QUANTIFYING CATCHMENT-SCALE PARTICULATE ORGANIC MATTER (POM) LOSS FOLLOWING FIRE, RELATIVE TO BACKGROUND POM FLUXES

By
Katherine E. Condon

A Thesis Submitted to the Faculty of the
DEPARTMENT OF HYDROLOGY AND WATER RESOURCES
In Partial Fulfillment of the Requirements
For the Degree of

MASTER OF SCIENCE
WITH A MAJOR IN HYDROLOGY

In the Graduate College

THE UNIVERSITY OF ARIZONA
2013

STATEMENT BY AUTHOR

This thesis has been submitted in partial fulfillment of requirements for an advanced degree at The University of Arizona and is deposited in the University Library to be made available to borrowers under rules of the Library.

Brief quotations from this dissertation are allowable without special permission, provided that accurate acknowledgment of source is made. Requests for permission for extended quotation from or reproduction of this manuscript in whole or in part may be granted by the copyright holder.

SIGNED: _____
Katherine E. Condon

APPROVAL BY THESIS DIRECTOR

This thesis has been approved on the date shown below:

_____ ____August 5, 2013_____
Dr. Paul D. Brooks Date
Professor of Hydrology and Water Resources

ACKNOWLEDGEMENTS

This research was made possible by the support of the National Science Foundation and their Jemez-Santa Catalina Critical Zone Observatory. I am grateful to the Valles Caldera National Preserve for their cooperation and assistance in accessing research sites. Many people graciously lent their time and expertise to help with this project and to provide me with encouragement along the way. In particular, I would like to thank Caitlin Orem and Michael Pohlmann for assisting with field work; Caitlin also generously shared LiDAR data which helped make these analyses possible. Thank you to Dr. Bruce Finney and Dr. Million Hailemichael at the ILEIA lab at the University of Idaho for running samples and providing valuable expertise. Tim Corley, Allison Peterson, Vanessa Boocher, Courtney Porter, and David Huckle provided much-appreciated help and advice in the lab. Thank you also to Dr. Erika Gallo, Clare Stielstra and Joel Biederman, who offered wise words and useful feedback. GIS support from Matej Durcik was immensely helpful, as was the expertise and guidance of Dr. Julia Perdrial, Dr. Craig Rasmussen, Dr. Jenifer McIntosh, and Dr. Kathleen Lohse.

Like many others in the Department of Hydrology and Water Resources, I have relied frequently on Olivia, Thomas and Erma, and I am grateful for their patient assistance. I have also been fortunate to have the encouragement, love, and support of my family and my partner James. Finally, I would like to express my deep gratitude to my committee members Dr. Tom Meixner and Dr. Jon Pelletier, and in particular to my advisor Dr. Paul Brooks, who has worked tirelessly to help guide me toward stronger science and a clearer story.

DEDICATION

I dedicate this thesis to the memory of my mother, Deborah Gail Condon, whose devotion to her own higher education has served as inspiration to me for years, and will continue to do so throughout my life.

TABLE OF CONTENTS

TABLE OF CONTENTS - *Continued*

TABLE OF CONTENTS - *Continued*

ABSTRACT

This study investigates translocation of particulate carbon and nitrogen from burned and unburned catchments within New Mexico's Valles Caldera National Preserve following severe wildfire. My research questions are: (1) how much carbon and nitrogen is eroded from burned slopes and re-deposited in debris fans? and (2) how do these quantities compare to fluvial export of particulate carbon and nitrogen from nearby unburned catchments? Results indicate that the ~200 kg ha^{-1} of nitrogen per depositional area on the debris fans represents ~50 to 100 years' worth of atmospheric inputs. In total, 124 times more carbon and 21 times more nitrogen were deposited on the two fans than was exported in particulate form from all three unburned catchments combined in water year 2012. My findings suggest that post-fire erosion may increase nitrogen loading to downslope environments, with the potential to alter the biogeochemical budgets of both aquatic and terrestrial systems.

1. INTRODUCTION

1.1 Introduction

1.1.1 Impact of Wildfire on Carbon and Nitrogen Pools

Wildfires are occurring with increasing frequency in the western United States, burning larger swaths of forest at higher intensities than in the past (Miller et al. 2009; Westerling et al. 2006). In the last decade, wildland fires have consumed between 1.5 to 4 million ha in the US every year (NIFC 2013), driven by a combination of historic management practices and warmer, drier climate conditions (Littell et al. 2009; McKelvey & Busse 1996; Westerling & Bryant 2008). This trend is predicted to continue, as a fuel surplus remains in the forests of the western US, and the fire season continues to become longer, warmer, and drier (Krawchuk et al. 2009; Marlon et al. 2012; Pechony & Shindell 2010). Forested montane catchments supply the majority of the water used in the western United States while simultaneously serving as a major carbon sink (Bales et al. 2006; Schimel et al. 2002; Serreze et al. 1999). There is therefore a strong need to better understand the hydrological and biogeochemical response of catchments to wildfire, and particularly to severe burns.

During fire, carbon and nitrogen from soil, litter, and above-ground biomass are lost to the atmosphere via combustion (Figure A1). Studies of severe, stand-replacing fire have reported as much as 30% of above-ground carbon and over 70% of above-ground nitrogen lost to burning (Johnson et al. 2004; Meigs et al. 2009), and litter losses may be

as high as 100% (Campbell et al. 2007). Soil loss estimates vary greatly, but research suggests that high severity burns average up to twice the soil carbon and nitrogen losses caused by moderate or low severity fires (Homann et al. 2011).

1.1.1 Impact of post-fire erosion on carbon and nitrogen pools and fluxes

Following fire, several mechanisms combine to increase fluvial erosion, exporting even more carbon and nitrogen from burned catchments (Figure A1). The loss of vegetative cover decreases interception and evapotranspiration, making more precipitation available for runoff (Anderson et al. 1976). Simultaneously, the loss of organic material, the alteration of the soil structure, and in some cases, the presence of pyrogenic hydrophobic compounds in burned soils, have the combined effect of reducing soil infiltration rates and capacity (DeBano 2000). As well, the removal of canopy and litter cover exposes more bare soil and ash on the forest floor to erosion (DeBano et al. 1998). Finally, since most fires occur in the dry, early summer months in the western US, the intense late summer convective storms that follow can trigger massive debris flows and mass wasting events (Cannon 2001; Meyer & Wells 1997; Robichaud et al. 2007).

Post-fire debris flows are capable of exporting highly variable but sometimes very large amounts of sediment from catchments. In a study of 95 burned catchments, less than half of the sites generated debris flows (Cannon 2001), but data on observed post-fire debris flows at 34 sites suggest average and median erosion rates of 230,000 and 150,000 kg ha^{-1} (Gartner et al. 2004; Shakesby & Doerr 2006). Following severe wildfire

in the Cascade Mountains, Baird et al. (1999) estimated losses to surface erosion at 280 kg C ha^{-1} and 14 kg N ha^{-1} in ponderosa pine and Douglas fir forest, and higher losses of 640 kg C and 22 kg N ha-1 in lodgepole pine and Engelmann spruce forest. Another study quantified the material moved by fluvial erosion following the Gondola Basin fire in the Lake Tahoe basin, and estimated that between 25 to 110 kg N ha^{-1} were translocated down gradient (Johnson et al. 2007). However, estimates of the carbon and nitrogen mass moved by post-fire erosion and debris flows are rare and complicated by a lack of pre-fire data.

It remains unclear how much eroded material is deposited and retained lower in the watershed, and whether carbon and nutrients in this sediment are sequestered or continue to actively cycle in a new location (Figure A1). To fully quantify losses to erosion, catchment sediment budgets must account for both erosion rates and sediment yield, i.e. what is input to the stream versus what is exported from the watershed. It is clear that there are large disparities between these amounts; studies in the US indicate that total sediment yield is roughly 10 to 20% of estimated erosion rates (Stallard 1998; Trimble & Crosson 2000). Although the process of erosion may increase mineralization of soil organic carbon (Van Hemelryck et al. 2011), if the replacement of carbon on the hillslopes (Harden et al. 1999) combined with burial and sequestration at the deposition site (Gregorich et al. 1998) exceeds the erosional losses, then erosion may result in a net carbon sink (Berhe et al. 2007). Because the loss of soil organic matter may seriously limit post-fire vegetative regeneration at some sites (Neary et al. 1999), more research is

needed into the quantity and possible implications of post-fire translocation and retention of carbon and nitrogen.

1.1.3 Quantifying particulate C and N background fluxes

Assessing the potential importance of post-fire carbon and nitrogen fluxes to both terrestrial and aquatic ecosystems requires knowledge of background levels of particulate fluxes from unburned catchment ecosystems. Logistical difficulties in quantifying particulate organic matter (POM), together with approaches that focus on baseflow carbon and nitrogen cycling, have resulted in relatively few studies on POM export from undisturbed catchments. Catchment carbon and nitrogen budgets have often excluded particulates, assuming that the bulk of fluxes take place in the dissolved form (defined as less than either 0.45 or 0.7 microns). For example, in a survey of large river systems, Hope (1994) found that particulates comprise only 10% of fluvial total organic carbon (TOC) on average. However, these samples were biased towards routine low flow or baseflow samples, and more recent work suggests that this ratio varies greatly among catchments and ecosystems (Horowitz 2008). (Horowitz 2008). In a recent review of published carbon flux data, annual particulate organic carbon export in seven montane catchments ranged widely, from 10 up to 79% of the TOC flux, averaging 39% (σ = 26%) (Alvarez-Cobelas et al. 2012; Kaushal & Lewis 2005; Rai & Sharma 1998). In systems driven by large monsoon events, particulate carbon and nitrogen have been observed to constitute 92 and 83% of total fluxes, respectively (Brooks et al. 2007).

These studies indicate a need for more complete baseline data on POM fluxes, and a knowledge gap that further complicates efforts to contextualize disturbance-related fluxes of C and N.

1.1.4 Stoichiometry and stable isotopes of burned and unburned POM

The sources of suspended sediment in streams and rivers vary by catchment and ecosystem as well as on a seasonal and event-scale within the same catchment. Elemental and isotopic analysis can identify characteristics that help distinguish between sources. For instance, a lower carbon to nitrogen (C:N) ratio may indicate a greater percentage of algal organic matter, indicating a higher proportion of autochthonous (in-stream) sediment sources (Dodds et al. 2004).

Stable isotopes may also be used as tracers to identify sources of sediment. It is well-established that stable carbon isotopes can be used to differentiate plant species contributing to the organic matter in litter and soils (Deines 1980). Certain plant photosynthetic pathways fractionate stable carbon isotopes more than others. It is therefore possible to determine percentages of C_3 and C_4 plant biomass in a soil by measuring the ratio of ^{12}C to ^{13}C. Because C_3 plant biomass averages 26‰ VPDB (Vienna PeeDee Belemnite standard) and C_4 plant biomass averages 12‰ VPDB, a simple mixing model using a weighted average can determine the percent contribution from each. Algal carbon is also often enriched in $\delta^{13}C$ compared to C_3 terrestrial plants, offering a potential tracer that can help identify in-stream (autochthonous) materials (Smith & Epstein 1971).

Processes affecting the ratio of ^{14}N to ^{15}N in soil and plant matter are complex, because ecosystem nitrogen cycles through many different pathways. Microbially mediated processes favor the lighter ^{14}N, and if the end product is removed via plant uptake, leaching, or gaseous losses, this leaves the soil comparatively enriched in ^{15}N (Nadelhoffer & Fry 1988; Sharp 2007).

Recently, it has been suggested that combustion at high temperatures may cause volatilization of lighter carbon and nitrogen isotopes, and correspondingly isotopically heavier organic material in partially burned soils (Saito et al. 2007). There is potential to use this knowledge to help trace the source of organic matter exported from a catchment by post-fire erosion.

1.2 Study Site Descriptions

1.2.1 Valles Caldera National Preserve, New Mexico

The Valles Caldera National Preserve (VCNP; 106°33’23”W, 35°52’19”N) is located in the headwaters of the Jemez River Basin in the Jemez Mountains of north-central New Mexico, at the site of a caldera formed 1.13 Ma (Figure A2; (Goff & Gardner 1994). Elevations range from 2300 in the lower grasslands to 3432 m at the summit of the Redondo Peak resurgent dome. Parent material at the site is rhyolitic. The forested uplands are predominately well-drained, rocky, cryic sandy loams, while the grasslands are darker mollics with greater water-holding capacity and organic matter content (Rodriguez & Archer 2010).

The site is semi-arid and seasonally snow-covered. Precipitation and temperature vary with elevation. Mean annual temperatures are around 3°C, and a SNOTEL site 5 km from Redondo Peak averages approximately 750 mm annual precipitation at an elevation of 2794 m (NRCS 2013). Typically about half of annual precipitation falls as snow between October and April, and the remainder falls during the late summer monsoon rains (Bowen 1996). Annual peak snowmelt discharge for the Redondo Peak catchments typically occurs in the month of April.

At the highest elevations, the hillslopes of the resurgent domes are predominately forested with Engelmann spruce (*Picea engelmannii*) and corkbark fir (*Abies lasiocarpa var. arizonica*) (Muldavin et al. 2006; Muldavin & Tonne 2003). Between 2740 and 3040 m, mixed conifer species, such as Douglas fir (*Pseudotsuga menziesii*), white fir (*Abies concolor*) and blue spruce (*Picea pungens*), are interspersed with aspen stands (*Populus tremuloides*). Below 2740 m, the hillslopes are forested with ponderosa pine (*Pinus ponderosa*) and Gambel oak (*Quercus gambelii*). The valley bottoms of the caldera consist of Rocky Mountain upper and lower montane grasslands. Grassland vegetation includes C_3 plants such as Parry's oatgrass (*Danthonia parryi*), Kentucky bluegrass (*Poa pratensis*), and Arizona fescue (*Festuca arizonica*), as well as C_4 species such as mountain muhly (*Muhlenbergia montana*) and pine dropseed (*Blepharoneuron tricholepis*).

In the summer of 2011, the western side of the Preserve was burned by the Las Conchas Fire, the largest in New Mexico's recorded history at the time. It was caused by a tree falling on a power line on 26 June 2011 and burned a total of 634 km^2, 80 of which

lie inside the VCNP, before containment on August 2 (USDA Forest Service 2011). The burn severity within the VCNP was 27% high, 33% moderate, and 32% low (Figure A3). The US Geological Survey assessed the debris flow hazard for the fire area as very high, predicting increased erosion and sedimentation rates (Tillery et al. 2011).

Following the fire, intense monsoon rains caused large debris flows from burned slopes, depositing new material at alluvial fans along the piedmonts of the Cerro del Medio resurgent dome (Figure A4). At these sites, as in classic alluvial fans, sediment is fluvially eroded from the hillslopes over time and deposited where the break in slope causes the flowing water to decrease in energy and velocity. The resulting alluvium is often poorly sorted due to the rapid decrease in sediment-carrying capacity, although finer material carried by sheetflow can be found along the fan edge (Blair & McPherson 1994). The older alluvium at the Cerro del Medio fans is well-vegetated with grasses, making areas covered in new sediment deposits easily identifiable.

1.2.2 Study Catchments

This study focuses on nine catchments of varying size: two burned catchments on Cerro del Medio, four burned zero-order basins (ZOBs) on Rabbit Mountain along the caldera rim, and three unburned catchments on Redondo Peak (Figure A2; Figure A3). The main study examines the Cerro del Medio and Redondo Peak sites, presented in the Appendix A manuscript. The ZOBs are presented separately in Appendix B.

The study catchments vary in size from 0.095 km^2 to 3.729 km^2, with mean slopes ranging from 9 to 21° (Table A1). The pre-fire or unburned vegetation at all sites consists mainly of spruce-fir mixed conifers at the upper elevations and ponderosa pine at the lower elevations (Muldavin et al. 2006). The two burned catchments on the southwestern slopes of Cerro del Medio will be referred to as Debris Fan 1 (DF1) and Debris Fan 2 (DF2). In total, 81 and 97% of the catchment areas burned, respectively, and 25 and 39% burned at high severity (USDA Forest Service 2011). They both subsequently produced large debris flows that deposited on their respective alluvial fans in the valley bottom (Figure A4). The catchments face mainly southwest, with elevations ranging from about 2650 to 3000 m (Table A1).

The four zero-order basin (ZOB) sites (named Instrumented, Orem, Gibbson, and Condon) on the northeast side of Rabbit Mountain exhibit a range of burn extents and severity. The entire Instrumented ZOB was burned, 74% of it at high severity. The Orem ZOB was nearly entirely burned as well, 44% of it at high severity. Both produced smaller-scale debris flows which deposited in culverts along NM Route 4 at the base of the slopes (Figure A3; culverts not shown). The Condon and Gibbson ZOBs showed no sign of debris flow deposition at any time following the fire, despite burn extents of 88 and 70%, respectively, with 53 and 32% of their areas burned at high severity. The Rabbit Mountain ZOBs all face mainly north and northwest, with elevations similar to Cerro del Medio ranging from 2650 to 3000 m (Table A1).

1.3 Thesis Format

The format of this thesis is outlined by the University of Arizona Graduate College's Manual for Theses and Dissertations and is therefore subject to repetition of information. The first chapter describes the context and relevance of this work. The second chapter describes the present study and briefly summarizes the findings described in Appendix A.

Appendix A is a scientific manuscript on the post-fire fluvial translocation of particulate carbon and nitrogen and is planned for submission to an as yet undecided venue. The manuscript repeats the introduction, conclusions and implications presented in Chapters 1 and 2, and further discusses the results of this research. Appendices B-G describe additional research and data that were collected as part of this study.

2. PRESENT STUDY

Please note: the context, methods, results and conclusions of this study are presented in a manuscript for publication entitled "Quantifying catchment-scale particulate organic matter (POM) loss following fire, relative to background POM fluxes", included with this document as Appendix A. The following section summarizes the methods and findings of this paper.

2.1 Present Study

Montane forested catchments supply water to millions in the western US while also serving as important carbon sinks. As wildfires continue to increase in magnitude, frequency, and severity, it becomes more and more critical to understand and quantify post-fire biogeochemical responses. However, our understanding is limited by a lack of information on how much C and N is translocated by episodic post-fire erosion and retained elsewhere in the watershed, and how these fluxes compare with baseline undisturbed particulate fluxes. To address these knowledge gaps, this study quantifies the fluvial export of particulate carbon and nitrogen from burned and unburned catchments within the Valles Caldera National Park in northern New Mexico's Jemez River Basin, following the 2011 Las Conchas wildfire. Specifically, we address two research questions: (1) how much carbon and nitrogen is eroded from burned slopes and re-

deposited below in debris fans? and (2) how do these quantities compare to fluvial export of particulate carbon and nitrogen in streamwater from nearby unburned catchments?

The study site is located in the Valles Caldera National Preserve (VCNP), in the headwaters of the Jemez River Basin of north-central New Mexico. The site is semi-arid and seasonally snow-covered, with a bimodal precipitation pattern where in a typical year, ~50% falls as snow between October and April, and the rest falls during the late summer monsoon rains (NRCS 2013). The hillslopes of the caldera wall and the resurgent domes are forested with ponderosa pine and mixed conifers, with interspersed aspen stands, while the valley bottom of the caldera is Rocky Mountain upper and lower montane grasslands (Muldavin et al. 2006). In 2011, the western side of the Preserve was burned by the Las Conchas Fire, the largest in New Mexico's recorded history at the time. Following the fire, intense monsoon rains caused large debris flows from burned slopes, depositing new material at alluvial fans and in culverts.

This study focuses on nine catchments of varying size, located on three resurgent domes: the extensively burned Cerro del Medio and Rabbit Mountain, and the unburned Redondo Peak. The two catchments on the southwestern slopes of Cerro del Medio burned at moderate and high severity, and subsequently produced large debris flows that deposited on their respective alluvial fans in the valley bottom. The four zero-order basins (ZOBs) of Rabbit Mountain were also moderately to severely burned. Two of these– the Orem ZOB and the Instrumented ZOB – produced smaller-scale debris flows that deposited in culverts at the base of their slopes. The unburned Redondo Peak sites include three larger catchments: Upper Jaramillo, History Grove, and La Jara.

Systematic transect surveys of the post-fire alluvial deposition were conducted in June 2012, ten months after the fire, following one monsoon and one snowmelt season during which sediment was eroded, deposited, and translocated again by multiple runoff events. Transects were surveyed at four sites: the two Cerro del Medio debris fans (DF1 and DF2), and at two culverts at the base of the burned Orem and Instrumented ZOBs on the northeast side of Rabbit Mountain. Observations of deposition type and amount were collected along each transect at regular 5 m intervals, following methods similar to Murphy et al. (2006). First, the predominant type of alluvial deposition was determined by visual inspection and categorized as: fines, sand /gravel, cobble, ash, mixed litter/ash, litter, woody debris, erosion, or vegetation. A trowel was then used to dig to the underlying grassland vegetation and the depth of the deposit was recorded to the nearest half centimeter. Length and diameter were measured for large woody debris to obtain volume, using a modification of methods from (Brown 1974). Length and width were also measured for any isolated piles of material separate from the larger depositional splays. The farthest extents of new deposition were recorded as waypoints on the GPS unit (Figure A5; Figure A6). At DF1, 5 transects were surveyed, with a total of 186 survey points recording deposit type and depth. At DF 2, 9 transects were surveyed, with a total of 251 survey points (Table A2).

At each of the two debris-filled culverts, a single longitudinal transect was surveyed in 5-meter intervals following the same methods described for the two fans. GPS waypoints were recorded to outline the edges of the alluvial deposits (Figure B2). At

the Instrumented ZOB culvert, 83 survey points were recorded. At the smaller Orem ZOB culvert, 40 survey points were recorded (Table A2).

Samples of the different alluvial types were taken in May and June of 2012. The May sampling locations were chosen using Light Detection and Ranging (LiDAR) imagery showing pre- and post-fire elevations to locate areas of post-fire deposition (Orem & Pelletier). In June, samples representing different deposit types were taken randomly when surveying the transects. A total of 23 samples and 33 samples were collected at DF1 and DF2 respectively, along with 8 and 13 samples from the Orem ZOB and Instrumented ZOB culverts (Table A2). Cores of the deposits were collected following a modification of standard soil sampling methods, similar to the methods described by Brooks et al. (1996), Hart and Gunther (1989), and Distefano and Gholz (1986). Cores were collected using a 3 cm diameter metal cylinder and a trowel, and stored in Ziploc bags on ice for transport. A small subsample was weighed and dried at 105°C for at least 48 hours to determine gravimetric water content and bulk density. The remainder was sieved through a 2 mm mesh screen, dried for 24 hours at 60°C, and ground in a ball mill. These samples then underwent elemental analysis with isotope ratio mass spectrometry (EA-IRMS) to determine bulk carbon and nitrogen content and stable isotopes.

Volumetric carbon and nitrogen concentrations were calculated using bulk density and the percent by weight determined by EA-IRMS analysis. Concentrations for the cobble, sand and gravel, and fines categories were calculated from the EA-IRMS detection limits, since the carbon and nitrogen contents were below detection. Woody

debris concentrations were calculated using the surveyed dimensions along with mean literature values for carbon and nitrogen content of large woody debris in mixed conifer forests.

Mapping of the fan survey data was done in ESRI ArcGIS 9.3. A polygon outline of each fan or culvert was created using the GPS waypoints marking the outer edges of the deposition, the surveyed transect depth data, and LiDAR data for the sites showing differenced pre- and post-fire elevations at the site (Orem & Pelletier). The areal percentage of each fan covered by different deposit types was calculated from the transect survey data, and an estimate of the percentage of each fan covered by each type of deposit was calculated by averaging the transect coverages for each fan.

Two methods were used to calculate total debris fan C and N content, providing a range of estimates for the total mass deposited. The first and simpler method, Method A, used a mean depth for each deposit type at each debris fan, calculated from the transect points. This method assumes that sediment amount and type are randomly distributed and that the systematic sampling provides a reasonable estimate of mean and variability. A quasi-Gaussian distribution can be present in sampling data even if deposition is not random on the landscape. Initial analyses of deposit depth approached a Gaussian distribution of all sample points, providing support for this approach.

Another simple method for predicting soil characteristics is to look for correlations with terrain, landscape position, and other spatial variables. This technique is strongest when the soil characteristics of interest are controlled by the flow of water, which is in turn controlled by the terrain (Gessler et al. 1995; Moore et al. 1993). In

Method B, two basic spatial variables were compared with the transect survey data: distance downslope from the fan apex, and distance from the center of the splay. The debris fan carbon and nitrogen contents were then calculated using spatially interpolated depths and frequencies for different deposit types instead of mean values.

At the two burned ZOB culverts, the total volume of alluvial deposition retained in the culverts was calculated using the mapped culvert area, the depth of deposition at each point along the longitudinal transect, and the width of the deposition at each point. Since the alluvial deposition at these two sites is much smaller and more uniform than the debris fan deposition, mean bulk density and mean carbon and nitrogen contents were used to calculate total mass.

Soil profile cores were collected at DF1, DF2, the Orem and Instrumented ZOB culverts, and at a third Rabbit Mountain site (Condon ZOB) which showed no new post-fire alluvial deposition in its culvert (Table A2). Soil profile cores were obtained March 2012 using an Environmentalist Sub-soil Sampler. A total of 13 cores were taken, ranging in length from 20 to 80 cm. They were transported on ice, laid horizontally to reduce compaction of the core, and frozen in order to better retain their shape when cut open. During subsampling, the frozen soil core tubes were sliced in half lengthwise, photographed and described, and then divided into 10 cm layers. One half of each layer was set aside to be archived. The remaining samples were weighed, sieved, dried, and ground according to the same protocols as the alluvial samples, and processed for EA-IRMS analysis.

Continuous discharge monitoring is conducted throughout the year at the Redondo Peak catchments for the University of Arizona Critical Zone Observatory. Surface water grab samples are collected weekly through the snowmelt season, biweekly through the summer months, and monthly through the winter. Daily samples during snowmelt and event samples during the monsoon were collected using an automated sampler (Teledyne Isco; http://www.isco.com/products/products1.asp?PL=201) at catchment outlets. For this research, the 0.7 μm glass fiber filters used to separate the dissolved from the particulate fractions were retained and analyzed for total suspended sediment, particulate carbon, and particulate nitrogen, following methods modified from Brooks et al. (2007) . Grab sample filters with sufficient sediment were retained for analysis, supplemented by Isco sample filters to better represent a range of seasons. The resulting carbon and nitrogen percentages by weight were used to calculate the total carbon and nitrogen mass. Volumetric concentrations were calculated as the total carbon and nitrogen mass, divided by the entire volume of water filtered for that sample.

Particulate carbon (PC) and particulate nitrogen (PN) flux rates describe the mass exported by streamflow over time, for example as grams per day or kilograms per year. Discharge data available in 15 minute intervals at the three Redondo Peak catchment flumes were used to calculate flux rates for each sample. A regression analysis did not reveal any significant relationships between discharge and TSS, PC, or PN concentrations at any of the three sites. Mean carbon and nitrogen concentrations at each site were tested for significant differences among seasons, between rising or falling discharge, and between high or low flows (JMP Version 10SAS Institute). Rising and falling discharge

produced significantly different mean concentrations at La Jara and Upper Jaramillo for PC, and at La Jara for PN (unequal variance ANOVA or paired t-test with $P < 0.05$). When significantly different, these concentrations were used with discharge to calculate daily flux rates. Otherwise, a single mean value was used for the entire hydrograph (at History Grove for PC and at History Grove and Upper Jaramillo for PN). Finally, total annual flux rates with standard error were calculated for each catchment by summing daily flux rates across the water year 2012 hydrograph.

2.2 Conclusions and Implications

2.2.1 Post-fire debris flow C and N

Different types of alluvial deposit materials were found with varying frequency along different transects and at different positions within the fans. Fines, sand/gravel, and cobble occur most frequently in the center of the fan, while ash, mixed litter/ash, and litter are less frequent in the center and occur more often moving out toward the edges (Figure A7). The depth of litter and ash deposits increases moving down gradient, fitting a weak but significant power law relationship between depth and the distance from the fan apex ($R^2 = 0.27$, $P < 0.01$; Figure A9). The depth of the heavier fractions – sand/gravel, cobble, and fines – is more strongly predicted by scaled distance from the center of the fan, decreasing in depth exponentially moving out toward the fan edges ($R^2 = 0.68$, $P < 0.01$; Figure A9). Similar patterns were described by Meyer and Wells (1997)

in Yellowstone National Park following post-fire debris flows on small alluvial fans. Our work demonstrates how simple empirical relationships can be used to tease out spatial patterns for different size fractions, quantifying how heavier, more mineral deposits become sparser toward the fan edges, while more organic litter and ash become deeper and more prevalent down gradient. The potential catchment-scale biogeochemical implications of this fluvial sorting have rarely been examined in studies of debris flows and alluvial fans, but here we observe that organic-rich materials are translocated farther from their source to be deposited in and near riparian grasslands.

The two methods used to calculate total C and N content in the alluvial fans provide different estimates (Table A5). Using Method A, the mean depth method, Debris Fan 1 contains 75,705 kg C (SE = 1841) and 977 kg N (SE = 59) while Method B using spatial interpolation yielded estimates of 155,090 kg C and 3720 kg N. For Debris Fan 2, the Method A results are 91,730 kg C (SE = 11,966) and 4122 kg N (SE = 346), while Method B results are 106,332 kg C and 2353 kg N at Debris Fan 2 (Table A6). Assuming that Method B's spatial interpolation provides the more accurate description of the fans, the two fans contain similar amounts of carbon and nitrogen per unit of deposition area, with ~9500 and 10,100 kg C ha^{-1} at DF1 and DF2 respectively, and ~200 kg N ha^{-1} at each fan. However, Debris Fan 1 contains about 40% more per unit of contributing catchment area: 1140 versus 804 kg C ha^{-1}, and 27 versus 18 kg N ha^{-1} (Table A6). Few studies have quantified the carbon and nitrogen content of translocated material following fire, and those that exist often look primarily at losses from a hillslope perspective. However, one study that quantified the material moved and deposited by fluvial erosion

following the Gondola Basin fire in the Lake Tahoe basin estimated between 25 to 110 kg N ha^{-1} were translocated (Johnson et al. 2007). Per unit of contributing catchment area, this is on the order of the 14 to 91 kg N ha^{-1} estimated on the Cerro del Medio debris fans by Method A; the Method B results also fall within this range.

The alluvial deposition retained in the burned Orem ZOB culvert contains 283 kg of carbon and 15 kg of nitrogen. The Instrumented ZOB culvert is larger and retained 1572 kg of carbon and 81 kg of nitrogen. The culverts have similar loading per unit of depositional area, at ~44,200 and 51,800 kg C ha^{-1} and 2300 and 2700 kg N m^{-2}. Per unit of contributing catchment, however, the Instrumented ZOB retained about 7 times as much carbon and nitrogen: 119.9 versus 16.8 kg C $ha^{-1}$and 6.2 versus 0.9 kg N ha^{-1}. Although the culverts are far more concentrated in carbon and nitrogen than the debris fan alluvial deposits, the carbon retained in total represents less than 0.1% of the carbon remaining in the burned catchment surface soils. The very high concentrations of carbon and nitrogen deposition suggest that localized effects of catchment-scale post-fire translocation may be dramatic where changes in slope function as a sediment trap. No alluvial deposition was observed at the culverts at the outlet of the Gibbson ZOB or the Condon ZOB. This failure to produce debris flows at their outlets suggests that any post-fire erosion was retained within the catchment.

2.2.2 Streamflow particulate C and N

The Redondo Peak catchment hydrographs follow the bimodal precipitation pattern at the site, with the highest flows during the snowmelt season, and event-specific peaks during the late summer monsoon (Figure A10). The mean annual discharge (± σ) in water year 2012 at the Redondo Peak catchments was $2.63*10^5 \pm 1.25*10^4$ L day^{-1} at History Grove, $2.32*10^5 \pm 9.80*10^3$ L day^{-1} at La Jara, and $3.70*10^5 \pm 4.29*10^4$ L day^{-1} at Upper Jaramillo. The estimated daily carbon and nitrogen fluxes from the three Redondo Peak catchments are highly variable over the hydrograph (Figure A11); due to the strong control of discharge, predicted fluxes are highest during the snowmelt season. Daily estimated PC fluxes for water year 2012 averaged 2.2 ± 3.5 (μ ± σ), 1.2 ± 0.9, and 2.4 ± 1.3 kg C day^{-1}, while PN fluxes averaged 0.2 ± 0.2, 0.2 ± 0.1, and 0.4 ± 0.2 kg N day^{-1} respectively at History Grove, La Jara, and Upper Jaramillo. Per hectare of catchment area, this equates to total annual fluxes of 3.4, 1.4, and 2.5 kg C and 0.3, 0.2, and 0.4 kg N, respectively (Table A6).

The majority of particulate carbon and nitrogen flux in water year 2012 took place during snowmelt, which made up 58, 42, and 47% of POM flux at History Grove, La Jara, and Upper Jaramillo respectively. Another 25, 39, and 30% of POM flux occurred during the summer monsoon from the respective catchments, and the remaining 17, 20, and 23% of the annual flux took place in the winter. The ratio of carbon to nitrogen increases logarithmically with TSS at each site (Figure A13). The relationship is strongest at History Grove ($R^2 = 0.73$, $P<0.0001$) and Upper Jaramillo ($R^2 = 0.65$, $P<0.0005$), and weaker but still significant at La Jara ($R^2 = 0.20$, $P<0.05$).

The PN fluxes from the Redondo Peak catchments are lower than comparable observations of other undisturbed headwater systems. Lewis (2002) has summarized data from 19 such sites in the United States, and found mean annual PN fluxes of 2.62 ± 0.36 kg N ha^{-1}. Another study of montane headwater catchments in the US found annual PC fluxes of ~10 kg C ha^{-1} (Alvarez-Cobelas et al. 2012; Kaushal & Lewis 2005), and similar fluxes have also been reported in Himalayan headwaters (Rai & Sharma 1998). The predicted Redondo Peak catchment PC fluxes are several times smaller, at 1.4 to 3.4 kg C ha^{-1}.

2.2.3 Comparison of episodic and continuous particulate fluxes

In total, 124 times more carbon and 21 times more nitrogen was deposited on the two post-fire debris fans than was exported in particulate form from all three unburned Redondo Peak catchments combined in water year 2012. Per square meter of catchment area, the debris fan carbon is roughly 400 times greater than the total water year 2012 Redondo Peak fluxes, and the debris fan nitrogen is roughly 70 times greater. Total C:N ratios in the debris fan materials are about twice as high as the culvert deposit C:N ratios, and 7 times greater than the mean C:N ratios in the suspended particulate samples. The woody debris in the fans plays a large role in increasing the C:N ratios at the debris fans. However, the litter and ash deposition also has C:N ratios 2 to 3 times higher than was observed in Redondo Peak suspended particulates.

2.2.4 Conclusions

To fully quantify the impact of fire on catchment carbon and nitrogen budgets and biogeochemistry, it is important to assess the potential effects of erosion and translocation. Episodic mass wasting events following the Las Conchas wildfire translocated hundreds of times more particulate carbon and tens of times more particulate nitrogen per unit catchment area than is exported annually by nearby unburned streams. The ~200 kg ha^{-2} of nitrogen per depositional area being retained in the fans represents roughly 50 to 100 years' worth of atmospheric inputs. Translocation of nitrogen-rich organic matter from the drier forested hillslopes to the wetter grassland soils in the Valle Grande could potentially lead to faster nutrient cycling, as well as increased nitrogen-loading to N-limited aquatic systems.

REFERENCES

Alvarez-Cobelas M, Angeler DG, Sanchez-Carrillo S, Almendros G (2012) A worldwide view of organic carbon export from catchments. Biogeochemistry 107(1-3): 275-293

Anderson HW, Hoover MD, Reinhart KG (1976) Forests and water: effects of forest management on floods, sedimentation, and water supply. In: U.S. Department of Agriculture FS (ed). Pacific Southwest Forest and Range Experiment Station, Berkeley, CA. p 115

Baird M, Zabowski D, Everett RL (1999) Wildfire effects on carbon and nitrogen in inland coniferous forests. Plant Soil 209(2): 233-243

Bales RC, Molotch NP, Painter TH, Dettinger MD, Rice R, Dozier J (2006) Mountain hydrology of the western United States. Water Resour. Res. 42(8):

Berhe AA, Harte J, Harden JW, Torn MS (2007) The significance of the erosion-induced terrestrial carbon sink. Bioscience 57(4): 337-346

Blair TC, McPherson JG (1994) ALLUVIAL FANS AND THEIR NATURAL DISTINCTION FROM RIVERS BASED ON MORPHOLOGY, HYDRAULIC PROCESSES, SEDIMENTARY PROCESSES, AND FACIES ASSEMBLAGES. Journal of Sedimentary Research Section a-Sedimentary Petrology and Processes 64(3): 450-489

Bowen BM (1996) Rainfall and climate variation over a sloping New Mexico plateau during the North American monsoon. Journal of Climate 9(12): 3432-3442

Brooks PD, Haas PA, Huth AK (2007) Seasonal variability in the concentration and flux of organic matter and inorganic nitrogen in a semiarid catchment, San Pedro River, Arizona. J. Geophys. Res.-Biogeosci. 112(G3):

Brooks PD, Williams MW, Schmidt SK (1996) Microbial activity under alpine snowpacks, Niwot Ridge, Colorado. Biogeochemistry 32(2): 93-113

Brown JK (1974) Handbook for inventorying downed woody material. Intermountain Forest and Range Experiment Station, Forest Service, U.S. Dept. of Agriculture, Ogden, Utah

Campbell J, Donato D, Azuma D, Law B (2007) Pyrogenic carbon emission from a large wildfire in Oregon, United States. Journal of Geophysical Research: Biogeosciences 112(G4): G04014

Cannon SH (2001) Debris-flow generation from recently burned watersheds. Environmental & Engineering Geoscience 7(4): 321-341

DeBano LF (2000) The role of fire and soil heating on water repellency in wildland environments: a review. Journal of Hydrology 231: 195-206

DeBano LF, G. ND, F. FP (1998) Fire's effects on ecosystems. J. Wiley, New York

Deines P (1980) The isotopic composition of reduced organic carbon. In: Fritz P & Fontes JC (eds) Handbook of Environmental Isotopic Geochemistry. Elsevier, Amsterdam. p 329-406

Distefano JF, Gholz HL (1986) A PROPOSED USE OF ION-EXCHANGE RESINS TO MEASURE NITROGEN MINERALIZATION AND NITRIFICATION IN INTACT SOIL CORES. Communications in Soil Science and Plant Analysis 17(9): 989-998

Dodds WK, Marti E, Tank JL, Pontius J, Hamilton SK, Grimm NB, Bowden WB, McDowell WH, Peterson BJ, Valett HM, Webster JR, Gregory S (2004) Carbon and nitrogen stoichiometry and nitrogen cycling rates in streams. Oecologia 140(3): 458-467

Gartner JE, Bigio ER, Cannon SH (2004) Compilation of Post Wildfire Runoff-Event Data from the Western United States. In: US Department of the Interior UGS (ed).

Gessler PE, Moore ID, McKenzie NJ, Ryan PJ (1995) SOIL-LANDSCAPE MODELING AND SPATIAL PREDICTION OF SOIL ATTRIBUTES. International Journal of Geographical Information Systems 9(4): 421-432

Goff F, Gardner JN (1994) EVOLUTION OF A MINERALIZED GEOTHERMAL SYSTEM, VALLES CALDERA, NEW-MEXICO. Econ. Geol. Bull. Soc. Econ. Geol. 89(8): 1803-1832

Gregorich EG, Greer KJ, Anderson DW, Liang BC (1998) Carbon distribution and losses: erosion and deposition effects. Soil & Tillage Research 47(3-4): 291-302

Harden JW, Sharpe JM, Parton WJ, Ojima DS, Fries TL, Huntington TG, Dabney SM (1999) Dynamic replacement and loss of soil carbon on eroding cropland. Glob. Biogeochem. Cycle 13(4): 885-901

Hart SC, Gunther AJ (1989) INSITU ESTIMATES OF ANNUAL NET NITROGEN MINERALIZATION AND NITRIFICATION IN A SUBARCTIC WATERSHED. Oecologia 80(2): 284-288

Homann PS, Bormann BT, Darbyshire RL, Morrissette BA (2011) Forest Soil Carbon and Nitrogen Losses Associated with Wildfire and Prescribed Fire. Soil Science Society of America Journal 75(5): 1926-1934

Hope D, Billett MF, Cresser MS (1994) A REVIEW OF THE EXPORT OF CARBON IN RIVER WATER - FLUXES AND PROCESSES. Environmental Pollution 84(3): 301-324

Horowitz AJ (2008) Determining annual suspended sediment and sediment-associated trace element and nutrient fluxes. Science of the Total Environment 400(1-3): 315-343

Johnson D, Murphy JD, Walker RF, Glass DW, Miller WW (2007) Wildfire effects on forest carbon and nutrient budgets. Ecological Engineering 31(3): 183-192

Johnson DW, Susfalk RB, Caldwell TG, Murphy JD, Miller WW, Walker RF (2004) Fire Effects on Carbon And Nitrogen Budgets in Forests. In: Wieder RK, Novák M & Vile M (eds) Biogeochemical Investigations of Terrestrial, Freshwater, and Wetland Ecosystems across the Globe. Springer Netherlands. p 263-275

Kaushal SS, Lewis WM (2005) Fate and transport of organic nitrogen in minimally disturbed montane streams of Colorado, USA. Biogeochemistry 74(3): 303-321

Krawchuk MA, Moritz MA, Parisien MA, Van Dorn J, Hayhoe K (2009) Global Pyrogeography: the Current and Future Distribution of Wildfire. PLoS One 4(4): 12

Lewis WM (2002) Yield of nitrogen from minimally disturbed watersheds of the United States. Biogeochemistry 57(1): 375-385

Littell JS, McKenzie D, Peterson DL, Westerling AL (2009) Climate and wildfire area burned in western U. S. ecoprovinces, 1916-2003. Ecol. Appl. 19(4): 1003-1021

Marlon JR, Bartlein PJ, Gavin DG, Long CJ, Anderson RS, Briles CE, Brown KJ, Colombaroli D, Hallett DJ, Power MJ, Scharf EA, Walsh MK (2012) Long-term perspective on wildfires in the western USA. Proceedings of the National Academy of Sciences 109(9): E535-E543

McKelvey KS, Busse KK (1996) Twentieth-century fire patterns on forest service lands. In *Sierra Nevada Ecosystem Project, Final Report to Congress, Vol. II, Assessments and Scientific Basis for Management Options.* In: Service UF (ed). University of California, Centers for Water and Wildland Resources, Davis, CA. p 1119-1138

Meigs GW, Donato DC, Campbell JL, Martin JG, Law BE (2009) Forest Fire Impacts on Carbon Uptake, Storage, and Emission: The Role of Burn Severity in the Eastern Cascades, Oregon. Ecosystems 12(8): 1246-1267

Meyer GA, Wells SG (1997) Fire-related sedimentation events on alluvial fans, Yellowstone National Park, USA. Journal of Sedimentary Research 67(5): 776-791

Miller JD, Safford HD, Crimmins M, Thode AE (2009) Quantitative Evidence for Increasing Forest Fire Severity in the Sierra Nevada and Southern Cascade Mountains, California and Nevada, USA. Ecosystems 12(1): 16-32

Moore ID, Gessler PE, Nielsen GA, Peterson GA (1993) SOIL ATTRIBUTE PREDICTION USING TERRAIN ANALYSIS. Soil Science Society of America Journal 57(2): 443-452

Muldavin E, Neville P, Jackson C, Neville T (2006) A Vegetation Map of Valles Caldera National Preserve New Mexico: Final Report for Cooperative Agreement No. 01CRAG0014. In., University of New Mexico, Albuquerque.

Muldavin E, Tonne P (2003) Vegetation Survey and Preliminary Ecological Assessment of Valles Caldera National Preserve, New Mexico. In: Service UF (ed). University of New Mexico, Albuquerque, NM. p 118

Murphy JD, Johnson DW, Miller WW, Walker RF, Carroll EF, Blank RR (2006) Wildfire Effects on Soil Nutrients and Leaching in a Tahoe Basin Watershed. J. Environ. Qual. 35(2): 479-489

Nadelhoffer KF, Fry B (1988) CONTROLS ON NATURAL N-15 AND C-13 ABUNDANCES IN FOREST SOIL ORGANIC-MATTER. Soil Science Society of America Journal 52(6): 1633-1640

National Interagency Fire Center (NIFC) (2013) Wildland fires and acres (1960-2012).

Natural Resources Conservation Service (NRCS) National Water and Climate Center (2013) Quemazon SNOTEL Site 708. In.

Neary DG, Klopatek CC, DeBano LF, Ffolliott PF (1999) Fire effects on belowground sustainability: a review and synthesis. Forest Ecology and Management 122(1-2): 51-71

Orem C, Pelletier JD Unpublished LiDAR data. In.

Pechony O, Shindell DT (2010) Driving forces of global wildfires over the past millennium and the forthcoming century. Proceedings of the National Academy of Sciences:

Rai SC, Sharma E (1998) Comparative assessment of runoff characteristics under different land use patterns within a Himalayan watershed. Hydrol. Process. 12(13-14): 2235-2248

Robichaud P, Elliot W, Pierson F, Hall D, Moffet C (2007) Predicting postfire erosion and mitigation effectiveness with a web-based probabilistic erosion model. Catena 71(2): 229-241

Rodriguez M, Archer V (2010) Valles Caldera National Preserve: Soils Existing Condition Report In: Service VCTaUF (ed). Jemez Springs, NM.

Saito L, Miller WW, Johnson DW, Qualls RG, Provencher L, Carroll E, Szameitat P (2007) Fire effects on stable isotopes in a Sierran forested watershed. J. Environ. Qual. 36(1): 91-100

SAS Institute I JMP v. 10. In., Cary, NC.

Schimel D, Kittel TGF, Running S, Monson R, Turnipseed A, Anderson D (2002) Carbon sequestration studied in western U.S. mountains

Eos, Transactions American Geophysical Union Volume 83, Issue 40. Eos, Transactions American Geophysical Union 83(40): 445-449

Serreze MC, Clark MP, Armstrong RL, McGinnis DA, Pulwarty RS (1999) Characteristics of the western United States snowpack from snowpack telemetry (SNOTEL) data. Water Resour. Res. 35(7): 2145-2160

Shakesby RA, Doerr SH (2006) Wildfire as a hydrological and geomorphological agent. Earth-Science Reviews 74(3-4): 269-307

Sharp Z (2007) Principles of Stable Isotope Geochemistry. Pearson Prentice Hall, Upper Saddle River, NJ

Smith BN, Epstein S (1971) Two Categories of 13C/12C Ratios for Higher Plants. Plant Physiology 47(3): 380-384

Stallard RF (1998) Terrestrial sedimentation and the carbon cycle: Coupling weathering and erosion to carbon burial. Glob. Biogeochem. Cycle 12(2): 231-257

Teledyne Isco (2013) Automatic Water Samplers. In. vol 7/22/2013.

Tillery AC, Darr MJ, Cannon SH, Michael JA (2011) Postwildfire Preliminary Debris Flow Hazard Assessment for the Area Burned by the 2011 Las Conchas Fire in North-Central New Mexico: U.S. Geological Survey Open-File Report 2011-1308. In. p 11

Trimble SW, Crosson P (2000) Land use - US soil erosion rates - Myth and reality. Science 289(5477): 248-250

USDA Forest Service (2011) Burned Area Emergency Response (BAER) Imagery Support Data Download. In. United States Forest Service.

Van Hemelryck H, Govers G, Van Oost K, Merckx R (2011) Evaluating the impact of soil redistribution on the in situ mineralization of soil organic carbon. Earth Surf. Process. Landf. 36(4): 427-438

Westerling AL, Bryant BP (2008) Climate change and wildfire in California. Clim. Change 87: S231-S249

Westerling AL, Hidalgo HG, Cayan DR, Swetnam TW (2006) Warming and earlier spring increase western US forest wildfire activity. Science 313(5789): 940-943

APPENDIX A: QUANTIFYING CATCHMENT-SCALE PARTICULATE ORGANIC MATTER (POM) LOSS FOLLOWING FIRE, RELATIVE TO BACKGROUND POM FLUXES

"Quantifying catchment-scale particulate organic matter (POM) loss following fire, relative to background POM fluxes"

Katherine E. Condon[1*], Jon Pelletier[2], Thomas Meixner[1], Kathleen A. Lohse[3], Craig Rasmussen[4], Jennifer C. McIntosh[1], Caitlin Orem[3], and Paul D. Brooks[1]

[1] Department of Hydrology and Water Resources,
University of Arizona, Tucson, AZ, 85721

[2] Department of Geosciences,
University of Arizona, Tucson, AZ, 85721

[3] Department of Biological Sciences,
Idaho State University, Pocatello, ID, 83209

[4] Department of Soil, Water, and Environmental Science
University of Arizona, Tucson, AZ, 85721

* Correspondence to: Katherine E. Condon, Department of Hydrology and Water Resources, 1133 E. James E. Rogers Way, University of Arizona, Tucson, AZ, 85721.

Email: condon@email.arizona.edu

Abstract

Increased erosion following wildfire is well-documented, but less clear is how translocation of organic material affects local carbon and nitrogen budgets. This study investigates the translocation of particulate carbon and nitrogen from burned and unburned catchments within New Mexico's Valles Caldera National Preserve following the 2011 Las Conchas wildfire. Our research questions are: (1) how much carbon and nitrogen is eroded from burned slopes and re-deposited below in debris fans? and (2) how do these quantities compare to fluvial export of particulate carbon and nitrogen in streamwater from nearby unburned catchments? Suspended sediment samples were taken throughout the 2012 water year and through the snowmelt period of 2013 at flumes in three unburned catchments. Alluvial deposit surveying and sampling was done at two debris fans at the base of severely burned catchments. Samples were analyzed for elemental carbon and nitrogen content, and the results were spatially interpolated across the terrain of the debris fans. Our results reveal that the ~200 kg ha^{-1} of nitrogen per depositional area on the debris fans represents ~ 50 to 100 years' worth of atmospheric inputs. In total, 124 times more carbon and 21 times more nitrogen were deposited on the two fans than was exported in particulate form from all three unburned catchments combined in water year 2012. Our results indicate that post-fire erosion may cause substantial nitrogen loading to downslope environments, with the potential to alter the biogeochemical budgets of both aquatic and terrestrial systems.

Introduction

Wildfires are occurring with increasing frequency in the western United States, burning larger swaths of forest at higher intensities than in the past (Miller et al. 2009; Westerling et al. 2006). In the last decade, wildland fires have consumed between 1.5 to 4 million ha in the US every year (NIFC 2013), driven by a combination of historic management practices and warmer, drier climate conditions (Littell et al. 2009; McKelvey & Busse 1996; Westerling & Bryant 2008). This trend is predicted to continue, as a fuel surplus remains in the forests of the western US, and the fire season continues to become longer, warmer, and drier (Krawchuk et al. 2009; Marlon et al. 2012; Pechony & Shindell 2010). Forested montane catchments supply the majority of the water used in the western United States while simultaneously serving as a major carbon sink (Bales et al. 2006; Schimel et al. 2002; Serreze et al. 1999).

During fire, carbon and nitrogen from soil, litter, and above-ground biomass are lost to the atmosphere via combustion. Studies of severe, stand-replacing fire have reported as much as 30% of above-ground carbon and over 70% of above-ground nitrogen lost to burning (Johnson et al. 2004; Meigs et al. 2009), and litter losses may be as high as 100% (Campbell et al. 2007). Soil loss estimates vary greatly, but research suggests that high severity burns average up to twice the soil carbon and nitrogen losses caused by moderate or low severity fires (Homann et al. 2011).

Following fire, several mechanisms combine to increase fluvial erosion, exporting even more carbon and nitrogen from burned catchments. The loss of vegetative cover

decreases interception and evapotranspiration, making more precipitation available for runoff (Anderson et al. 1976). Simultaneously, the loss of organic material, the alteration of the soil structure, and in some cases, the presence of pyrogenic hydrophobic compounds in burned soils, have the combined effect of reducing soil infiltration rates and capacity (DeBano 2000). As well, the removal of canopy and litter cover exposes more bare soil and ash on the forest floor to erosion (DeBano et al. 1998). Finally, since most fires occur in the dry, early summer months in the western US, the intense late summer convective storms that follow can trigger massive debris flows and mass wasting events (Cannon 2001; Meyer & Wells 1997; Robichaud et al. 2007).

Post-fire debris flows are capable of exporting highly variable but sometimes very large amounts of sediment from catchments. In a study of 95 burned catchments, less than half of the sites generated debris flows (Cannon 2001), but data on observed post-fire debris flows at 34 sites suggest average and median erosion rates of 230,000 and 150,000 kg ha^{-1} (Gartner et al. 2004; Shakesby & Doerr 2006). Following severe wildfire in the Cascade Mountains, Baird et al. (1999) estimated losses to surface erosion at 280 kg C ha^{-1} and 14 kg N ha^{-1} in ponderosa pine and Douglas fir forest, and higher losses of 640 kg C and 22 kg N ha-1 in lodgepole pine and Engelmann spruce forest. However, estimates of the carbon and nitrogen mass moved by post-fire erosion are rare, in part because of the complications in separating volatilization losses from erosive losses, as well as a lack of pre-fire data.

It remains unclear how much eroded material is deposited and retained lower in the watershed, and whether carbon and nutrients in this sediment are sequestered or

continue to actively cycle in a new location (Figure A1). To fully quantify losses to erosion, catchment sediment budgets must account for both erosion rates and sediment yield, i.e. what is input to the stream versus what is exported from the watershed. It is clear that there are large disparities between these amounts; studies in the US indicate that total sediment yield is roughly 10 to 20% of estimated erosion rates (Stallard 1998; Trimble & Crosson 2000). The process of erosion may increase mineralization of soil organic carbon (Van Hemelryck et al. 2011), if the replacement of carbon on the hillslopes (Harden et al. 1999) combined with burial and sequestration at the deposition site (Gregorich et al. 1998) exceeds the erosional losses, then erosion may result in a net carbon sink (Berhe et al. 2007). Because the loss of soil organic matter may seriously limit post-fire vegetative regeneration at some sites (Neary et al. 1999), more research is needed into the quantity and possible implications of post-fire translocation and retention of carbon and nitrogen.

Assessing the potential importance of post-fire carbon and nitrogen fluxes to both terrestrial and aquatic ecosystems requires knowledge of background levels of particulate fluxes from unburned catchment ecosystems. Logistical difficulties in quantifying particulate organic matter (POM), together with approaches that focus on baseflow carbon and nitrogen cycling, have resulted in relatively few studies on POM export from undisturbed catchments. Catchment carbon and nitrogen budgets have often excluded particulates, assuming that the bulk of fluxes take place in the dissolved form (defined as less than either 0.45 or 0.7 microns). For example, in a survey of large river systems, Hope (1994) found that particulates comprise only 10% of fluvial total organic carbon

(TOC) on average. However, these samples were biased towards routine low flow or baseflow samples, and more recent work suggests that this ratio varies greatly among catchments and ecosystems (Horowitz 2008). In a recent review of published carbon flux data, annual particulate organic carbon export in seven montane catchments ranged widely, from 10 up to 79% of the TOC flux, averaging 39% (σ = 26%) (Alvarez-Cobelas et al. 2012; Kaushal & Lewis 2005; Rai & Sharma 1998). In systems driven by large monsoon events, particulate carbon and nitrogen have been observed to constitute 92 and 83% of total fluxes, respectively (Brooks et al. 2007). These studies indicate a need for more complete baseline data on POM fluxes, and a knowledge gap that further complicates efforts to contextualize disturbance-related fluxes of C and N.

Our understanding of catchment biogeochemical responses to wildfire is limited by a lack of information on how much C and N is translocated by episodic post-fire erosion and retained down gradient, and how these fluxes compare with baseline undisturbed particulate fluxes. To address these knowledge gaps, this study quantifies the fluvial export of particulate carbon and nitrogen from burned and unburned catchments within the Valles Caldera National Park in northern New Mexico's Jemez River Basin, following the 2011 Las Conchas wildfire. Specifically, we address two research questions: (1) how much carbon and nitrogen is eroded from burned slopes and re-deposited below in debris fans? and (2) how do these quantities compare to fluvial export of particulate carbon and nitrogen in streamwater from nearby unburned catchments?

Site Description

Valles Caldera National Preserve, New Mexico

The Valles Caldera National Preserve (VCNP; 106°33’23”W, 35°52’19”N) is located in the headwaters of the Jemez River Basin in the Jemez Mountains of north-central New Mexico, at the site of a caldera formed 1.13 Ma (Figure A2; (Goff & Gardner 1994). Elevations range from 2300 in the lower grasslands to 3432 m at the summit of the Redondo Peak resurgent dome. Parent material at the site is rhyolitic. The forested uplands are predominately well-drained, rocky, cryic sandy loams, while the grasslands are darker mollics with greater water-holding capacity and organic matter content (Rodriguez & Archer 2010).

The site is semi-arid and seasonally snow-covered. Precipitation and temperature vary with elevation. Mean annual temperatures are around 3°C, and a SNOTEL site 5 km from Redondo Peak averages approximately 750 mm annual precipitation at an elevation of 2794 m (NRCS 2013). Typically about half of annual precipitation falls as snow between October and April, and the remainder falls during the late summer monsoon rains (Bowen 1996). Annual peak snowmelt discharge for the Redondo Peak catchments typically occurs in the month of April.

At the highest elevations, the hillslopes of the resurgent domes are predominately forested with Engelmann spruce (*Picea engelmannii*) and corkbark fir (*Abies lasiocarpa var. arizonica*) (Muldavin et al. 2006; Muldavin & Tonne 2003). Between 2740 and 3040

m, mixed conifer species, such as Douglas fir (*Pseudotsuga menziesii*), white fir (*Abies concolor*) and blue spruce (*Picea pungens*), are interspersed with aspen stands (*Populus tremuloides*). Below 2740 m, the hillslopes are forested with ponderosa pine (*Pinus ponderosa*) and Gambel oak (*Quercus gambelii*). The valley bottoms of the caldera consist of Rocky Mountain upper and lower montane grasslands. Grassland vegetation includes C_3 plants such as Parry's oatgrass (*Danthonia parryi*), Kentucky bluegrass (*Poa pratensis*), and Arizona fescue (*Festuca arizonica*), as well as C_4 species such as mountain muhly (*Muhlenbergia montana*) and pine dropseed (*Blepharoneuron tricholepis*).

In the summer of 2011, the western side of the Preserve was burned by the Las Conchas Fire, the largest in New Mexico's recorded history at the time. It was caused by a tree falling on a power line on 26 June 2011 and burned a total of 634 km^2, 80 of which lie inside the VCNP, before full containment on August 2 (USDA Forest Service 2011). The burn severity within the VCNP was 27% high, 33% moderate, and 32% low (Figure A3). The US Geological Survey assessed the debris flow hazard for the fire area as very high, predicting increased erosion and sedimentation rates (Tillery et al. 2011).

Following the fire, intense monsoon rains caused large debris flows from burned slopes, depositing new material at alluvial fans along the piedmonts of the Cerro del Medio resurgent dome (Figure A4). At these sites, as in classic alluvial fans, sediment is fluvially eroded from the hillslopes over time and deposited where the break in slope causes the flowing water to decrease in energy and velocity. The resulting alluvium is often poorly sorted due to the rapid decrease in sediment-carrying capacity, although

finer material carried by sheetflow can be found along the fan edge (Blair & McPherson 1994). The older alluvium at the Cerro del Medio fans is well-vegetated with grasses, making areas covered in new sediment deposits easily identifiable.

Study catchments

This study focuses on five catchments in total: two burned catchments on Cerro del Medio and three unburned catchments on Redondo Peak (Figure A2; Figure A3). The study catchments vary in size from 1.322 km^2 to 3.729 km^2, with mean slopes between 13 to 16° (Table A1). The pre-fire or unburned vegetation at all sites consists mainly of spruce-fir mixed conifers at the upper elevations and ponderosa pine at the lower elevations (Muldavin et al. 2006).

The two burned catchments on the southwestern slopes of Cerro del Medio will be referred to as Debris Fan 1 (DF1) and Debris Fan 2 (DF2). In total, 81 and 97% of the catchment areas burned, respectively, and 25 and 39% burned at high severity (USDA Forest Service 2011). They both subsequently produced large debris flows that deposited on their respective alluvial fans in the valley bottom (Figure A3; Figure A4). The catchments face mainly southwest, with elevations ranging from about 2650 to 3000 m (Table A1).

The unburned Redondo Peak sites include three larger catchments – Upper Jaramillo, History Grove, and La Jara – that drain from different sides of the same resurgent dome, and therefore represent a variety of aspects. Perennial streamflow from

all three catchments drains to the East Fork of the Jemez River, fed year-round by hydrological connections with the hillslopes (Liu et al. 2008). Elevations are higher than the Rabbit Mountain and Cerro del Medio sites, ranging from roughly 2683 to 3435 m (Table A1).

Methods

Alluvial deposit field surveys

Systematic transect surveys of the post-fire alluvial deposition were conducted at the two Cerro del Medio debris fans in June 2012, ten months after the fire, following one monsoon and one snowmelt season during which sediment was eroded, deposited, and translocated again by multiple runoff events.

At the two debris fans, linear East-West transects were established every 100 m down the length of the fan using a surveyors tape, compass, and a handheld Garmin GPS unit (NAD 83 with accuracy of ± 3-5 m) to record transect anchors and endpoints, following methods similar to Murphy et al. (2006). For a detailed description of standard soil transect methods, see Patterson and Carter (2006). Observations of deposition type and amount were collected along each transect at regular 5 m intervals (Figure A5; Figure A6). First, the predominant type of alluvial deposition was determined by visual inspection and categorized as: fines, sand /gravel, cobble, ash, mixed litter/ash, litter, woody debris, erosion, or vegetation. A trowel was then used to dig to the underlying

grassland vegetation and the depth of the deposit was recorded to the nearest half centimeter. Length and diameter were measured for large woody debris to obtain volume, using a modification of methods from (Brown 1974). Length and width were also measured for any isolated piles of material separate from the larger depositional splays. The farthest extents of new deposition were recorded as waypoints on the GPS unit (Figure A6). At DF1, 5 transects were surveyed, with a total of 186 survey points recording deposit type and depth. At DF 2, 9 transects were surveyed, with a total of 251 survey points (Table A2).

Alluvial deposit sampling

Samples of the different alluvial types were taken in May and June of 2012. The May sampling locations were chosen using Light Detection and Ranging (LiDAR) imagery showing pre- and post-fire elevations to locate areas of post-fire deposition (Orem & Pelletier). In June, samples representing different deposit types were taken randomly when surveying the transects. A total of 23 samples and 33 samples were collected at DF1 and DF2 respectively, along with 8 and 13 samples from the Orem ZOB and Instrumented ZOB culverts (Table A2).

Cores of the deposits were collected following a modification of standard soil sampling methods, similar to the methods described by Brooks et al. (1996), Hart and Gunther (1989), and Distefano and Gholz (1986). Cores were collected using a 3 cm diameter metal cylinder and a trowel, and stored in Ziploc bags on ice for transport. A

small subsample was weighed and dried at 105°C for at least 48 hours to determine gravimetric water content and bulk density. The remainder was sieved through a 2 mm mesh screen, dried for 24 hours at 60°C, and ground in a ball mill. These samples then underwent elemental analysis with isotope ratio mass spectrometry (EA-IRMS) to determine bulk carbon and nitrogen content and stable isotopes.

Acid fumigation was conducted on a subset of the samples to drive off inorganic carbonates following the methods of Harris et al. (2001). Samples were weighed into tared silver capsules and moistened with de-ionized water. The open tins were placed in a polystyrene tray in a vacuum desiccator under a fume hood, along with an open container of hydrochloric acid (12N). Suction was drawn and the samples were left to fumigate for 4 hours. Prior to fumigation, the vacuum desiccator was cleaned with acetone to remove any sources of carbon contamination including silicone grease, to prevent distortion of the samples' isotopic signatures (Harris et al. 2001; Lorrain et al. 2003). After fumigation, the samples were removed and oven-dried at 60°C for 4 hours. The carbon and nitrogen contents for the fumigated samples were compared to results for the same samples without fumigation. It was determined that the inorganic carbon and nitrogen in the samples was negligible and the remainder of the samples did not undergo acid fumigation.

Samples were double-packed into tared silver (acid-fumigated) or tin (non-fumigated) capsules and weighed, then shipped in 96-well polystyrene trays to Idaho State University's Interdisciplinary Laboratory for Elemental and Isotopic Analysis (ILEIA) for EA-IRMS analysis (Harris et al. 2001; Nadelhoffer & Fry 1988). A

preliminary set of samples was analyzed to determine packing weights, which revealed that the more mineral categories of fines, sand/gravel, and cobble were consistently below the detection limit for the analysis; these categories were excluded from further EA-IRMS analysis. For the litter and ash samples, one blank was included per 30 samples, in the form of a capsule with no sample material inside for soils, and a capsule packed with clean combusted filter material for the suspended stream particulates. One duplicate per 10 samples was also included.

Samples were analyzed using ECS 4010 (Elemental Combustion System 4010) interfaced to a Delta V advantage mass spectrometer through the ConFlo IV system (ThermoScientific; http://www.thermoscientific.com). The elemental analysis is done by an evolutionary "flash combustion/chromatographic separation techniques". The furnace temperature was kept at 1000°C; while the reduction oven was 650°C. The gases generated from the combustion of the samples are carried in a helium stream into a GC column held at 60°C. The gases then get separated before being diluted in the ConFlo IV and passed to the mass spectrometer for analysis. Isotope ratios of $\delta^{13}C$ are reported as ‰ values relative to the VPDB scale; whereas $\delta^{15}N$ values are reported as ‰ values relative to air-N_2. Three in-house standards (ISU Peptone, Costech Acetanilide and DORM-3) which are directly calibrated against international standards (IAEA-N-1, IAEA-N-2, USGS-25, USGS-40, USGS-41, USGS-24, IAEA-600) were used to normalize the raw data and as a quality control. ISU Peptone and Costech Acetanilide are used to set up a two-point calibration line. A third standard (DORM-3) is used to monitor the accuracy of the data (ILEIA 2012).

Volumetric carbon and nitrogen concentrations were calculated using bulk density and the percent by weight determined by EA-IRMS analysis. Concentrations for the cobble, sand and gravel, and fines categories were calculated from the EA-IRMS detection limits, since the carbon and nitrogen contents were below detection. Woody debris concentrations were calculated using the surveyed dimensions along with mean literature values for carbon and nitrogen content of large woody debris in mixed conifer forests.

Alluvial deposit mapping

Mapping of the fan survey data was done in ESRI ArcGIS 9.3 using geographic coordinate system North American 1983, projected into NAD 1983 UTM Zone 13N (Transverse Mercator). Transect anchor points were imported as x-y GPS coordinates, connected with polylines, and survey data points were inserted at 5 m intervals along each transect. A polygon outline of each fan or culvert was created using the GPS waypoints marking the outer edges of the deposition, the surveyed transect depth data, and LiDAR data for the sites showing differenced pre- and post-fire elevations at the site (Orem & Pelletier). The polygon fan areas were calculated and recorded for later computations.

The areal percentage of each fan covered by different deposit types was calculated from the transect survey data. Any points along the transects where deposition was part of a larger contiguous splay were assigned a 5 m^2 area. At points where isolated

depositional piles or levees were observed, area was calculated using the dimensions measured in the field. Points where no deposition was observed were assigned zero coverage. The percentage of each transect covered by each type of material (fines, litter, etc.) was then calculated using the point observations and a total transect area. An estimate of the percentage of each fan covered by each type of deposit was calculated by averaging the transect coverages for each fan.

Calculation of total fan C and N content

Two methods were used to calculate total debris fan C and N content, providing a range of estimates for the total mass deposited. The first and simplest method used a mean depth for each deposit type at each debris fan, calculated from the transect points. This method assumes that sediment amount and type are randomly distributed and that the systematic sampling provides a reasonable estimate of mean and variability. Total carbon and nitrogen masses for each deposit type (m_d) at each fan were calculated using a mean volumetric carbon or nitrogen concentration for each deposit type (C_d), and the mean depth (d_d) and area (A_d) covered by that deposit type at that fan (Eqn. 1). These values were then summed for a total carbon or nitrogen mass for each fan (Eqn. 2).

$$m_d = C_d * d_d * A_d \qquad \text{Eqn. 1}$$

$$m_f = m_{ash} + m_{cobble} + m_{fines} + m_{litter} + m_{sand\ \&\ gravel} + m_{woody\ debris} \quad \text{Eqn. 2}$$

Standard error for this method was calculated using MATLAB (MathWorks Version R2011b) to perform delete-d jackknife subsampling (Efron & Tibshirani 1993; Wu 1986). A random subsample of size *d* was excluded from the *n* survey points over 10^6 iterations of the calculations described above. For the DF1 survey data, $n = 157$ and $d = 13$. For the DF2 survey data, $n = 174$ and $d = 14$.

The debris fan carbon and nitrogen contents were then calculated by a second method, using spatially interpolated depths and frequencies for different deposit types instead of mean values. A very simple method for predicting soil characteristics is to look for correlations with terrain, landscape position, and other spatial variables. This technique is strongest when the soil characteristics of interest are controlled by the flow of water, which is in turn controlled by the terrain (Gessler et al. 1995; Moore et al. 1993). Two basic spatial variables were compared with the transect survey data: distance downslope from the fan apex, and distance from the center of the splay.

The distance that each survey point lay from the fan apex was calculated using the point-distance tool in ArcToolbox (ESRI ArcGIS 9.3.1). A scaled distance from center value was also calculated for each survey point, using a center point assigned to each transect. For instance, if the alluvial deposits begin and end at the 20 and 80 m points on a transect, and the center point is at 40 m, then the scaled distance from center for the 60 m point is $(60 - 40) / (80 - 40) = 0.5$, i.e. the point is halfway from the center to the

edge of the deposits. These two spatial variables were then plotted against the deposit depth measurements and the frequency of deposit types. Any strong correlations were tested for significance.

Rasters of 10 m^2 cell size covering both fans were created using the Spatial Analyst Raster Calculator (ESRI ArcGIS 9.3.1) for the following variables: the Euclidian distance from the fan apex (D), the distance to the edge of the fan (X_{edge}), and the distance to a polyline marking the splay center (X_{center}). The center of the splay was drawn using the digital elevation model (DEM) data to create a "ridgeline" polyline shape, using methods similar to delineating a stream channel network, but with negative elevation values to reverse flow accumulation to the highest points. The scaled distance to the center (R) was then calculated for each cell via Eqn. 3.

$$R = \frac{X_{center}}{X_{center} + X_{edge}} \qquad \text{Eqn. 3}$$

The scaled distance to center, R, was used to predict the percent of cell area covered by each deposit type ($\phi_{deposit}$) and the depth of cobble, sand and gravel, and fines (d_{heavy}). D was used to predict the depth of litter and ash deposits (d_{light}). A single mean depth dimension was used for woody debris regardless of location on the fan. For each given deposit type, a mean carbon or nitrogen mass per area ($\gamma_{deposit}$) was calculated from the mean concentration (c) for each deposit type and the 10 m^2 cell area (A_{cell}; Eqn. 4). The product of this areal concentration γ, the depth d, and the fractional coverage ϕ

gives the mass for that deposit type in that cell (m_{cell}). Summing across deposit types and across cells then gives the total carbon or nitrogen mass for the entire fan (Eqn. 5).

$$\gamma_{deposit} = c_{deposit} A_{cell} \quad \text{Eqn. 4}$$

$$m_{cell} = \phi_{heavy}\gamma_{heavy}d_{heavy} + \phi_{ash}\gamma_{ash}d_{ash} + \ldots + \phi_{litter}\gamma_{litter}d_{litter} \quad \text{Eqn. 5}$$

Streamwater suspended sediment sampling

Continuous discharge monitoring and regular surface water sampling are conducted at the Redondo Peak catchments for the University of Arizona Critical Zone Observatory. Grab samples are collected weekly through the snowmelt season, biweekly through the summer months, and monthly through the winter. Daily samples during snowmelt and event samples during the monsoon are collected using an automated sampler (Teledyne Isco; http://www.isco.com/products/products1.asp?PL=201) at catchment outlets. For this research, the 0.7 μm glass fiber filters used to separate the dissolved from the particulate fractions were retained and analyzed for total suspended sediment, particulate carbon, and particulate nitrogen, following methods modified from Brooks et al. (2007) . Grab sample filters with sufficient sediment were retained for analysis, supplemented by Isco sample filters to better represent a range of seasons. In

total, 26 grab sample filters were analyzed at History Grove, 41 grab and 13 Isco sample filters were analyzed at Upper Jaramillo, and 24 grab and 23 Isco sample filters at La Jara (Table A2).

Samples were collected in clean, combusted (4 hours at 500°C) amber glass bottles, transported on ice, and analyzed within two days. The bottles were shaken before filtering through combusted (4 hours at 500°C) Whatman 0.7 μm glass fiber filters using vacuum pods. Between 50 to 250 mL were filtered for each sample, and the volume recorded to the nearest 50 mL. The filters were then stored frozen in plastic zipper bags until time of analysis, when they were thawed at 4°C overnight, dried for 24 hours at 60°C in combusted tared tin dishes, and weighed.

An average clean filter weight was determined using twenty clean, combusted filters that had been filtered with 100 mL of de-ionized water, frozen, thawed, and oven-dried according to the same protocol. The filters lost an average mass of 3.8 mg ($\sigma = 1.2$) during the filtering, freezing, and drying process, compared with unused combusted filters. The mass of the clean, thawed, dried filters ranged from 124.8 to 131.4 mg, and averaged 129.1 mg ($\sigma = 0.3$). This average clean filter mass was subtracted from the dried filter masses to calculate total suspended sediment (TSS). When filters with very low sample mass produced negative TSS values, they were classified as "below detection limit" and excluded from further analysis.

The oven-dried and weighed filters were sliced in half. One half was weighed to determine the exact percent by mass that each section represented. The other section was scraped with a clean steel spatula to obtain as much of the retained sediment as possible

while limiting the amount of glass fiber filter material for packing into the 5 x 9 mm capsules required for EA-IRMS analysis.

The resulting carbon and nitrogen percentages by weight were used to calculate the total carbon and nitrogen mass on the scraped filter half, which was assumed to represent half of the total filtrate material. Duplicates were included in order to compare results using different halves of the same filter. Finally, volumetric concentrations were calculated as the twice the total carbon and nitrogen mass on the filter half, divided by the entire volume of water filtered for that sample.

Streamwater particulate C and N flux calculations

Particulate carbon (PC) and particulate nitrogen (PN) flux rates describe the mass exported by streamflow over time, for example as grams per day or kilograms per year. Discharge data available in 15 minute intervals at the three Redondo Peak catchment flumes were used to calculate flux rates for each sample. Mean carbon and nitrogen concentrations at each site were tested for significant differences among subsets (JMP Version 10SAS Institute). Rising and falling discharge produced significantly different mean concentrations at La Jara and Upper Jaramillo for PC, and at La Jara for PN (unequal variance ANOVA or paired t-test with $P < 0.05$). When significantly different, these concentrations were used with discharge to calculate daily flux rates. Otherwise, a single mean value was used for the entire hydrograph (at History Grove for PC and at History Grove and Upper Jaramillo for PN). Finally, total annual flux rates with standard

error were calculated for each catchment by summing daily flux rates across the water year 2012 hydrograph.

Results

Spatial variability in alluvial deposits

Different types of alluvial deposit materials were found with varying frequency along different transects and at different positions within the fans. Fines, sand/gravel, and cobble occur most frequently in the center of the fan, while ash, mixed litter/ash, and litter are less frequent in the center and occur more often moving out toward the edges (Figure A7). Areal coverage by post-fire deposits of any type ranged from 52% to 87% of the total transect area (Table A3), and averaged about 70% coverage at both fans (Figure A8). Fines dominated at both sites, covering 37.1 and 27.6 percent of the DF1 and DF2 transects, respectively. Sand or gravel occurred frequently along the DF1 transects (26.9 percent coverage) but about half as frequently on DF2 (13.5 percent). Ash and litter deposits covered a far greater percentage of the DF2 transects than DF1, with ash at nearly 14.9 percent versus 1.1 percent, and litter at 8.2 percent versus 1.8 percent.

Depth of the post-fire deposits follows two clear patterns moving down the length of the fan and out from the center. The depth of litter and ash deposits increases moving down gradient, fitting a weak but significant power law relationship between depth and the distance from the fan apex ($R^2 = 0.27$, $P < 0.01$; Figure A9). The depth of the heavier

fractions – sand/gravel, cobble, and fines – is more strongly predicted by scaled distance from the center of the fan, decreasing in depth exponentially moving out toward the fan edges ($R^2 = 0.68$, $P < 0.01$; Figure A9). These relationships were used to spatially interpolate depth across the debris fans.

C and N content of alluvial deposits

On average, ash deposits had lower carbon and nitrogen contents than litter, with 1.89% C and 0.12% N for ash (w/w; SE = 22.4 and 18.9%), versus 9.65 % C and 0.43% N for litter (w/w; SE = 9.4 and 8.6%; Table A4). C:N ratios were higher for litter, averaging 22.8 (SE = 5%) versus 14.5 (SE = 12%) for ash (Table A4). Cobble, sand/gravel, and fines were below the EA-IRMS detection limit of 0.0001% C and 0.00002% N, and those limits were used for further calculations (Table A4). Woody debris C:N ratios were highest, based on literature value estimates of 0.1750 % C and 0.0002 % N (Harmon & Sexton 1996; Prescott et al. 1989).

The two methods used to calculate total C and N content in the alluvial fans provide different estimates (Table A5). Using the mean depth method, Debris Fan 1 contains 75,705 kg C (SE = 1841) and 977 kg N (SE = 59), while spatial interpolation yielded estimates of 155,090 kg C (SE = 5016) and 3720 kg N (SE = 200). For Debris Fan 2, the mean depth method results are 91,730 kg C (SE = 11,966) and 4122 kg N (SE = 346), while spatial interpolation results in 106,332 kg C (SE = 2493) and 2353 kg N (SE = 107) at Debris Fan 2 (Table A6).

Assuming that the spatial interpolation results are a more realistic description of the fans, the two fans contain similar amounts of carbon and nitrogen per unit of deposition area, with 0.95 and 1.01 kg C m^{-2} at DF1 and DF2 respectively, and 0.02 kg N m^{-2} at each fan. However, Debris Fan 1 contains about 40% more per unit of contributing catchment area: 1140 versus 804 kg C ha^{-1}, and 27 versus 18 kg N ha^{-1} (Table A6).

Particulate C and N fluxes in streamflow

The Redondo Peak catchment hydrographs follow the bimodal precipitation pattern at the site, with the highest flows during the snowmelt season, and event-specific peaks during the late summer monsoon (Figure A10). The mean annual discharge ($\pm \sigma$) in water year 2012 at the Redondo Peak catchments was $2.63*10^5 \pm 1.25*10^4$ L day^{-1} at History Grove, $2.32*10^5 \pm 9.80*10^3$ L day^{-1} at La Jara, and $3.70*10^5 \pm 4.29*10^4$ L day^{-1} at Upper Jaramillo. Discharge peaked at History Grove at $3.03*10^5$ L day^{-1} on March 26, at La Jara at $2.59*10^5$ L day^{-1} on April 1, and at Upper Jaramillo at $5.38*10^5$ L day^{-1} on April 4.

The coefficients of variation for the duplicate filter halves tended to be high, with mean values of 18.8% and 12.4%, for carbon and nitrogen respectively. There was no significant correlation between daily mean discharge and total suspended sediment, particulate carbon concentration, or particulate nitrogen concentration at any of the sites. Separate regressions calculated for different seasons, for high or low discharge, and for

rising or falling discharge also did not reveal any significant relationships between TSS and discharge at any of the three catchments.

Mean total suspended sediment concentrations at the La Jara catchment were significantly higher in winter ($\mu \pm \sigma$ = 72.1 ± 71.4 mg/L) than during snowmelt (19.8 ± 15.0 mg/L) and monsoon (10.0 ± 5.8 mg/L) (Tukey-Kramer HSD, $P<0.05$; Table A9). Similarly at History Grove, winter TSS (113.5 ± 88.1 mg/L) was significantly higher than post-peak snowmelt (13.7 ± 15.2 mg/L) or monsoon (36.7 ± 34.9 mg/L) (Tukey-Kramer HSD, $P<0.05$; Table A8). History Grove TSS was also significantly higher at low flows (45.3 ± 53.9 mg/L) compared with high (17.4 ± 9.5; paired t-test for unequal variance, $P<0.05$; Table A8). No significant differences in TSS concentrations were found at Upper Jaramillo among any of the data subsets.

The particulate carbon (PC) fraction of TSS was significantly higher during low flows at History Grove (14.9% ± 9.7%) versus high flows (4.6% ± 8.0%), as well as in summer (16.0% ± 9.7%) versus winter (6.1% ± 3.9%), and during rising discharge (17.5% ± 3.9%) versus falling (7.1% ± 11.1%; $P<0.05$; Table A8). Similarly at La Jara, the PC fraction was significantly higher in summer (15.6% ± 9.1%) than in winter (8.7% ± 9.3%; Table A9). However, at La Jara, PC fraction, PC concentration, and particulate nitrogen (PN) fraction were all significantly higher during falling discharge as opposed to rising (Table A9). No other significant differences were detected for PN (fraction or concentration) among subsets at any of the three sites. At Upper Jaramillo, the PC concentration was significantly higher during falling discharge (3.61 ± 0.67 mg/L) versus rising (0.88 ± 0.35 mg/L), but no other significant differences were detected (Table A10).

The mean (± σ) C:N ratios for all samples were 7.7 ± 5.6 at History Grove, 5.5 ± 2.3 at La Jara, and 6.1 ± 3.5 at Upper Jaramillo.

The estimated daily carbon and nitrogen fluxes from the three Redondo Peak catchments are highly variable over the hydrograph (Figure A11). Daily PC fluxes for water year 2012 averaged 2.2 ± 3.5 (μ ± σ), 1.2 ± 0.9, and 2.4 ± 1.3 kg C day^{-1}, while PN fluxes averaged 0.2 ± 0.2, 0.2 ± 0.1, and 0.4 ± 0.2 kg N day^{-1} respectively at History Grove, La Jara, and Upper Jaramillo. Per hectare of catchment area, this equates to total annual fluxes of 3.4, 1.4, and 2.5 kg C and 0.3, 0.2, and 0.4 kg N, respectively.

The ratio of carbon to nitrogen increases logarithmically with TSS at each site (Figure A13). The relationship is strongest at History Grove ($R^2 = 0.73$, $P<0.0001$) and Upper Jaramillo ($R^2 = 0.65$, $P<0.0005$), and weaker but still significant at La Jara ($R^2 = 0.20$, $P<0.05$).

The majority of particulate carbon and nitrogen flux in water year 2012 took place during snowmelt, which made up 58, 42, and 47% of POM flux at History Grove, La Jara, and Upper Jaramillo respectively. Another 25, 39, and 30% of POM flux occurred during the summer monsoon from the respective catchments, and the remaining 17, 20, and 23% of the annual flux took place in the winter.

Comparison of episodic and continuous fluxes

In total, 124 times more carbon and 21 times more nitrogen was deposited on the two post-fire debris fans than was exported in particulate form from all three unburned

Redondo Peak catchments combined in water year 2012. Per square meter of catchment area, the debris fan carbon is roughly 400 times greater than the total water year 2012 Redondo Peak fluxes, and the debris fan nitrogen is roughly 70 times greater. Total C:N ratios in the debris fan materials are about 7 times greater than the mean C:N ratios in the suspended particulate samples. The woody debris in the fans plays a large role in increasing the C:N ratios at the debris fans. However, the litter and ash deposition also has C:N ratios 3 to 4 times higher than was observed in Redondo Peak suspended particulates.

Discussion

Post-fire erosion can affect catchment biogeochemistry in a multitude of ways. Some studies suggest that erosion may lead to a net carbon sink (Berhe et al. 2007), or potentially a net carbon source (Van Hemelryck et al. 2011), depending on replenishment and sedimentation and burial processes downslope. Because carbon uptake in montane forests is potentially nitrogen-limited (Johnson 2006), the impact of wildfire on nitrogen cycling in forests and forest soils is of growing interest (Smithwick et al. 2005). Nitrogen inputs above 50 to 60 kg ha^{-1} yr^{-1} may lead to nitrate leaching from undisturbed forest soils (Gundersen et al. 2006). However, little research has been done into how post-fire erosion and translocation of organic material might affect unburned sites downslope and downstream. Our results suggest that the carbon deposited in post-fire debris flows following the Las Conchas fire is not large compared with either upslope or grassland soil

carbon pools. However, nitrogen loading to lower, wetter areas is more substantial, and may be an overlooked but important effect of wildfire-induced erosion and sedimentation.

Depositional patterns

Preferential deposition of finer ash and litter occurred along the margins and down gradient on the debris fans, while heavier fractions like sand/gravel and cobble dominate in the center. This is in keeping with the traditional sheetflow alluvial fan model described by Blair and McPherson (1994), where heavier materials are poorly sorted in the center of the fan, surrounded by finer materials along the edges. Similar patterns were described by Meyer and Wells (1997) in Yellowstone National Park following post-fire debris flows on small alluvial fans. Our work demonstrates how simple empirical relationships can be used to tease out spatial patterns for different size fractions, quantifying how litter and ash with higher carbon and nitrogen contents, and higher C:N ratios, become deeper and more prevalent down gradient. The potential catchment-scale biogeochemical implications of this fluvial sorting have rarely been examined in studies of debris flows and alluvial fans, but here we observe that organic-rich materials are translocated farther from their source to be deposited in and near riparian grasslands.

C and N content of depositional materials

Few studies have quantified the carbon and nitrogen content of translocated material following fire, and those that exist often focus on surface erosion from the perspective of hillslope losses (Baird et al. 1999). However, one study which quantified the material moved and retained elsewhere by fluvial erosion following the Gondola Basin fire in the Lake Tahoe basin estimated between 25 to 110 kg N ha^{-1} were translocated (Johnson et al. 2007). Per unit of contributing catchment area, this is on the order of the 14 to 91 kg N ha^{-1} estimated on the Cerro del Medio debris fans by Method A; the Method B results also fall within this range.

Deep channelization at the fan apex suggests that much of the coarser material in the debris flows may be eroded subsurface soils. The more carbon and nitrogen-rich litter deposits can easily be sourced to the forested hillslopes, as they are comprised of pine needles and small twigs that did not originate in the grasslands. The ash is of ambiguous origin, as it may represent either more completely combusted upslope forest litter, or more easily combusted grasses from the valley floor. In either case, the lower carbon and nitrogen contents, and lower C:N ratios, of the debris flow ash deposits versus litter are reflective of more complete combustion of the fuel source. A decrease in C:N is observed when organic material burns at temperatures between 200 and 500°C, where carbon will volatilize more completely than nitrogen; the longer the burning continues, the larger the decrease (Neary et al. 1999; Saito et al. 2007). Saito et al. (2007) observed a decrease in soil C:N of ~9 when burn temperatures reached 400°C; the difference between the mean C:N ratios of litter and ash samples in our results is ~5 (Figure A12).

Preliminary results from surface soil sampling at similar mixed conifer zero-order basin sites elsewhere in the VCNP indicate unburned soils with organic carbon contents of 3.1 ± 1.8 kg m^{-2} (Pers. Comm., K. Lohse 2012). This result suggests that the 800 to 1100 kg C per catchment hectare retained in the alluvial fan deposits is equivalent to roughly 3% of surface soil carbon from the contributing catchments. Although the deposition represents a small fraction of the hillslope carbon source, from the perspective of the grasslands where the organic matter has been deposited and retained, carbon and nitrogen loading is much more substantial, at ~10,000 kg C ha^{-1} and 200 kg N ha^{-1} of depositional area (Table A6). Atmospheric deposition of nitrogen occurs at the research site at a rate of roughly 2 to 4 kg N ha^{-1} (NADP Fenn et al. 2003; 2012). Per unit area, the nitrogen being retained in the fan therefore represents roughly 50 to 100 years' worth of atmospheric inputs.

Particulate C and N fluxes in streamflow

Baseline fluvial export of POM is a function of concentration multiplied by discharge. In water year 2012, discharge was below the historic average in the Jemez River basin; downstream of the Valles Caldera, the Jemez River USGS stream gage site reported mean annual discharge at 53% of average based on the past 58 years of record (USGS 2013). However, there is a lack of correlation between discharge and total suspended sediment concentrations, which suggests that loading in these streams is

limited by sediment supply rather than the kinetic energy of the stream water (Vansickle & Beschta 1983).

Low C:N ratios in stream particulates may point to more decomposed organic matter (Conen et al. 2008), or more algal material, indicators of autochthonous (in-stream) (Dodds et al. 2004). Conversely, higher C:N ratios may indicate terrestrial sources like soil or litter. At all three sites, C:N ratios are low when TSS is low, following a clear pattern that suggests that autochthonous sources dominate at these times, a pattern that is commonly observed in stream sediments (Gao et al. 2007; Meybeck 1982; Onstad et al. 2000; Zhang et al. 2009). The higher C:N ratios that characterize higher particulate concentrations likely indicate soil organic matter or terrestrial litter or detritus, suggesting a hydrologic connection with upland soils at those times.

The PN fluxes from the Redondo Peak catchments are lower than comparable observations of other undisturbed headwater systems. Lewis (2002) has summarized data from 19 such sites in the United States, and found mean annual PN fluxes of 2.62 ± 0.36 kg N ha^{-1}. Another study of montane headwater catchments in the US found annual PC fluxes of ~10 kg C ha^{-1} (Alvarez-Cobelas et al. 2012; Kaushal & Lewis 2005), and similar fluxes have also been reported in Himalayan headwaters (Rai & Sharma 1998). The predicted Redondo Peak catchment PC fluxes are several times smaller, at 1.4 to 3.4 kg C ha^{-1}. Compared to the post-fire debris flow material retained on the Cerro del Medio alluvial fans, the total annual particulate fluxes from all three Redondo streams represent roughly 400 times less carbon and 70 times less nitrogen in total. When the predominately autochthonous origin of the streamflow particulates is taken into account,

the difference in terrestrial carbon and nitrogen transport by the streamflow versus the post-fire episodic flux is even greater.

C and N loading to riparian grasslands and streams

Translocation of organic matter from the drier forested hillslopes down gradient to the lower and wetter valley grassland soils could potentially lead to faster nutrient cycling in a less moisture-limited system, since nitrification and soil respiration are controlled in part by moisture availability (Lundquist et al. 1999; Peters et al. 2011; Stark & Firestone 1995; Stielstra In review; Tipping et al. 1999). However, Valles Caldera grassland soils are not N-limited, but rather phosphorous (P) limited, so increased productivity and carbon uptake due solely to N-fertilization would not necessarily be expected (Van Horn et al. 2012). Although this study did not quantify the phosphorous content of the new depositional material, volcanic parent material as is found in at the site is typically rich in P (Jones et al. 1979).

Although the addition of charcoal to ponderosa pine forest soils has been shown to increase nitrification, the same study found that no such effect occurs in grassland soils which typically have higher nitrification rates to begin with (DeLuca et al. 2006). Excess nitrogen translocated to the valley grasslands therefore has the potential to leach into streams or groundwater, with possible ecological and public health implications (Carpenter et al. 1998). Nutrient enrichment in streams can adversely affect water quality through eutrophication, causing algal blooms that lead to oxygen depletion and mortality

in aquatic organisms (Galloway et al. 2003; Vitousek et al. 1997). Streams in the Valles Caldera have been shown to be N-limited (Van Horn et al. 2012), so N-loading to surface waters at the site has potential ecological implications such as acidification (Stoddard 1994).

Continued research into the response of the Valle grassland streams, soils, and vegetation below the debris fans will further elucidate how post-fire deposition is affecting biogeochemistry at the site. Recommended avenues for investigation include soil trace gas efflux monitoring to quantify mineralization rates in the alluvial deposition, soil water sampling to determine possible nitrate and ammonium leaching, and elemental analysis of the alluvial deposits for phosphorous, to quantify loading to the potentially P-limited grasslands.

Conclusions

To fully quantify the impact of fire on catchment carbon and nitrogen budgets and biogeochemistry, it is important to assess the potential effects of erosion and translocation. Episodic mass wasting events following the Las Conchas wildfire translocated hundreds of times more particulate carbon and tens of times more particulate nitrogen per unit catchment area than is exported annually by nearby unburned streams. The ~200 kg ha^{-2} of nitrogen per depositional area being retained in the fans represents roughly 50 to 100 years' worth of atmospheric inputs. Translocation of nitrogen-rich organic matter from the drier forested hillslopes to the wetter grassland soils in the Valle

Grande could potentially lead to faster nutrient cycling, as well as increased nitrogen-loading to N-limited aquatic systems.

References

Alvarez-Cobelas M, Angeler DG, Sanchez-Carrillo S, Almendros G (2012) A worldwide view of organic carbon export from catchments. Biogeochemistry 107(1-3): 275-293

Anderson HW, Hoover MD, Reinhart KG (1976) Forests and water: effects of forest management on floods, sedimentation, and water supply. In: U.S. Department of Agriculture FS (ed). Pacific Southwest Forest and Range Experiment Station, Berkeley, CA. p 115

Baird M, Zabowski D, Everett RL (1999) Wildfire effects on carbon and nitrogen in inland coniferous forests. Plant Soil 209(2): 233-243

Bales RC, Molotch NP, Painter TH, Dettinger MD, Rice R, Dozier J (2006) Mountain hydrology of the western United States. Water Resour. Res. 42(8):

Berhe AA, Harte J, Harden JW, Torn MS (2007) The significance of the erosion-induced terrestrial carbon sink. Bioscience 57(4): 337-346

Blair TC, McPherson JG (1994) ALLUVIAL FANS AND THEIR NATURAL DISTINCTION FROM RIVERS BASED ON MORPHOLOGY, HYDRAULIC PROCESSES, SEDIMENTARY PROCESSES, AND FACIES ASSEMBLAGES. Journal of Sedimentary Research Section a-Sedimentary Petrology and Processes 64(3): 450-489

Bowen BM (1996) Rainfall and climate variation over a sloping New Mexico plateau during the North American monsoon. Journal of Climate 9(12): 3432-3442

Brooks PD, Haas PA, Huth AK (2007) Seasonal variability in the concentration and flux of organic matter and inorganic nitrogen in a semiarid catchment, San Pedro River, Arizona. J. Geophys. Res.-Biogeosci. 112(G3):

Brooks PD, Williams MW, Schmidt SK (1996) Microbial activity under alpine snowpacks, Niwot Ridge, Colorado. Biogeochemistry 32(2): 93-113

Brown JK (1974) Handbook for inventorying downed woody material. Intermountain Forest and Range Experiment Station, Forest Service, U.S. Dept. of Agriculture, Ogden, Utah

Campbell J, Donato D, Azuma D, Law B (2007) Pyrogenic carbon emission from a large wildfire in Oregon, United States. Journal of Geophysical Research: Biogeosciences 112(G4): G04014

Cannon SH (2001) Debris-flow generation from recently burned watersheds. Environmental & Engineering Geoscience 7(4): 321-341

Carpenter SR, Caraco NF, Correll DL, Howarth RW, Sharpley AN, Smith VH (1998) Nonpoint pollution of surface waters with phosphorus and nitrogen. Ecol. Appl. 8(3): 559-568

Conen F, Zimmermann M, Leifeld J, Seth B, Alewell C (2008) Relative stability of soil carbon revealed by shifts in delta N-15 and C : N ratio. Biogeosciences 5(1): 123-128

DeBano LF (2000) The role of fire and soil heating on water repellency in wildland environments: a review. Journal of Hydrology 231: 195-206

DeBano LF, G. ND, F. FP (1998) Fire's effects on ecosystems. J. Wiley, New York

DeLuca TH, MacKenzie MD, Gundale MJ, Holben WE (2006) Wildfire-Produced Charcoal Directly Influences Nitrogen Cycling in Ponderosa Pine Forests. Soil Sci. Soc. Am. J. 70(2): 448-453

Distefano JF, Gholz HL (1986) A PROPOSED USE OF ION-EXCHANGE RESINS TO MEASURE NITROGEN MINERALIZATION AND NITRIFICATION IN INTACT SOIL CORES. Communications in Soil Science and Plant Analysis 17(9): 989-998

Dodds WK, Marti E, Tank JL, Pontius J, Hamilton SK, Grimm NB, Bowden WB, McDowell WH, Peterson BJ, Valett HM, Webster JR, Gregory S (2004) Carbon and nitrogen stoichiometry and nitrogen cycling rates in streams. Oecologia 140(3): 458-467

Efron B, Tibshirani R (1993) An introduction to the bootstrap. Chapman & Hall, New York

Environmental Systems Resource Institute (ESRI) (2009) ArcGIS v. 9.3.1. In., Redlands, California.

Fenn ME, Haeuber R, Tonnesen GS, Baron JS, Grossman-Clarke S, Hope D, Jaffe DA, Copeland S, Geiser L, Rueth HM, Sickman JO (2003) Nitrogen emissions, deposition, and monitoring in the western United States. Bioscience 53(4): 391-403

Galloway JN, Aber JD, Erisman JW, Seitzinger SP, Howarth RW, Cowling EB, Cosby BJ (2003) The nitrogen cascade. Bioscience 53(4): 341-356

Gao QZ, Tao Z, Yao GR, Ding J, Liu ZF, Liu KX (2007) Elemental and isotopic signatures of particulate organic carbon in the Zengjiang River, southern China. Hydrol. Process. 21(10): 1318-1327

Gartner JE, Bigio ER, Cannon SH (2004) Compilation of Post Wildfire Runoff-Event Data from the Western United States. In: US Department of the Interior UGS (ed).

Gessler PE, Moore ID, McKenzie NJ, Ryan PJ (1995) SOIL-LANDSCAPE MODELING AND SPATIAL PREDICTION OF SOIL ATTRIBUTES. International Journal of Geographical Information Systems 9(4): 421-432

Goff F, Gardner JN (1994) EVOLUTION OF A MINERALIZED GEOTHERMAL SYSTEM, VALLES CALDERA, NEW-MEXICO. Econ. Geol. Bull. Soc. Econ. Geol. 89(8): 1803-1832

Gregorich EG, Greer KJ, Anderson DW, Liang BC (1998) Carbon distribution and losses: erosion and deposition effects. Soil & Tillage Research 47(3-4): 291-302

Gundersen P, Schmidt IK, Raulund-Rasmussen K (2006) Leaching of nitrate from temperate forests – effects of air pollution and forest management. Environmental Reviews 14(1): 1-57

Harden JW, Sharpe JM, Parton WJ, Ojima DS, Fries TL, Huntington TG, Dabney SM (1999) Dynamic replacement and loss of soil carbon on eroding cropland. Glob. Biogeochem. Cycle 13(4): 885-901

Harmon ME, Sexton J (1996) Guidelines for Measurements of Woody Detritus in Forest Ecosystems. In. U.S. LTER Network Office, University of Washington, Seattle, WA. p 73

Harris D, Horwath WR, van Kessel C (2001) Acid fumigation of soils to remove carbonates prior to total organic carbon or carbon-13 isotopic analysis. Soil Science Society of America Journal 65(6): 1853-1856

Hart SC, Gunther AJ (1989) INSITU ESTIMATES OF ANNUAL NET NITROGEN MINERALIZATION AND NITRIFICATION IN A SUBARCTIC WATERSHED. Oecologia 80(2): 284-288

Homann PS, Bormann BT, Darbyshire RL, Morrissette BA (2011) Forest Soil Carbon and Nitrogen Losses Associated with Wildfire and Prescribed Fire. Soil Science Society of America Journal 75(5): 1926-1934

Hope D, Billett MF, Cresser MS (1994) A REVIEW OF THE EXPORT OF CARBON IN RIVER WATER - FLUXES AND PROCESSES. Environmental Pollution 84(3): 301-324

Horowitz AJ (2008) Determining annual suspended sediment and sediment-associated trace element and nutrient fluxes. Science of the Total Environment 400(1-3): 315-343

Interdisciplinary Laboratory for Elemental and Isotopic Analysis at Idaho State University (ILEIA) (2012) Elemental and Isotopic Analysis Methods and Standards. In.

Johnson D, Murphy JD, Walker RF, Glass DW, Miller WW (2007) Wildfire effects on forest carbon and nutrient budgets. Ecological Engineering 31(3): 183-192

Johnson DW (2006) Progressive N limitation in forests: Review and implications for long-term responses to elevated CO2. Ecology 87(1): 64-75

Johnson DW, Susfalk RB, Caldwell TG, Murphy JD, Miller WW, Walker RF (2004) Fire Effects on Carbon And Nitrogen Budgets in Forests. In: Wieder RK, Novák M & Vile M (eds) Biogeochemical Investigations of Terrestrial, Freshwater, and Wetland Ecosystems across the Globe. Springer Netherlands. p 263-275

Jones JP, Singh BB, Fosberg MA, Falen AL (1979) PHYSICAL, CHEMICAL, AND MINERALOGICAL CHARACTERISTICS OF SOILS FROM VOLCANIC ASH IN NORTHERN IDAHO .2. PHOSPHORUS SORPTION. Soil Science Society of America Journal 43(3): 547-552

Kaushal SS, Lewis WM (2005) Fate and transport of organic nitrogen in minimally disturbed montane streams of Colorado, USA. Biogeochemistry 74(3): 303-321

Krawchuk MA, Moritz MA, Parisien MA, Van Dorn J, Hayhoe K (2009) Global Pyrogeography: the Current and Future Distribution of Wildfire. PLoS One 4(4): 12

Lewis WM (2002) Yield of nitrogen from minimally disturbed watersheds of the United States. Biogeochemistry 57(1): 375-385

Littell JS, McKenzie D, Peterson DL, Westerling AL (2009) Climate and wildfire area burned in western U. S. ecoprovinces, 1916-2003. Ecol. Appl. 19(4): 1003-1021

Lohse KA (2012) Personal Communication. In: Condon KE (ed).

Lorrain A, Savoye N, Chauvaud L, Paulet YM, Naulet N (2003) Decarbonation and preservation method for the analysis of organic C and N contents and stable isotope ratios of low-carbonated suspended particulate material. Analytica Chimica Acta 491(2): 125-133

Lundquist EJ, Jackson LE, Scow KM (1999) Wet-dry cycles affect dissolved organic carbon in two California agricultural soils. Soil Biol. Biochem. 31(7): 1031-1038

Marlon JR, Bartlein PJ, Gavin DG, Long CJ, Anderson RS, Briles CE, Brown KJ, Colombaroli D, Hallett DJ, Power MJ, Scharf EA, Walsh MK (2012) Long-term perspective on wildfires in the western USA. Proceedings of the National Academy of Sciences 109(9): E535-E543

Mathworks (2011) MATLAB R2011b, version 7.13.0.564. In., Natick, MA.

McKelvey KS, Busse KK (1996) Twentieth-century fire patterns on forest service lands. In *Sierra Nevada Ecosystem Project, Final Report to Congress, Vol. II, Assessments and Scientific Basis for Management Options.* In: Service UF (ed). University of California, Centers for Water and Wildland Resources, Davis, CA. p 1119-1138

Meigs GW, Donato DC, Campbell JL, Martin JG, Law BE (2009) Forest Fire Impacts on Carbon Uptake, Storage, and Emission: The Role of Burn Severity in the Eastern Cascades, Oregon. Ecosystems 12(8): 1246-1267

Meybeck M (1982) CARBON, NITROGEN, AND PHOSPHORUS TRANSPORT BY WORLD RIVERS. American Journal of Science 282(4): 401-450

Meyer GA, Wells SG (1997) Fire-related sedimentation events on alluvial fans, Yellowstone National Park, USA. Journal of Sedimentary Research 67(5): 776-791

Miller JD, Safford HD, Crimmins M, Thode AE (2009) Quantitative Evidence for Increasing Forest Fire Severity in the Sierra Nevada and Southern Cascade Mountains, California and Nevada, USA. Ecosystems 12(1): 16-32

Moore ID, Gessler PE, Nielsen GA, Peterson GA (1993) SOIL ATTRIBUTE PREDICTION USING TERRAIN ANALYSIS. Soil Science Society of America Journal 57(2): 443-452

Muldavin E, Neville P, Jackson C, Neville T (2006) A Vegetation Map of Valles Caldera National Preserve New Mexico: Final Report for Cooperative Agreement No. 01CRAG0014. In., University of New Mexico, Albuquerque.

Muldavin E, Tonne P (2003) Vegetation Survey and Preliminary Ecological Assessment of Valles Caldera National Preserve, New Mexico. In: Service UF (ed). University of New Mexico, Albuquerque, NM. p 118

Murphy JD, Johnson DW, Miller WW, Walker RF, Carroll EF, Blank RR (2006) Wildfire Effects on Soil Nutrients and Leaching in a Tahoe Basin Watershed. J. Environ. Qual. 35(2): 479-489

Nadelhoffer KF, Fry B (1988) CONTROLS ON NATURAL N-15 AND C-13 ABUNDANCES IN FOREST SOIL ORGANIC-MATTER. Soil Science Society of America Journal 52(6): 1633-1640

National Atmospheric Deposition Program (NADP) (2012) 2011 Annual Summary. In: Sheppard L (ed). Illinois State Water Survey, University of Illinois at Urbana-Champaign, Champaign, Illinois.

National Interagency Fire Center (NIFC) (2013) Wildland fires and acres (1960-2012).

Natural Resources Conservation Service (NRCS) National Water and Climate Center (2013) Quemazon SNOTEL Site 708. In.

Neary DG, Klopatek CC, DeBano LF, Ffolliott PF (1999) Fire effects on belowground sustainability: a review and synthesis. Forest Ecology and Management 122(1-2): 51-71

Onstad GD, Canfield DE, Quay PD, Hedges JI (2000) Sources of particulate organic matter in rivers from the continental USA: Lignin phenol and stable carbon isotope compositions. Geochimica Et Cosmochimica Acta 64(20): 3539-3546

Orem C, Pelletier JD Unpublished LiDAR data. In.

Patterson GT, Carter MR (2006) Soil Sampling and Handling. In: Carter MR & Gregorich EG (eds) Soil Sampling and Methods of Analysis. Canadian Society of Soil Science.

Pechony O, Shindell DT (2010) Driving forces of global wildfires over the past millennium and the forthcoming century. Proceedings of the National Academy of Sciences:

Peters NE, Bohlke JK, Brooks PD, Burt TP, Gooseff MN, Hamilton DP, Mulholland PJ, Roulet NT, Turner JV (2011) Hydrology and Biogeochemistry Linkages. In: Wilderer P (ed) Treatise on Water Science. Oxford Academic Press, Oxford. p 271-304

Prescott CE, Corbin JP, Parkinson D (1989) INPUT, ACCUMULATION, AND RESIDENCE TIMES OF CARBON, NITROGEN, AND PHOSPHORUS IN 4 ROCKY-

MOUNTAIN CONIFEROUS FORESTS. Canadian Journal of Forest Research-Revue Canadienne De Recherche Forestiere 19(4): 489-498

Rai SC, Sharma E (1998) Comparative assessment of runoff characteristics under different land use patterns within a Himalayan watershed. Hydrol. Process. 12(13-14): 2235-2248

Robichaud P, Elliot W, Pierson F, Hall D, Moffet C (2007) Predicting postfire erosion and mitigation effectiveness with a web-based probabilistic erosion model. Catena 71(2): 229-241

Rodriguez M, Archer V (2010) Valles Caldera National Preserve: Soils Existing Condition Report In: Service VCTaUF (ed). Jemez Springs, NM.

Saito L, Miller WW, Johnson DW, Qualls RG, Provencher L, Carroll E, Szameitat P (2007) Fire effects on stable isotopes in a Sierran forested watershed. J. Environ. Qual. 36(1): 91-100

SAS Institute I JMP v. 10. In., Cary, NC.

Schimel D, Kittel TGF, Running S, Monson R, Turnipseed A, Anderson D (2002) Carbon sequestration studied in western U.S. mountains

Eos, Transactions American Geophysical Union Volume 83, Issue 40. Eos, Transactions American Geophysical Union 83(40): 445-449

Serreze MC, Clark MP, Armstrong RL, McGinnis DA, Pulwarty RS (1999) Characteristics of the western United States snowpack from snowpack telemetry (SNOTEL) data. Water Resour. Res. 35(7): 2145-2160

Shakesby RA, Doerr SH (2006) Wildfire as a hydrological and geomorphological agent. Earth-Science Reviews 74(3-4): 269-307

Smithwick EAH, Turner MG, Mack MC, Chapin FS (2005) Postfire soil N cycling in northern conifer forests affected by severe, stand-replacing wildfires. Ecosystems 8(2): 163-181

Stallard RF (1998) Terrestrial sedimentation and the carbon cycle: Coupling weathering and erosion to carbon burial. Glob. Biogeochem. Cycle 12(2): 231-257

Stark JM, Firestone MK (1995) MECHANISMS FOR SOIL-MOISTURE EFFECTS ON ACTIVITY OF NITRIFYING BACTERIA. Appl. Environ. Microbiol. 61(1): 218-221

Stielstra C (In review) QUANTIFYING THE ROLE OF HYDROLOGIC VARIABILITY IN CONTROLLING SOIL CARBON FLUX AT TWO SEMI-ARID MONTANE SITES.

Stoddard JL (1994) Long-term changes in watershed retention of nitrogen: its causes and aquatic consequences. In: Baker LA (ed) Environmental Chemistry of Lakes and Reservoirs. American Chemical Society, Washington, DC. p 223-284

Survey UG (2013) Water resources data for the United States, Water Year 2012: U.S. Geological Survey Water Data Report WDR-US-2012, site 08324000. In. vol 22 July 2013.

Teledyne Isco (2013) Automatic Water Samplers. In. vol 7/22/2013.

ThermoScientific (2013) ConFlo IV universal Continuous Flow interface. In. vol 7/22/2013.

Tillery AC, Darr MJ, Cannon SH, Michael JA (2011) Postwildfire Preliminary Debris Flow Hazard Assessment for the Area Burned by the 2011 Las Conchas Fire in North-Central New Mexico: U.S. Geological Survey Open-File Report 2011-1308. In. p 11

Tipping E, Woof C, Rigg E, Harrison AF, Ineson P, Taylor K, Benham D, Poskitt J, Rowland AP, Bol R, Harkness DD (1999) Climatic influences on the leaching of dissolved organic matter from upland UK Moorland soils, investigated by a field manipulation experiment. Environment International 25(1): 83-95

Trimble SW, Crosson P (2000) Land use - US soil erosion rates - Myth and reality. Science 289(5477): 248-250

USDA Forest Service (2011) Burned Area Emergency Response (BAER) Imagery Support Data Download. In. United States Forest Service.

Van Hemelryck H, Govers G, Van Oost K, Merckx R (2011) Evaluating the impact of soil redistribution on the in situ mineralization of soil organic carbon. Earth Surf. Process. Landf. 36(4): 427-438

Van Horn DJ, White CS, Martinez EA, Hernandez C, Merrill JP, Parmenter RR, Dahm CN (2012) Linkages Between Riparian Characteristics, Ungulate Grazing, and Geomorphology and Nutrient Cycling in Montane Grassland Streams. Rangeland Ecology & Management 65(5): 475-485

Vansickle J, Beschta RL (1983) SUPPLY-BASED MODELS OF SUSPENDED SEDIMENT TRANSPORT IN STREAMS. Water Resour. Res. 19(3): 768-778

Vitousek PM, Aber JD, Howarth RW, Likens GE, Matson PA, Schindler DW, Schlesinger WH, Tilman D (1997) Human alteration of the global nitrogen cycle: Sources and consequences. Ecol. Appl. 7(3): 737-750

Westerling AL, Bryant BP (2008) Climate change and wildfire in California. Clim. Change 87: S231-S249

Westerling AL, Hidalgo HG, Cayan DR, Swetnam TW (2006) Warming and earlier spring increase western US forest wildfire activity. Science 313(5789): 940-943

Wu CFJ (1986) JACKKNIFE, BOOTSTRAP AND OTHER RESAMPLING METHODS IN REGRESSION-ANALYSIS - DISCUSSION. Annals of Statistics 14(4): 1261-1295

Zhang S, Lu XX, Sun HQ, Han JT, Higgitt DL (2009) Geochemical characteristics and fluxes of organic carbon in a human-disturbed mountainous river (the Luodingjiang River) of the Zhujiang (Pearl River), China. Science of the Total Environment 407(2): 815-825

APPENDIX B: ALLUVIAL DEPOSITION RETAINED IN ZERO-ORDER BASIN (ZOB) CULVERTS

Site Descriptions

The four zero-order basin (ZOB) sites (named Instrumented, Orem, Gibbson, and Condon) are on the northeast side of Rabbit Mountain, along the caldera rim (Figure A2). The ZOBs all face mainly north and northwest, with elevations similar to Cerro del Medio ranging from 2650 to 3000 m (Table A1). They exhibit a range of burn extents and severity (Figure A3). The 100% of the Instrumented ZOB was burned, 74% of it at high severity. The Orem ZOB was nearly entirely burned as well, 44% of it at high severity. Both produced smaller-scale debris flows which deposited in culverts along NM Route 4 at the base of the slopes (Figure A3; Figure B1). The Condon and Gibbson ZOBs showed no sign of debris flow deposition at any time following the fire, despite burn extents of 88 and 70%, respectively, with 53 and 32% of their areas burned at high severity.

Methods

At each of the two debris-filled culverts, a single longitudinal transect was surveyed in 5-meter intervals following the same methods described for the two fans. GPS waypoints were recorded to outline the edges of the alluvial deposits (Figure B2). At the Instrumented ZOB culvert, 83 survey points were recorded. At the smaller Orem ZOB culvert, 40 survey points were recorded (Table A2).

The total volume of alluvial deposition retained in the culverts was calculated using the mapped culvert area, the depth of deposition at each point along the longitudinal transect, and the width of the deposition at each point. Since the alluvial deposition at these two sites is much smaller and more uniform than the debris fan deposition, mean bulk density and mean carbon and nitrogen contents were used to calculate total mass.

Results and Discussion

The alluvial deposition retained in the burned Orem ZOB culvert contains 283 kg of carbon and 15 kg of nitrogen. The Instrumented ZOB culvert is larger and retained 1572 kg of carbon and 81 kg of nitrogen. The culverts have similar loading per unit of depositional area, at ~44,200 and 51,800 kg C ha^{-1} and 2300 and 2700 kg N m^{-2}. Per unit of contributing catchment, however, the Instrumented ZOB retained about 7 times as much carbon and nitrogen: 119.9 versus 16.8 kg C $ha^{-1}$and 6.2 versus 0.9 kg N ha^{-1}.

Preliminary results from post-fire soil sampling in the burned Instrumented ZOB indicate that the surface (upper 5 cm) soil organic carbon content is in the range of 12,000 to 22,000 kg m^2 (Pers. Comm., K. Lohse 2012). Although the culverts are far more concentrated in carbon and nitrogen than the debris fan alluvial deposits, the carbon retained in total represents less than 0.1% of the carbon remaining in the burned catchment surface soils. The very high concentrations of carbon and nitrogen deposition

suggest that localized effects of catchment-scale post-fire translocation may be dramatic where changes in slope function as a sediment trap.

No alluvial deposition was observed at the culverts at the outlet of the Gibbson ZOB or the Condon ZOB. This failure to produce debris flows at their outlets suggests that any post-fire erosion was retained within the catchment. Cannon (2001) demonstrated that debris flow generation and characteristics are variable among catchments and controlled by drainage morphology, lithology, and water-repellency of the soils. Drainage morphology is notably different between the sites, with the debris-flow producing ZOBs having steeper slopes at the outlets.

Future Work

The Orem and Instrumented ZOB culverts have essentially served as sediment traps, providing us with an artificial zone of preferential deposition at the base of severely burned slopes. They are easily accessible and with a clear spatial delimitation, and in the future could potentially serve as a source of data on the cycling, uptake, and mineralization of carbon and nitrogen in partially burned and eroded litter and surface soils. Gas efflux measurements and re-sampling of carbon and nitrogen and stable isotopes may be a potential avenue of future investigation. Recent work by Stephan et al. (2012) has shown an increase in foliar N concentrations in re-vegetating understory following fire; a comparison of the foliar composition of grasses growing in the culvert deposition with other nearby vegetation might also be informative.

References

Cannon SH (2001) Debris-flow generation from recently burned watersheds. Environmental & Engineering Geoscience 7(4): 321-341

Lohse KA (2012) Personal Communication. In: Condon KE (ed).

Stephan K, Kavanagh KL, Koyama A (2012) Effects of spring prescribed burning and wildfires on watershed nitrogen dynamics of central Idaho headwater areas. Forest Ecology and Management 263(0): 240-252

APPENDIX C: STREAM PARTICULATE CARBON AND NITROGEN STABLE ISOTOPES

Introduction

The sources of suspended sediment in streams and rivers vary by catchment and ecosystem as well as on a seasonal and event-scale within the same catchment. Elemental and isotopic analysis can identify characteristics that help distinguish between sources. For instance, a lower carbon to nitrogen (C:N) ratio may indicate a greater percentage of algal organic matter, indicating a higher proportion of autochthonous (in-stream) sediment sources (Dodds et al. 2004).

Stable isotopes may also be used as tracers to identify sources of sediment. It is well-established that stable carbon isotopes can be used to differentiate plant species contributing to the organic matter in litter and soils (Deines 1980). Certain plant photosynthetic pathways fractionate stable carbon isotopes more than others. It is therefore possible to determine percentages of C_3 and C_4 plant biomass in a soil by measuring the ratio of ^{12}C to ^{13}C. Because C_3 plant biomass averages 26‰ VPDB (Vienna PeeDee Belemnite standard) and C_4 plant biomass averages 12‰ VPDB, a simple mixing model using a weighted average can determine the percent contribution from each. Algal carbon is also often enriched in $\delta^{13}C$ compared to C_3 terrestrial plants, offering a potential tracer that can help identify in-stream (autochthonous) materials (Smith & Epstein 1971).

Processes affecting the ratio of ^{14}N to ^{15}N in soil and plant matter are complex, because ecosystem nitrogen cycles through many different pathways. Microbially mediated processes favor the lighter ^{14}N; if the depleted end product is removed via plant

uptake, leaching, or gaseous losses, this leaves the soil comparatively enriched in ^{15}N (Nadelhoffer & Fry 1988; Sharp 2007).

Recently, it has been suggested that combustion at high temperatures may cause volatilization of lighter carbon and nitrogen isotopes, and a corresponding enrichment of the organic material left behind in partially burned soils (Saito et al. 2007). There is potential to use this knowledge to help trace the source of organic matter exported from a catchment by post-fire erosion.

Methods

Samples were collected in clean, combusted (4 hours at 500°C) amber glass bottles, transported on ice, and analyzed within two days. The bottles were shaken before filtering through combusted (4 hours at 500°C) Whatman 0.7 μm glass fiber filters using vacuum pods. Between 50 to 250 mL were filtered for each sample, and the volume recorded to the nearest 50 mL. The filters were then stored frozen in plastic zipper bags until time of analysis, when they were thawed at 4°C overnight, dried for 24 hours at 60°C in combusted tared tin dishes, and weighed.

An average clean filter weight was determined using twenty clean, combusted filters that had been filtered with 100 mL of de-ionized water, frozen, thawed, and oven-dried according to the same protocol. The filters lost an average mass of 3.8 mg ($\sigma = 1.2$) during the filtering, freezing, and drying process, compared with unused combusted filters. The mass of the clean, thawed, dried filters ranged from 124.8 to 131.4 mg, and

averaged 129.1 mg ($\sigma = 0.3$). This average clean filter mass was subtracted from the dried filter masses to calculate total suspended sediment (TSS). When filters with very low sample mass produced negative TSS values, they were classified as “below detection limit” and excluded from further analysis.

The oven-dried and weighed filters were sliced in half. One half was weighed to determine the exact percent by mass that each section represented. The other section was scraped with a clean steel spatula to obtain as much of the retained sediment as possible while limiting the amount of glass fiber filter material for packing into the 5 x 9 mm capsules required for EA-IRMS analysis.

Samples were analyzed using ECS 4010 (Elemental Combustion System 4010) interfaced to a Delta V advantage mass spectrometer through the ConFlo IV system (ThermoScientific; http://www.thermoscientific.com/). The elemental analysis is done by an evolutionary "flash combustion/chromatographic separation techniques". The furnace temperature was kept at 1000°C; while the reduction oven was 650°C. The gases generated from the combustion of the samples are carried in a helium stream into a GC column held at 60°C. The gases then get separated before being diluted in the ConFlo IV and passed to the mass spectrometer for analysis. Isotope ratios of $\delta^{13}C$ are reported as ‰ values relative to the VPDB scale; whereas $\delta^{15}N$ values are reported as ‰ values relative to air-N_2. Three in-house standards (ISU Peptone, Costech Acetanilide and DORM-3) which are directly calibrated against international standards (IAEA-N-1, IAEA-N-2, USGS-25, USGS-40, USGS-41, USGS-24, IAEA-600) were used to normalize the raw data and as a quality control. ISU Peptone and Costech Acetanilide are used to set up a

two-point calibration line. A third standard (DORM-3) is used to monitor the accuracy of the data (ILEIA 2012).

Results and Discussion

The coefficients of variation for the duplicate filter halves tended to be high, with mean values of 18.8%, 12.4%, -0.2%, and 22.9% for bulk carbon, bulk nitrogen, $\delta^{13}C$, and $\delta^{15}N$, respectively. Relationships between stable isotopic signatures and TSS or C:N were generally weak and not significant, with the exception of $\delta^{13}C$ at History Grove, which decreases logarithmically as the C:N ratio increases (Figure C1). This likely indicates a stronger algal signature (i.e. less negative $\delta^{13}C$ values) when C:N is high. Since $\delta^{13}C$ at La Jara did differ significantly across seasons or between high and low flows in this data (Table A8), more targeted sampling and analysis is needed to further analyze this trend.

References

Deines P (1980) The isotopic composition of reduced organic carbon. In: Fritz P & Fontes JC (eds) Handbook of Environmental Isotopic Geochemistry. Elsevier, Amsterdam. p 329-406

Dodds WK, Marti E, Tank JL, Pontius J, Hamilton SK, Grimm NB, Bowden WB, McDowell WH, Peterson BJ, Valett HM, Webster JR, Gregory S (2004) Carbon and nitrogen stoichiometry and nitrogen cycling rates in streams. Oecologia 140(3): 458-467

Interdisciplinary Laboratory for Elemental and Isotopic Analysis at Idaho State University (ILEIA) (2012) Elemental and Isotopic Analysis Methods and Standards. In.

Nadelhoffer KF, Fry B (1988) CONTROLS ON NATURAL N-15 AND C-13 ABUNDANCES IN FOREST SOIL ORGANIC-MATTER. Soil Science Society of America Journal 52(6): 1633-1640

Saito L, Miller WW, Johnson DW, Qualls RG, Provencher L, Carroll E, Szameitat P (2007) Fire effects on stable isotopes in a Sierran forested watershed. J. Environ. Qual. 36(1): 91-100

Sharp Z (2007) Principles of Stable Isotope Geochemistry. Pearson Prentice Hall, Upper Saddle River, NJ

Smith BN, Epstein S (1971) Two Categories of 13C/12C Ratios for Higher Plants. Plant Physiology 47(3): 380-384

ThermoScientific (2013) ConFlo IV universal Continuous Flow interface. In. vol 7/22/2013.

APPENDIX D: IN-SITU SOIL CORE CARBON AND NITROGEN AND STABLE ISOTOPES

Methods

Soil profile cores were collected at DF1, DF2, the Orem and Instrumented ZOB culverts, and at a third Rabbit Mountain site (Condon ZOB) which showed no new post-fire alluvial deposition in its culvert (Table A2). Soil profile cores were obtained March 2012 using an Environmentalist Sub-soil Sampler. A total of 13 cores were taken, ranging in length from 20 to 80 cm. They were transported on ice, laid horizontally to reduce compaction of the core, and frozen in order to better retain their shape when cut open. During subsampling, the frozen soil core tubes were sliced in half lengthwise, photographed and described, and then divided into 10 cm layers. One half of each layer was set aside to be archived. The remaining samples were weighed, sieved, dried, and ground according to the same protocols as the alluvial samples, and processed for EA-IRMS analysis.

Samples were analyzed using ECS 4010 (Elemental Combustion System 4010) interfaced to a Delta V advantage mass spectrometer through the ConFlo IV system (ThermoScientific; http://www.thermoscientific.com/). The elemental analysis is done by an evolutionary "flash combustion/chromatographic separation techniques". The furnace temperature was kept at 1000°C; while the reduction oven was 650°C. The gases generated from the combustion of the samples are carried in a helium stream into a GC column held at 60°C. The gases then get separated before being diluted in the ConFlo IV and passed to the mass spectrometer for analysis. Isotope ratios of $\delta^{13}C$ are reported as ‰ values relative to the VPDB scale; whereas $\delta^{15}N$ values are reported as ‰ values relative to air-N_2. Three in-house standards (ISU Peptone, Costech Acetanilide and DORM-3)

which are directly calibrated against international standards (IAEA-N-1, IAEA-N-2, USGS-25, USGS-40, USGS-41, USGS-24, IAEA-600) were used to normalize the raw data and as a quality control. ISU Peptone and Costech Acetanilide are used to set up a two-point calibration line. A third standard (DORM-3) is used to monitor the accuracy of the data (ILEIA 2012).

Results and Discussion

No consistent changes in isotopic signature with depth along the soil profile were seen; however, sampling at a finer resolution and deeper into the soil profile might reveal a clearer pattern in future research. More thorough sampling of the debris fan alluvium using these techniques could provide insight in the future as to the carbon contents buried at depth in the fans. However, this preliminary sampling indicates that deeper layers (>20cm) were below the detection limit of the EA-IRMS analysis (0.0001% C and 0.00002% N, w/w).

References

Interdisciplinary Laboratory for Elemental and Isotopic Analysis at Idaho State University (ILEIA) (2012) Elemental and Isotopic Analysis Methods and Standards. In.

ThermoScientific (2013) ConFlo IV universal Continuous Flow interface. In. vol 7/22/2013.

APPENDIX E: ALLUVIAL DEPOSIT STABLE ISOTOPES

Methods

Cores of the alluvial deposits were collected following a modification of standard soil sampling methods, similar to the methods described by Brooks et al. (1996), Hart and Gunther (1989), and Distefano and Gholz (1986). Cores were collected using a 3 cm diameter metal cylinder and a trowel, and stored in Ziploc bags on ice for transport. A small subsample was weighed and dried at 105°C for at least 48 hours to determine gravimetric water content and bulk density. The remainder was sieved through a 2 mm mesh screen, dried for 24 hours at 60°C, and ground in a ball mill. These samples then underwent elemental analysis with isotope ratio mass spectrometry (EA-IRMS) to determine bulk carbon and nitrogen content and stable isotopes.

Samples were analyzed using ECS 4010 (Elemental Combustion System 4010) interfaced to a Delta V advantage mass spectrometer through the ConFlo IV system (ThermoScientific; http://www.thermoscientific.com/). The elemental analysis is done by an evolutionary "flash combustion/chromatographic separation techniques". The furnace temperature was kept at 1000°C; while the reduction oven was 650°C. The gases generated from the combustion of the samples are carried in a helium stream into a GC column held at 60°C. The gases then get separated before being diluted in the ConFlo IV and passed to the mass spectrometer for analysis. Isotope ratios of $\delta^{13}C$ are reported as ‰ values relative to the VPDB scale; whereas $\delta^{15}N$ values are reported as ‰ values relative to air-N_2. Three in-house standards (ISU Peptone, Costech Acetanilide and DORM-3) which are directly calibrated against international standards (IAEA-N-1, IAEA-N-2, USGS-25, USGS-40, USGS-41, USGS-24, IAEA-600) were used to normalize the raw

data and as a quality control. ISU Peptone and Costech Acetanilide are used to set up a two-point calibration line. A third standard (DORM-3) is used to monitor the accuracy of the data (ILEIA 2012).

Results and Discussion

The burned litter and ash are not enriched in ^{15}N or ^{13}C compared to the unburned soil core samples, as would be expected if the lighter isotopes had preferentially volatilized during the fire. The ash is also not more enriched in ^{15}N compared to the burned litter. On the contrary, the burned litter samples are the most depleted in ^{15}N (mean $\delta^{15}N = 2.13‰$), the ash is somewhat less depleted (mean $\delta^{15}N = 3.68‰$), and the unburned soil profile is the most enriched (mean $\delta^{15}N = 4.75‰$). This may be due in part to a larger percentage of fresh litter in the burned soil material, which presumably originated from the organic horizon on the forested slopes. Older, more decomposed soils are generally observed to be more enriched in ^{15}N (Dawson et al. 2002; Dijkstra et al. 2006). Although this enrichment with depth was not observed within the soil profile, we may be seeing a similar effect looking at the burned litter versus the deeper undisturbed soils.

Another possible interpretation of the data is that the ash and the burned litter deposits originate from different plant biomass sources. Because grass combusts more quickly and completely than woody plants, we might expect the ash to consist of predominantly burned grasses. However, although the ash $\delta^{13}C$ values are significantly less negative than the burned soil, it is only by a very small margin (0.8‰). The mean ash $\delta^{13}C$ value of -24.59‰ does not suggest a C_4 signature in the ash; C_4 grasses also occur

infrequently at this site (Muldavin et al. 2006). These data were not utilized further in this study, but may hopefully serve as a launching point for others in the future; see Appendix F for all supplementary data tables.

References

Brooks PD, Williams MW, Schmidt SK (1996) Microbial activity under alpine snowpacks, Niwot Ridge, Colorado. Biogeochemistry 32(2): 93-113

Dawson TE, Mambelli S, Plamboeck AH, Templer PH, Tu KP (2002) Stable isotopes in plant ecology. Annual Review of Ecology and Systematics 33: 507-559

Dijkstra P, Ishizu A, Doucett R, Hart SC, Schwartz E, Menyailo OV, Hungate BA (2006) C-13 and N-15 natural abundance of the soil microbial biomass. Soil Biol. Biochem. 38(11): 3257-3266

Distefano JF, Gholz HL (1986) A PROPOSED USE OF ION-EXCHANGE RESINS TO MEASURE NITROGEN MINERALIZATION AND NITRIFICATION IN INTACT SOIL CORES. Communications in Soil Science and Plant Analysis 17(9): 989-998

Hart SC, Gunther AJ (1989) INSITU ESTIMATES OF ANNUAL NET NITROGEN MINERALIZATION AND NITRIFICATION IN A SUBARCTIC WATERSHED. Oecologia 80(2): 284-288

Interdisciplinary Laboratory for Elemental and Isotopic Analysis at Idaho State University (ILEIA) (2012) Elemental and Isotopic Analysis Methods and Standards. In.

Muldavin E, Neville P, Jackson C, Neville T (2006) A Vegetation Map of Valles Caldera National Preserve New Mexico: Final Report for Cooperative Agreement No. 01CRAG0014. In., University of New Mexico, Albuquerque.

ThermoScientific (2013) ConFlo IV universal Continuous Flow interface. In. vol 7/22/2013.

APPENDIX F: SUPPLEMENTAL DATA

Summary

The following data are included as supplemental tables at the end of this document, in the hopes that they may assist in future Critical Zone Observatory research at these sites. Table F1 provides the results of the Elemental Analysis with Isotopic Ratio Mass Spectrometry, performed by the ILEIA Lab at Idaho State University. Table F2 provides the results of the glass-fiber filter particulate carbon and nitrogen concentrations for the Redondo Peak catchments, also analyzed at the same laboratory.

APPENDIX F: TABLES

LIST OF TABLES

Table A1. Summary of catchment characteristics for all sites. Where relevant, mean values ± standard deviation are above in normal typeface and ranges are below in italics.

	Site	Area (km^2)	Elevation (m)	Mean slope (°)	Aspect (°)	Area Burned (%)	
						High Severity	Total
Burned	Debris Fan 2	1.322	2802 ± 87 *2652-2985*	15 ± 8 *0-43*	191 ± 70 SW	25.2	80.7
	Debris Fan 1	1.361	2858 ± 83 *2668-3014*	14 ± 7 *0-38*	207 ± 70 SSW	39.1	96.5
Unburned	History Grove	2.434	2947 ± 98 *2683-3303*	13 ± 6 *0-41*	119 ± 60 ESE	0.0	0.0
	Upper Jaramillo	3.100	2917 ± 101 *2720-3311*	13 ± 8 *0-45*	222 ± 134 NNW	0.0	0.0
	La Jara	3.729	3107 ± 156 *2706-3435*	16 ± 8 *0-43*	111 ± 68 ENE	0.0	0.0

Table A2. Data collected and samples analyzed at burned and unburned sites in May and June 2012. EA-IRMS indicates elemental analysis with isotope ratio mass spectrometry. GFF TSS indicates streamwater total suspended sediment on glass fiber filters. * indicates that this sample type was not applicable at this site.

Site	Deposit Type and Depth	Alluvial Deposit Bulk Density	Alluvial Deposit EA-IRMS	GFF TSS	GFF EA-IRMS
Debris Fan 2	251	23	13	*	*
Debris Fan 1	186	33	5	*	*
History Grove	*	*	*	26	15
Upper Jaramillo	*	*	*	54	14
La Jara	*	*	*	47	26
Grand Total	**437**	**56**	**18**	**127**	**55**

Table A3. Percent of transect areas covered by each type of alluvial material at Debris Fan 1 and Debris Fan 2. ● indicates that no such deposits were observed along this transect. Totals indicate percent of transect area covered by any type of new deposition.

	Transect	**Ash**	**Cobble**	**Fines**	**Litter**	**Sand & Gravel**	**Woody Debris**	***Total***
Debris Fan 1	1	5.3	●	63.5	9.4	●	●	*78.1*
	2	●	●	10.7	0.2	64.3	●	*75.2*
	3	●	●	61.9	●	●	●	*61.9*
	4	●	2.9	28.8	0.2	20	11.5	*63.3*
	5	●	3.7	20.6	3.3	50	1.9	*79.4*
Debris Fan 2	1	●	●	33.3	33.3	●	●	*66.7*
	2	60	●	●	1.1	●	●	*61.1*
	3	16	7.9	13.2	0.1	15.8	2.6	*55.6*
	4	40	●	20	●	26.7	●	*86.7*
	5	4.2	16.7	12.5	21.2	20.8	●	*75.4*
	6	●	●	52.9	3.6	14.7	●	*71.2*
	7	●	●	42.9	10	7.1	7.1	*67.1*
	8	●	5.7	57.1	3.1	20	●	*85.9*
	9	16.7	●	16.7	2.3	16.7	●	*52.3*

Table A4. Mean carbon and nitrogen content (% mass) with standard deviation and percent standard error for debris fan samples.

	Ash	**Litter & ash**	**Litter**	**Woody debris**	**Cobble**	**Fines**	**Sand & gravel**
N	7	5	7	*	**	**	**
Carbon (w/w, %)	1.894	7.854	9.649	0.175	0.0001	0.0001	0.0001
Std Dev	*1.123*	*2.4551*	*2.400*				
Std Error	*22.40%*	*14.00%*	*9.40%*				
Nitrogen (w/w, %)	0.1207	0.3720	0.4329	0.0002	0.00002	0.00002	0.00002
Std Dev	*0.0603*	*0.1117*	*0.0990*				
Std Error	*18.90%*	*13.40%*	*8.60%*				
C:N Ratio	14.48	21.12	22.76	875	5	5	5
Std Dev	*4.45*	*3.15*	*3.02*				
Std Error	*11.61%*	*6.67%*	*5.41%*				

*Literature values (Harmon & Sexton 1996; Prescott et al. 1989)

**Below detection limit

Table A5. Area covered by different deposit types and volumetric content of carbon and nitrogen, on Debris Fan 1 and Debris Fan 2, according to Method A using mean depths. Standard error margins calculated using a delete-d jackknife subsampling approach are included for the Total C and N mass of the fans.

Deposit Type	Fraction of fan	Area (m^2)	Mean depth (m)	Mean C content (g/cm^3)	Mean N content (g/cm^3)
Ash	0.0105	1,214	0.0700	0.02743	0.00175
Cobble	0.0131	1,514	0.0700	0.00010	0.00002
Fines	0.3709	42,791	0.0463	0.00010	0.00002
Litter	0.0177	2,047	0.0711	0.07179	0.00317
Litter & ash	0.0082	947	0.0800	0.05444	0.00259
Sand & gravel	0.2686	30,986	0.0944	0.00010	0.00002
Woody debris	0.0267	3,075	0.1083	0.17500	0.00021
FAN 1 TOTALS	**0.7157**	**82,575**			
Ash	0.1491	15,669	0.0611	0.02743	0.00175
Cobble	0.0336	3535	0.1129	0.00010	0.00002
Fines	0.2762	29,026	0.0478	0.00010	0.00002
Litter	0.0817	8585	0.0848	0.07179	0.00317
Litter & ash	0.0041	433	0.0610	0.05444	0.00259
Sand & gravel	0.1353	14221	0.0752	0.00010	0.00002
Woody debris	0.0109	1143	0.0575	0.17500	0.00021
FAN 2 TOTALS	**0.6910**	**72,612**			

Table A6. Estimated carbon and nitrogen mass in post-fire deposition retained in debris fans. Masses are presented in total kilograms, per hectare of catchment area, and per hectare of depositional area, ± standard error margins. Method A uses mean depths for different types of deposition, and Method B spatial interpolates depth and deposit type based on position on the fan.

		Carbon		
Debris Fan	Method	*kg*	*kg/ha catchment*	*kg/ha depositional area*
1	A	75,705 ± 1841	556 ± 14	4642 ± 113
	B	155,090 ± 5016	1140 ± 37	9509 ± 308
2	A	91,730 ± 11,966	694 ± 91	8744 ± 1141
	B	106,332 ± 2493	804 ± 19	10,137 ± 238
		Nitrogen		
Debris Fan	Method	*kg*	*kg/ha catchment*	*kg/ha depositional area*
1	A	977 ± 59	14 ± 7	60 ± 4
	B	3720 ± 200	27 ± 1	228 ± 12
2	A	4122 ± 346	91 ± 31	393 ± 33
	B	2353 ± 107	18 ± 1	224 ± 10

Table A7. Mean ± standard deviation of daily discharge at Redondo Peak catchments in water year 2012 (Q, in 10^3 L/day), with observed suspended sediment data, including total suspended sediment (TSS, in mg/L), particulate carbon concentration (PC, in mg/L), particulate nitrogen concentration (PN, in mg/L), particulate C:N ratio, particulate carbon flux (PC, in g/day), and particulate nitrogen flux (PN, in g/day).

	History Grove	**La Jara**	**Upper Jaramillo**
Q (10^3 L/d)	263 ± 13	232 ± 10	370 ± 43
TSS (mg/L)	39.0 ± 47.2	22.5 ± 26.3	31.7 ± 32.4
PC (mg/L)	5.0 ± 8.0	1.7 ± 1.6	3.1 ± 2.9
PN (mg/L)	0.4 ± 0.4	0.3 ± 0.1	0.4 ± 0.3
C:N	7.7 ± 5.6	5.5 ± 2.3	6.1 ± 3.5
PC (g/day)	1755 ± 2331	1845 ± 2394	4542 ± 5570
PN (g/day)	206 ± 238	316 ± 276	646 ± 503

Table A8. History Grove mean ± standard deviation for particulate carbon and particulate nitrogen (as mg/L and as fraction of total suspended sediment), C:N ratio, suspended sediment $\delta^{13}C$ (‰ VPDB), and suspended sediment $\delta^{15}N$ (‰ air). The number of observations, given in parentheses, is the same for each constituent in subsequent columns until otherwise indicated. Bolded values indicate statistically significant differences between categories ($P < 0.05$; unequal variance ANOVA or paired t-test).

	TSS (mg/L)	**PC (mg/L)**	**PC (% of TSS)**	**PN (mg/L)**	**PN (% of TSS)**	**C:N**	**$\delta^{13}C$ (VPDB ‰)**	**$\delta^{15}N$ (air ‰)**
Winter Baseflow	**113.5 ± 88.1 (3)**	15.14 ± 20.71 (2)	10.9 ± 9.4	0.94 ± 0.93	1.7 ± 1.0	10.22 ± 11.98	-26.39 ± 0.46	4.74 ± NA (1)
Pre-peak Snowmelt	**37.1 ± 16.2 (4)**	5.01 ± 3.39 (2)	10.6 ± 3.1	0.52 ± 0.24	1.1 ± 0.1	9.20 ± 2.21	-26.26 ± 0.37	4.28 ± 1.02 (2)
Post-peak Snowmelt	**13.7 ± 15.2 (8)**	0.81 ± 0.64 (5)	5.5 ± 2.7	0.22 ± 0.03	1.8 ± 0.9	3.40 ± 2.13	-26.13 ± 0.18	3.06 ± 2.38 (2)
All Snowmelt	**21.5 ± 15.3 (12)**	2.01 ± 2.53 (7)	7.0 ± 3.6	0.31 ± 0.18	1.6 ± 0.8	5.06 ± 3.44	-26.17 ± 0.22	3.67 ± 1.65 (4)
Monsoon	**36.7 ± 34.9 (6)**	5.23 ± 4.67 (5)	18.9 ± 11.1	0.43 ± 0.23	2.0 ± 1.1	10.40 ± 4.75	-26.28 ± 0.39	1.33 ± 2.84 (5)
High Flows	**17.4 ± 9.5 (4)**	1.12 ± 0.59 (3)	**4.6 ± 8.0**	0.24 ± 0.05	1.4 ± 1.1	**3.82 ± 1.29**	**-26.06 ± 0.16**	5.00 ± 3.54 (1)
Low Flows	**45.3 ± 53.9 (15)**	6.58 ± 8.82 (9)	**14.9 ± 9.7**	0.50 ± 0.42	1.9 ± 0.8	**9.31 ± 6.23**	**-26.29 ± 0.29**	2.19 ± 2.29 (8)
Summer	42.3 ± 53.4 (10)	7.29 ± 9.93 (8)	**16.0 ± 9.7**	0.53 ± 0.47	2.0 ± 1.1	**9.97 ± 5.81**	-26.28 ± 0.37	2.30 ± 2.85 (7)
Winter	36.0 ± 43.1 (11)	2.03 ± 2.77 (6)	**6.1 ± 3.9**	0.32 ± 0.19	1.5 ± 0.5	**4.68 ± 3.76**	-26.19 ± 0.21	3.31 ± 1.82 (3)
Rising Discharge	37.4 ± 50.7 (9)	7.34 ± 4.86 (6)	**17.5 ± 3.9**	0.53 ± 0.24	2.0 ± 0.9	9.82 ± 5.43	**-26.41 ± 0.11**	**1.44 ± 0.47 (6)**
Falling Discharge	41.2 ± 50.4 (10)	3.09 ± 11.18 (6)	**7.1 ± 11.1**	0.34 ± 0.53	1.6 ± 1.0	6.06 ± 5.79	**-26.05 ± 0.36**	**4.61 ± 2.69 (3)**

Table A9. La Jara mean ± standard deviation for particulate carbon and particulate nitrogen (as mg/L and as fraction of total suspended sediment), C:N ratio, suspended sediment $\delta^{13}C$ (‰ VPDB), and suspended sediment $\delta^{15}N$ (‰ air). The number of observations, given in parentheses, is the same for each constituent in subsequent columns until otherwise indicated. Bolded values indicate statistically significant differences between categories ($P < 0.05$; unequal variance ANOVA or paired t-test).

	TSS (mg/L)	**PC (mg/L)**	**PC (% of TSS)**	**PN (mg/L)**	**PN (% of TSS)**	**C:N**	**$\delta^{13}C$ (VPDB ‰)**	**$\delta^{15}N$ (air ‰)**
Winter Baseflow	**72.1 ± 71.4 (3)**	1.10 ± 0.36 (3)	2.7 ± 2.0	0.23 ± 0.03 (3)	0.6 ± 0.4	4.66 ± 1.12	-26.20 ± 0.36 (4)	2.33 ± 0.62 (3)
Pre-peak Snowmelt	**19.7 ± 15.4 (10)**	1.57 ± 1.00 (6)	13.0 ± 11.7	0.26 ± 0.06 (6)	2.5 ± 2.2	5.45 ± 2.38	-26.30 ± 0.26 (6)	3.95 ± 3.47 (6)
Post-peak Snowmelt	**19.9 ± 15.2 (18)**	2.19 ± 2.49 (10)	10.8 ± 9.1	0.33 ± 0.23 (10)	2.6 ± 3.4	5.43 ± 3.04	-26.18 ± 0.43 (10)	3.12 ± 7.31 (8)
All Snowmelt	**19.8 ± 15.0 (28)**	1.96 ± 1.88 (16)	11.6 ± 10.2	0.30 ± 0.17 (6)	2.5 ± 2.8	5.44 ± 2.64	-26.22 ± 0.35 (16)	3.47 ± 5.51 (14)
Monsoon	**10.0 ± 5.8 (6)**	1.37 ± 1.05 (6)	14.2 ± 8.8	0.26 ± 0.07 (5)	3.0 ± 0.8	6.01 ± 2.05	-26.11 ± 0.43 (6)	2.59 ± 2.79 (6)
High Flows	16.9 ± 14.2 (23)	1.97 ± 1.60 (11)	14.3 ± 9.6	0.31 ± 0.14 (11)	3.3 ± 2.4	4.89 ± 2.35	-26.14 ± 0.36 (11)	3.64 ± 4.47 (9)
Low Flows	31.7 ± 37.9 (14)	1.52 ± 0.00 (14)	8.7 ± 0.0	0.26 ± 0.00 (13)	1.6 ± 0.0	5.94 ± 0.00	-26.23 ± 0.00 (15)	2.74 ± 0.00 (14)
Summer	18.1 ± 18.5 (10)	2.30 ± 2.28 (9)	**15.6 ± 9.1**	0.35 ± 0.22 (8)	3.6 ± 3.2	6.30 ± 2.48	-26.16 ± 0.39 (9)	2.44 ± 2.23 (9)
Winter	24.1 ± 28.8 (27)	1.39 ± 1.00 (16)	**8.7 ± 9.3**	0.25 ± 0.08 (16)	1.8 ± 1.7	5.04 ± 2.24	-26.21 ± 0.35 (17)	3.51 ± 5.50 (14)
Rising Discharge	25.2 ± 33.5 (20)	**1.09 ± 1.73 (13)**	**8.9 ± 11.5**	**0.22 ± 0.14 (12)**	2.4 ± 3.3	4.85 ± 2.27	-26.19 ± 0.28 (13)	3.68 ± 3.16 (12)
Falling Discharge	21.7 ± 15.6 (13)	**2.92 ± 1.62 (9)**	**15.0 ± 8.3**	**0.40 ± 0.16 (9)**	2.3 ± 1.5	6.75 ± 2.57	-26.23 ± 0.40 (10)	3.09 ± 5.78 (8)

Table A10. Upper Jaramillo mean ± standard deviation for particulate carbon and particulate nitrogen (as mg/L and as fraction of total suspended sediment), C:N ratio, suspended sediment $\delta^{13}C$ (‰ VPDB), and suspended sediment $\delta^{15}N$ (‰ air). The number of observations, given in parentheses, is the same for each constituent in subsequent columns until otherwise indicated. Bolded values indicate statistically significant differences between categories ($P < 0.05$; unequal variance ANOVA or paired t-test).

	TSS (mg/L)	**PC (mg/L)**	**PC (% of TSS)**	**PN (mg/L)**	**PN (% of TSS)**	**C:N**	**$\delta^{13}C$ (VPDB ‰)**	**$\delta^{15}N$ (air ‰)**
Winter Baseflow	82.2 ± 97.6 (2)	NA (0)	NA	NA	NA	NA	NA	NA
Pre-peak Snowmelt	32.7 ± 27.2 (13)	4.15 ± 4.03 (2)	15.9 ± 16.0	0.64 ± 0.43	2.4 ± 1.8	5.64 ± 2.53	-25.98 ± 0.13	3.95 ± 4.50 (2)
Post-peak Snowmelt	28.3 ± 27.6 (21)	2.99 ± 3.16 (9)	9.3 ± 2.8	0.41 ± 0.26	2.3 ± 1.8	5.91 ± 3.85	-26.60 ± 0.60	2.38 ± 1.52 (5)
All Snowmelt	30.0 ± 27.1 (34)	3.21 ± 3.14 (11)	10.5 ± 6.3	0.45 ± 0.28	2.4 ± 1.7	5.86 ± 3.53	-26.49 ± 0.60	2.82 ± 2.34 (7)
Monsoon	17.1 ± 11.3 (3)	2.58 ± 1.97 (3)	16.8 ± 10.4	0.34 ± 0.07	2.8 ± 1.8	6.97 ± 4.02	-26.30 ± 0.39	2.66 ± 0.40 (2)
High Flows	31.0 ± 28.2 (31)	2.90 ± 2.25 (9)	8.8 ± 9.4	0.41 ± 0.11	2.3 ± 0.9	5.52 ± 4.28	-26.52 ± 0.13	2.10 ± 0.81 (5)
Low Flows	34.4 ± 47.9 (8)	3.38 ± 3.27 (5)	17.5 ± 6.6	0.45 ± 0.30	2.7 ± 1.9	7.13 ± 3.16	-26.31 ± 0.69	3.65 ± 2.52 (4)
Summer	36.2 ± 32.2 (12)	3.33 ± 2.91 (10)	12.2 ± 6.2	0.42 ± 0.23	2.5 ± 1.9	6.81 ± 3.78	-26.54 ± 0.61	2.41 ± 1.37 (6)
Winter	29.7 ± 32.9 (27)	2.42 ± 3.07 (4)	11.2 ± 10.8	0.44 ± 0.34	2.3 ± 1.0	4.33 ± 2.13	-26.21 ± 0.30	3.53 ± 3.26 (3)
Rising Discharge	24.7 ± 26.7 (11)	**0.88 ± 0.35 (3)**	9.7 ± 7.8	0.27 ± 0.25	3.0 ± 1.9	**3.21 ± 3.85**	-26.33 ± 0.75	2.70 ± 1.53 (1)
Falling Discharge	35.8 ± 35.3 (26)	**3.61 ± 0.67 (9)**	10.5 ± 3.2	0.44 ± 0.07	1.9 ± 1.0	**7.23 ± 1.93**	-26.57 ± 0.14	2.18 ± 0.37 (7)

Table B1. Summary of catchment characteristics for all sites. Where relevant, mean values ± standard deviation are above in normal typeface and ranges are below in italics.

	Scale	Site	Area (km^2)	Elevation (m)	Mean slope (°)	Aspect (°)	Area Burned (%)	
							High Severity	Total
Burned	ZOB	Condon ZOB	0.095	2762 ± 75 *2655-2973*	21 ± 7 *1-38*	298 ± 72 NW	53.1	87.5
		Instrumented ZOB	0.131	2785 ± 64 *2662-2934*	21 ± 6 *2-37*	96 ± 120 NNE	74.0	100.0
		Orem ZOB	0.169	2803 ± 59 *2679-2950*	13 ± 5 *1-32*	202 ± 126 WNW	43.8	97.5
		Gibson ZOB	0.579	2835 ± 91 *2663-3002*	21 ± 8 *1-41*	276 ± 72 WNW	31.7	69.8
	Catchment	Debris Fan 2	1.322	2802 ± 87 *2652-2985*	15 ± 8 *0-43*	191 ± 70 SW	25.2	80.7
		Debris Fan 1	1.361	2858 ± 83 *2668-3014*	14 ± 7 *0-38*	207 ± 70 SSW	39.1	96.5
Unburned	Catchment	History Grove	2.434	2947 ± 98 *2683-3303*	13 ± 6 *0-41*	119 ± 60 ESE	0.0	0.0
		Upper Jaramillo	3.100	2917 ± 101 *2720-3311*	13 ± 8 *0-45*	222 ± 134 NNW	0.0	0.0
		La Jara	3.729	3107 ± 156 *2706-3435*	16 ± 8 *0-43*	111 ± 68 ENE	0.0	0.0

Table B2. Data collected and samples analyzed at burned and unburned sites in May and June 2012. EA-IRMS indicates elemental analysis with isotope ratio mass spectrometry * indicates that this sample type was not applicable at this site.

Site	Deposit Type and Depth	In Situ Soil EA-IRMS	Alluvial Deposit Bulk Density	Alluvial Deposit EA-IRMS
Instrumented ZOB	83	3	13	5
Orem ZOB	40	5	8	3
Condon ZOB	*	4	*	*
Grand Total	**123**	**12**	**21**	**8**

Table B1. Total carbon and nitrogen deposited in ZOB culverts, in total kilograms, per hectare of catchment area, and per hectare of depositional area, ± standard error margins.

	Carbon		
ZOB	*kg*	*kg/ha catchment*	*kg//ha depositional area*
Orem	283 ± 3	16.8 ± 0.18	44,200 ± 500
Instrumented	1572 ± 20	119.9 ± 1.5	51,800 ± 600
	Nitrogen		
	kg	*kg/ha catchment*	*kg/ha depositional area*
Orem	15 ± 1	0.9 ± 0.0	2300 ± 100
Instrumented	81 ± 2	6.2 ± 0.1	2700 ± 100

Table F1. Results of gravimetric bulk density and EA-IRMS analysis of soil and alluvial deposition samples. F1 indicates Debris Fan 1, F2 indicates Debris Fan 2, C1 indicates Instrumented ZOB Culvert, C2 indicates Orem ZOB Culvert, and T denotes a specific transect and the distance along it (e.g. F2-T4-25 was sampled at Debris Fan 2, at the 25 m mark on Transect 4). In-situ cores are labeled by site (F1, C1, etc.) then by duplicate core A or B from the same site, then by the 10cm subsampled layer, with 1 indicating 0-10cm depth, 2 indicating 10-20cm depth, and so on.

Sample ID	**Sample Type**	**Bulk Density (g/cm^3)**	**C % (w/w)**	**d13C % VPDB**	**N % (w/w)**	**d15N % air**
F1-13	Ash	1.561	2.33	-25.749384	0.17	3.472098
F1-13	Ash	1.561	2.32	-25.763132	0.16	3.385925
F1-14	Ash	1.065	2.72	-24.952	0.19	3.527857
F1-15	Ash	1.574	0.22	-23.3631	0.03	3.486291
F1-18	Ash	1.947	2.3	-24.0328	0.15	4.432167
F2-T1-12.4	Ash	1.239	0.61	-23.7009	0.05	4.60654
F2-T4-0	Ash	1.346	1.75	-24.3824	0.11	3.743796
F2-T4-25	Ash	1.424	3.33	-24.8037	0.15	2.780686
F2-04	Litter	0.679	8.47	-25.6384	0.42	2.207889
F2-T3-1.8	Litter	0.509	10.21	-24.4237	0.42	1.47694
F2-T5-150	Litter	0.627	8.25	-24.2047	0.34	3.247034
F2-T5-63.2	Litter	1.276	5.54	-25.6325	0.31	2.70161
F2-T6-3.5	Litter	0.949	10.76	-25.3694	0.44	2.625575
F2-T7-20	Litter	0.775	12.48	-25.4037	0.49	1.200172
F1-20	Litter and Ash	0.613	5.03	-24.604372	0.29	3.3778146
F1-20	Litter and Ash	0.613	4.17	-24.651508	0.27	3.4274908

Sample ID	Sample Type	Bulk Density (g/cm^3)	C % (w/w)	d13C % VPDB	N % (w/w)	d15N % air
F2-15	Litter and Ash	0.748	10.9	-25.3998	0.54	1.460719
F2-T1-1.5	Litter and Ash	0.841	8.88	-25.1857	0.42	2.220055
F2-T1-26.4	Litter and Ash	0.726	6.25	-25.4774	0.27	2.32549
F2-T2-0	Litter and Ash	0.491	8.64	-25.3674	0.35	1.774997
C1A1	In Situ Core	0.612	3	-26.372	0.22	3.788404
C1A2	In Situ Core	1.153	2.06	-26.7068	0.15	3.708313
C1A3	In Situ Core	1.054	1.11	-25.9281	0.1	4.563961
C2A1	In Situ Core	0.899	1.26	-24.698644	0.11	3.3798422
C2A1	In Situ Core	0.899	1.44	-24.5101	0.11	3.3474006
C2A2	In Situ Core	1.297	2.05	-25.1995	0.14	2.627603
C2A3	In Situ Core	0.610	6.06	-25.7189	0.33	2.513043
C2A4	In Situ Core	0.985	3.55	-26.3131	0.26	3.209524
C2A5	In Situ Core	0.958	2.15	-25.1445	0.16	4.864045
F1A2	In Situ Core	0.922	3.59	-22.441	0.3	5.970101
F1A3	In Situ Core	0.890	2.07	-20.9052	0.19	7.785817
F1A4	In Situ Core	1.094	1.56	-22.444	0.14	7.528312
F2B1	In Situ Core	1.220	3.46	-24.899	0.25	5.517946
F2B2	In Situ Core	1.033	2.49	-23.3278	0.2	6.230648
F2B3	In Situ Core	1.073	1.99	-22.1896	0.17	7.447208

Sample ID	Sample Type	Bulk Density (g/cm^3)	C % (w/w)	d13C % VPDB	N % (w/w)	d15N % air
F2B4	In Situ Core	1.060	1.2	-22.1238	0.11	6.631099
C1-04	Litter	1.054	5.14	-25.6885	0.26	1.430305
C1-05	Litter	0.557	9.13	-25.9065	0.49	1.691865
C1-581	Litter	0.785	5.96	-25.6698	0.34	2.106509
C1-583	Litter	1.116	6.53	-25.8044	0.37	1.619885
C1-584	Litter	0.724	11.59	-26.229582	0.57	1.8844872
C1-584	Litter	0.724	9.84	-25.818124	0.53	2.3782078
C2-04	Litter	0.604	8.27	-25.4784	0.47	1.659424
C2-12	Litter	0.491	8.26	-25.6276	0.49	2.344752
C2-8	Litter	0.536	8.86	-25.2721	0.49	2.158213

Table F2. Suspended particulate carbon and nitrogen and stable isotope data, for Redondo Peak catchments History Grove (Site ID =1), La Jara (Site ID = 2), and Upper Jaramillo (Site ID = 3). Sediment was collected on glass-fiber filters and underwent Elemental Analysis with Isotopic Ratio Mass Spectrometry (EA-IRMS). Missing or data is noted with an asterisk (*).

Site ID	Date & Time	Q at Site (L/d)	TSS (mg/L)	C (frac. of TSS)	N (frac. of TSS)	C:N ratio	$\delta^{15}N$ ‰ air	$\delta^{13}C$ ‰ VPDB
1	11/30/11 10:30	*	11.9	0.04185	0.023914	1.75	*	-26.0656
3	11/30/11 12:15	744942.7	13.2	*	*	*	*	*
1	3/10/12 10:00	*	57.9	0.128115	0.011896	10.77	3.554965	-26.523
2	3/11/12 12:00	2375623	3.1	0.236823	0.052133	4.54	3.165257	-26.5591
2	3/11/12 12:00	2375623	5.2	0.358212	0.061273	5.85	2.632267	-26.1646
3	3/12/12 2:00	459517.9	25.7	0.272482	0.03668	7.43	7.127802	-26.0666
3	3/26/12 11:00	1723099	28.6	0.045634	0.011831	3.86	0.768319	-25.8893
1	3/26/12 13:45	2617833	31.2	0.083744	0.010964	7.64	5.003581	-26.002
2	3/26/12 15:00	1648990	15.2	0.028381	0.012417	2.29	2.406371	-26.0549
2	3/26/12 22:00	1580486	15.9	*	*	*	*	*
3	3/26/12 22:00	2904261	25.2	*	*	*	*	*
2	3/27/12 13:45	1472837	8.4	0.157855	0.030274	5.21	*	-26.0059
3	3/27/12 22:00	2820385	58.6	*	*	*	*	*
3	3/28/12 22:00	2686715	5.9	*	*	*	*	*
3	3/29/12 22:00	2620553	12.4	*	*	*	*	*
2	3/30/12 22:00	1795785	9.9	*	*	*	*	*
3	3/30/12 22:00	2760671	14.9	*	*	*	*	*
3	3/31/12 22:00	3039749	71.2	*	*	*	*	*
3	4/1/12 22:00	2930211	12.6	*	*	*	*	*
3	4/2/12 11:30	2594699	9.4	*	*	*	*	*
2	4/2/12 14:30	1957259	12.4	0.045554	0.012527	3.64	-3.13843	-26.1214

Site ID	Date & Time	Q at Site (L/d)	TSS (mg/L)	C (frac. of TSS)	N (frac. of TSS)	C:N ratio	$\delta^{15}N$ ‰ air	$\delta^{13}C$ ‰ VPDB
3	4/2/12 22:00	1973147	19.9	*	*	*	*	*
3	4/3/12 22:00	2323399	94.6	*	*	*	*	*
3	4/4/12 22:00	2849674	46.6	*	*	*	*	*
3	4/9/12 10:00	2457996	0.4	*	*	*	*	*
1	4/9/12 11:45	1592719	10.9	0.023102	0.017968	1.29	*	-26.0549
2	4/9/12 12:30	1971938	14.4	0.027724	0.011882	2.33	19.8158	-25.5518
3	4/17/12 10:15	2672405	11.9	0.052088	0.020034	2.60	*	-26.5788
1	4/17/12 12:00	1108298	15.9	0.031154	0.012239	2.55	*	-26.1107
2	4/17/12 12:30	1778659	2.4	*	*	*	*	*
2	4/17/12 22:00	1800678	10.6	*	*	*	*	*
3	4/18/12 22:00	2604171	4.6	*	*	*	*	*
2	4/18/12 22:00	1827590	30.9	*	*	*	*	*
2	4/20/12 22:00	1864289	2.6	*	*	*	*	*
3	4/20/12 22:00	2729257	12.4	*	*	*	*	*
3	4/21/12 22:00	2752205	15.2	*	*	*	*	*
2	4/21/12 22:00	1905881	28.4	*	*	*	*	*
2	4/22/12 22:00	1913220	31.2	0.112187	0.014278	7.86	1.480441	-26.6627
3	4/22/12 22:00	2735994	15.9	*	*	*	*	*
2	4/24/12 9:45	1878968	6.9	0.051413	0.029379	1.75	*	-25.6474
1	4/24/12 10:45	785350	11.4	*	*	*	*	*
3	4/24/12 12:00	2880888	9.9	0.076347	0.022345	3.42	2.699638	-26.3036
2	4/24/12 22:00	1927900	22.5	*	*	*	*	*
3	4/24/12 22:00	2901115	39.9	*	*	*	*	*
3	4/25/12 22:00	2923535	37.9	*	*	*	*	*
2	4/26/12 22:00	1974385	17.1	*	*	*	*	*

Site ID	Date & Time	Q at Site (L/d)	TSS (mg/L)	C (frac. of TSS)	N (frac. of TSS)	C:N ratio	$\delta^{15}N$ ‰ air	$\delta^{13}C$ ‰ VPDB
2	4/29/12 22:00	1729727	5.1	*	*	*	*	*
3	4/29/12 22:00	2658472	7.9	*	*	*	*	*
2	4/30/12 22:00	1658777	25.1	*	*	*	*	*
3	4/30/12 22:00	2545076	43.9	*	*	*	*	*
3	5/1/12 10:30	2558315	3.9	0.125803	0.060572	2.08	*	-26.2566
1	5/1/12 12:30	533353	3.9	*	*	*	*	*
2	5/1/12 13:30	1604952	1.4	0.307123	0.110564	2.78	2.012807	-25.9727
3	5/1/12 22:00	2398805	25.9	*	*	*	*	*
3	5/2/12 22:00	2310621	78.6	0.068066	0.006031	11.29	3.786593	-26.5868
2	5/2/12 22:00	1387207	58.5	0.097591	0.012199	8.00	1.793389	-26.6333
2	5/3/12 22:00	1360295	42.8	0.146788	0.015372	9.55	2.625109	-26.2169
3	5/3/12 22:00	2173817	84.5	*	*	*	*	*
3	5/4/12 22:00	2044975	77.9	0.110848	0.012713	8.72	3.327302	-28.163
3	5/5/12 22:00	1932936	72.7	0.096868	0.008383	11.56	-0.10537	-26.2174
2	5/9/12 10:00	1294237	18.6	*	*	*	*	*
1	5/9/12 10:45	396344.9	6.4	0.078101	0.033773	2.31	*	-26.2145
3	5/9/12 12:00	1991092	7.9	0.075426	0.026764	2.82	*	-26.3702
3	5/12/12 9:10	1634796	9.2	0.138012	0.040776	3.38	*	-26.3271
3	5/29/12 10:45	847634.5	22.8	0.095883	0.013121	7.31	2.17043	-26.5788
1	5/29/12 12:15	203065.6	22.2	0.084552	0.012527	6.75	4.743663	-25.8845
3	6/19/12 10:45	573955.9	16.9	0.279925	0.024933	11.23	2.940809	-26.7375
1	6/19/12 12:15	183493	51.4	*	*	*	*	*
2	6/19/12 13:00	582284.4	9.9	0.001472	*	*	2.757182	-25.6585
2	6/19/12 13:15	572498.1	6.4	0.239367	0.034195	7.00	-1.30736	-26.2859
3	7/4/12 12:00	512494.1	28.6	0.073791	0.011479	6.43	2.369615	-26.1636

Site ID	Date & Time	Q at Site (L/d)	TSS (mg/L)	C (frac. of TSS)	N (frac. of TSS)	C:N ratio	$\delta^{15}N$ ‰ air	$\delta^{13}C$ ‰ VPDB
1	7/4/12 13:20	251997	99.9	0.128328	0.008105	15.83	4.096867	-26.0304
2	7/6/12 12:30	709506.2	5.2	0.099656	0.035987	2.77	1.323272	-25.5205
3	7/31/12 10:15	526502.3	5.9	0.151371	0.046576	3.25	*	-26
1	7/31/12 11:45	259336.8	16.6	0.365557	0.02721	13.43	-1.50969	-26.647
2	7/31/12 12:30	670361.1	9.2	0.142951	0.024861	5.75	4.188172	-26.6519
2	8/12/12 14:30	636109	7.9	0.228714	0.036758	6.22	6.915734	-26.3105
2	8/12/12 15:00	648341.9	21.2	0.142745	0.01721	8.29	1.691994	-26.2331
1	8/13/12 11:12	249550.5	32.5	0.129565	0.011089	11.68	2.533418	-26.74
1	8/13/12 11:30	242210.8	9.2	0.227522	0.034535	6.59	3.435844	-26.1391
1	8/13/12 12:00	239764.2	10.6	0.093017	0.020929	4.44	-1.92757	-25.8552
1	10/24/12 4:50	198172.4	169.9	0.175339	0.00938	18.69	4.741789	-26.7175
2	2/25/13 12:15	425703.7	154.6	0.006464	0.001361	4.75	1.632346	-26.2213
2	2/25/13 13:00	425703.7	32.6	0.04596	0.008016	5.73	2.554502	-26.5697
1	3/5/13 10:15	198172.4	158.6	*	*	*	*	*
2	3/5/13 11:00	425703.7	29.2	0.027254	0.007787	3.50	2.807292	-26.2996
3	3/5/13 13:15	413898.8	151.2	*	*	*	*	*
2	3/18/13 11:30	425703.7	30.6	0.02713	0.00829	3.27	9.606008	-25.9511
2	3/18/13 12:45	425703.7	33.2	0.058961	0.008844	6.67	4.128555	-26.4953
1	3/18/13 13:30	198172.4	19.2	*	*	*	*	*
1	3/25/13 11:30	198172.4	39.9	*	*	*	*	*
2	3/25/13 12:30	425703.7	52.6	0.068381	0.006796	10.06	1.747248	-26.5971
1	3/31/13 14:15	198172.4	15.9	0.0582	0.014227	4.09	1.378437	-26.3769
2	3/31/13 15:00	425703.7	22.6	0.082942	0.012836	6.46	-2.03859	-26.3808
2	4/8/13 11:00	425703.7	27.9	0.052198	0.007733	6.75	2.409594	-26.5599
1	4/8/13 11:45	198172.4	23.2	*	*	*	*	*

Site ID	Date & Time	Q at Site (L/d)	TSS (mg/L)	C (frac. of TSS)	N (frac. of TSS)	C:N ratio	$\delta^{15}N$ ‰ air	$\delta^{13}C$ ‰ VPDB
3	4/8/13 13:00	413898.8	10.6	*	*	*	*	*

References

Harmon ME, Sexton J (1996) Guidelines for Measurements of Woody Detritus in Forest Ecosystems. In. U.S. LTER Network Office, University of Washington, Seattle, WA. p 73

Prescott CE, Corbin JP, Parkinson D (1989) INPUT, ACCUMULATION, AND RESIDENCE TIMES OF CARBON, NITROGEN, AND PHOSPHORUS IN 4 ROCKY-MOUNTAIN CONIFEROUS FORESTS. Canadian Journal of Forest Research-Revue Canadienne De Recherche Forestiere 19(4): 489-498

APPENDIX G: FIGURES

LIST OF FIGURES

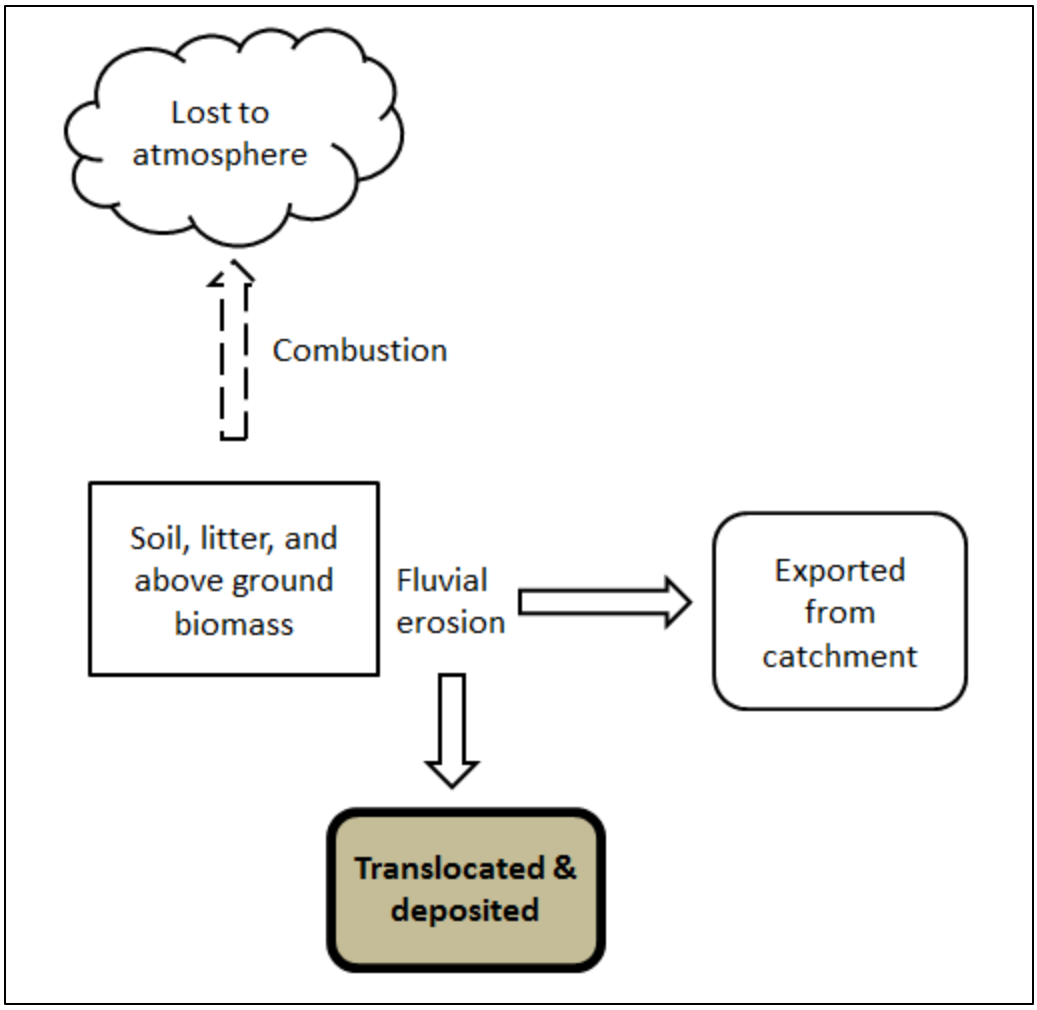

Figure A1. Conceptual diagram of possible carbon and nitrogen loss pathways during and following wildfire. This study quantifies the carbon and nitrogen that is translocated by fluvial erosion and deposited elsewhere in the catchment.

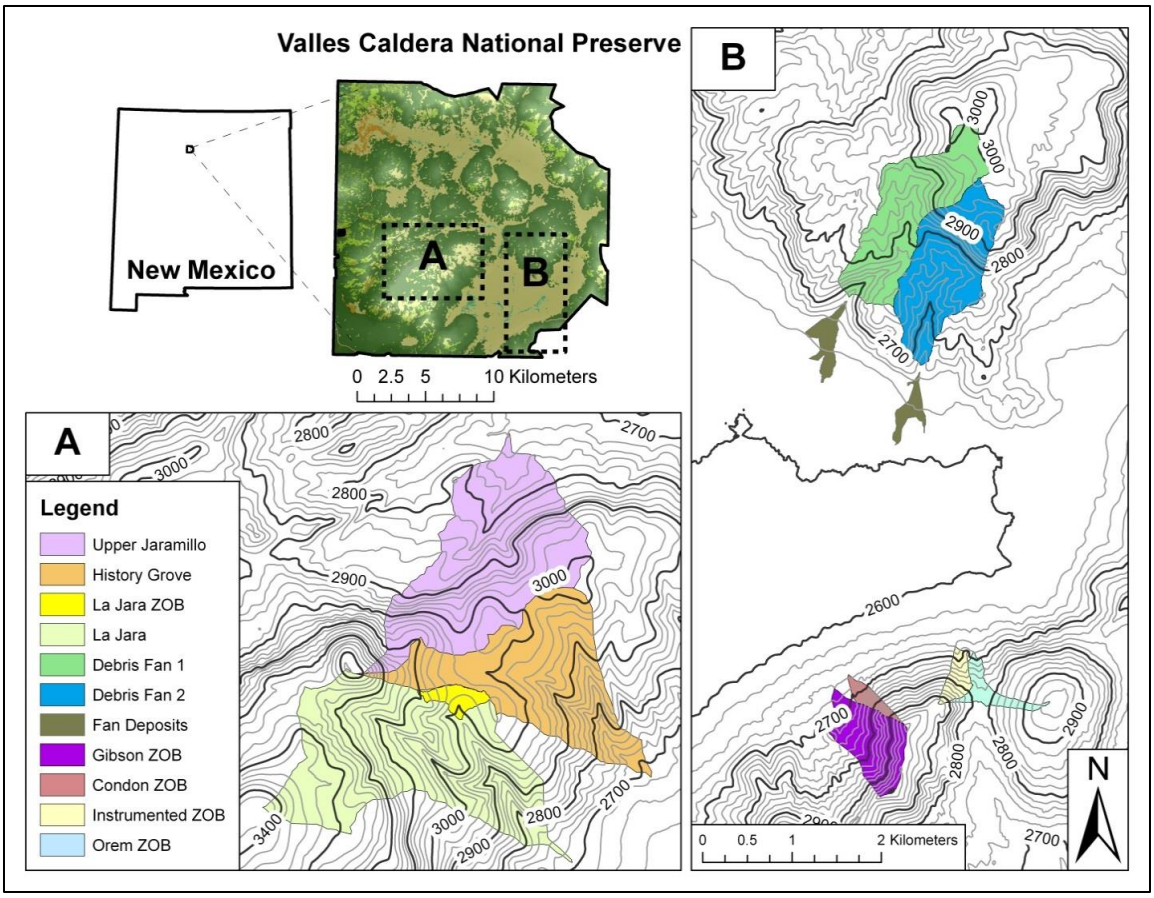

Figure A2. Maps of study catchments within Valles Caldera National Preserve, New Mexico. (A) Redondo Peak unburned catchments; (B) Cerro del Medio burned catchments with debris fans; (C) Rabbit Mountain burned and control catchments.

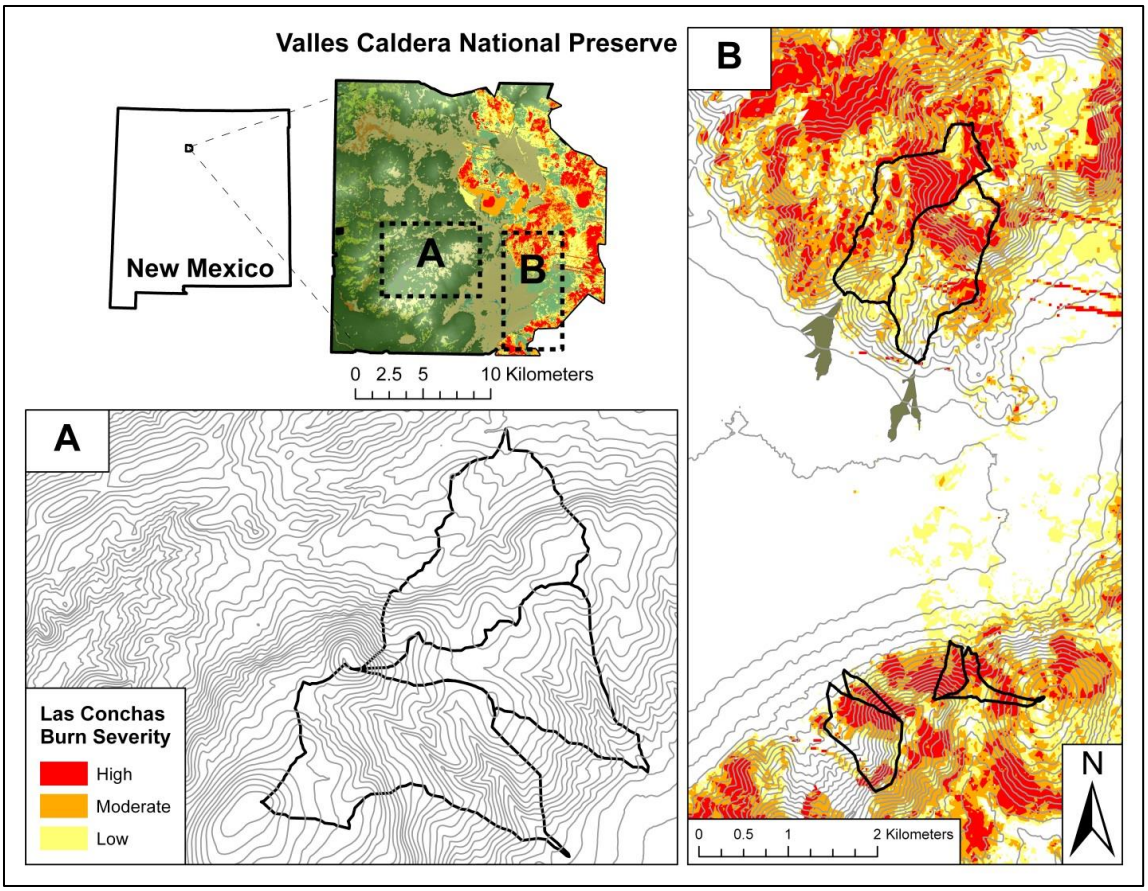

Figure A3. Extent and severity of Las Conchas wildfire within (A) Redondo Peak and (B) Fan 1 and Fan 2 catchments on Cerro del Medio to the north and Rabbit Mountain ZOBs to the south(USDA Forest Service 2011).

Figure A4. Aerial images of southern slopes of Cerro del Medio, before Las Conchas fire (top) and after (bottom). Images taken June 30, 2005 and May 4, 2012 (Google Earth, 2013).

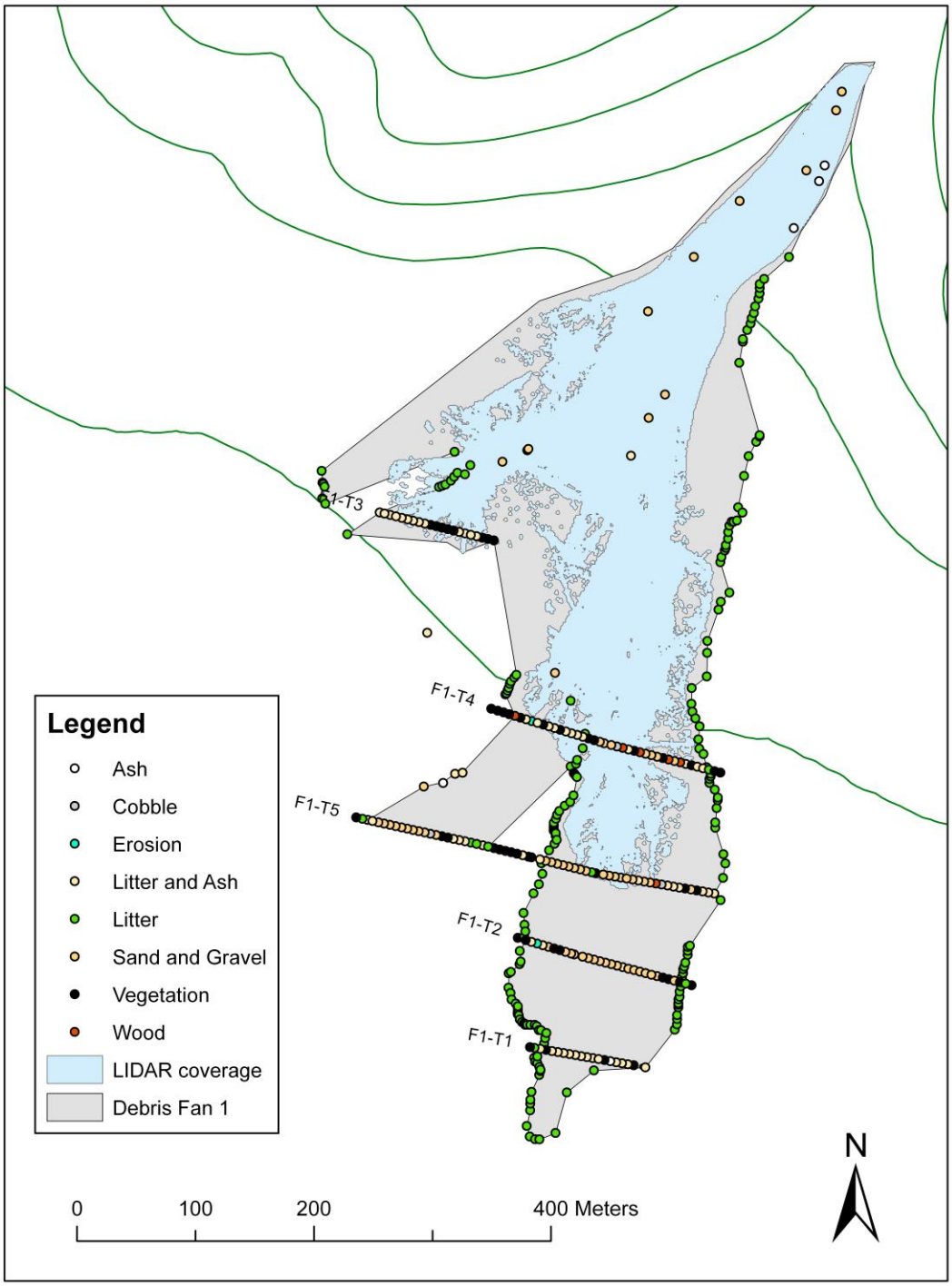

Figure A5. June 2012 sampling transects and outline of alluvial deposits at Debris Fan 1.

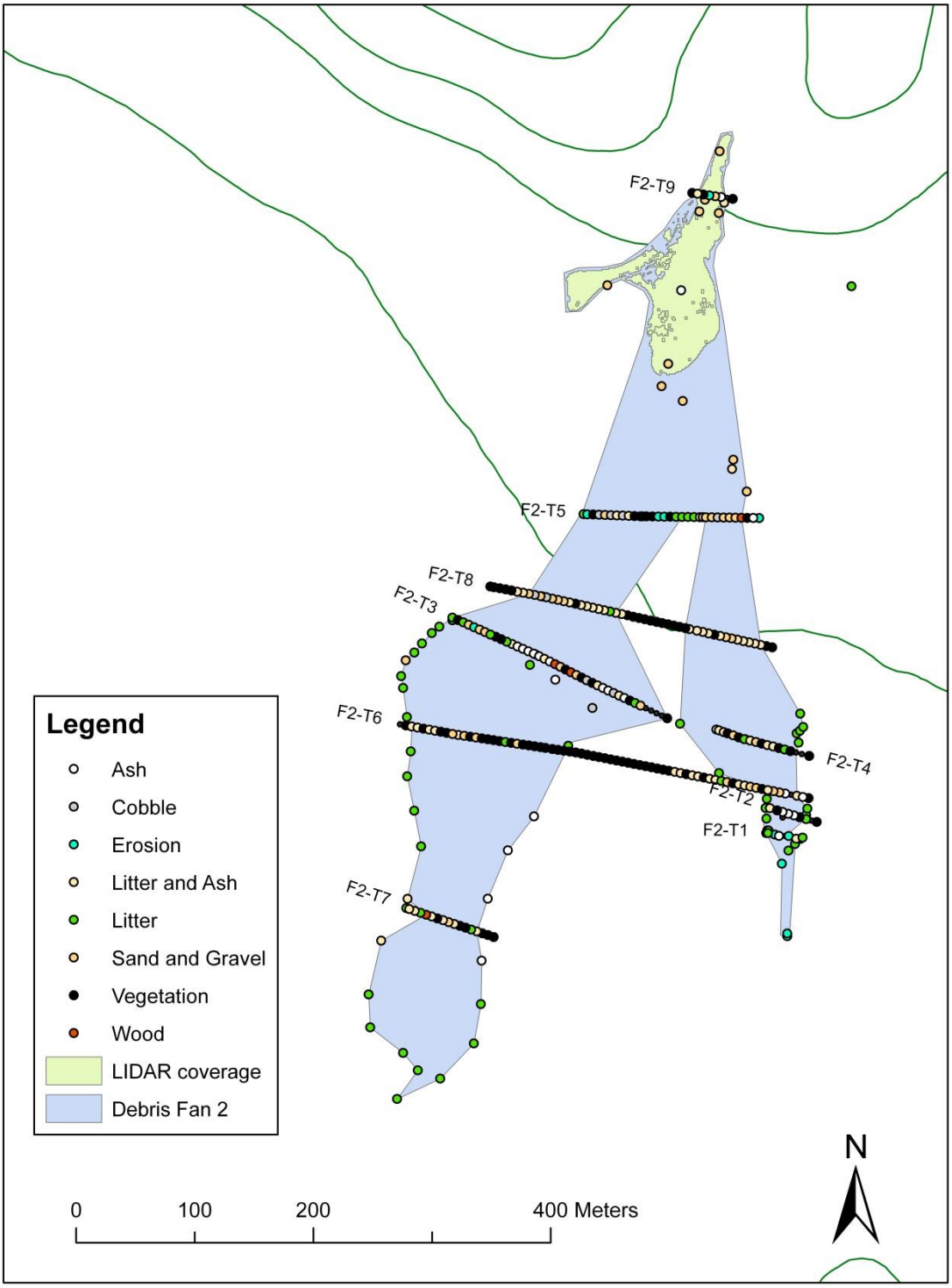

Figure A6. June 2012 sampling transects and outline of alluvial deposits at Debris Fan 2.

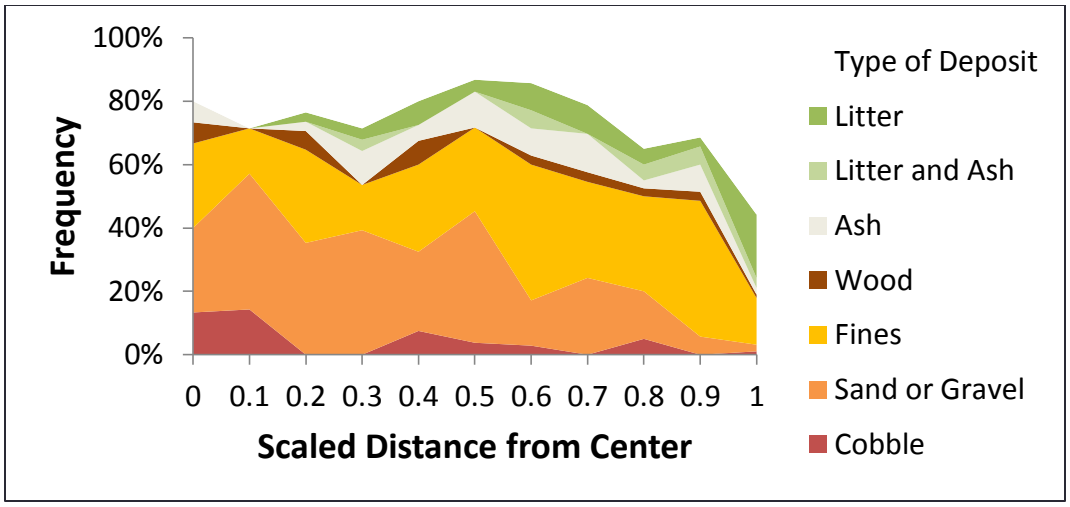

Figure A7. Frequency of deposit types along all transects in Debris Fans 1 and 2. The x-axis represents position on the transect, as a fraction of transect length from the center of the splay. Zero indicates the center of the splay, and one indicates the edge of the deposition to either side. For example, observations at 0.5 are halfway from the center of the splay to the edge of the debris fan.

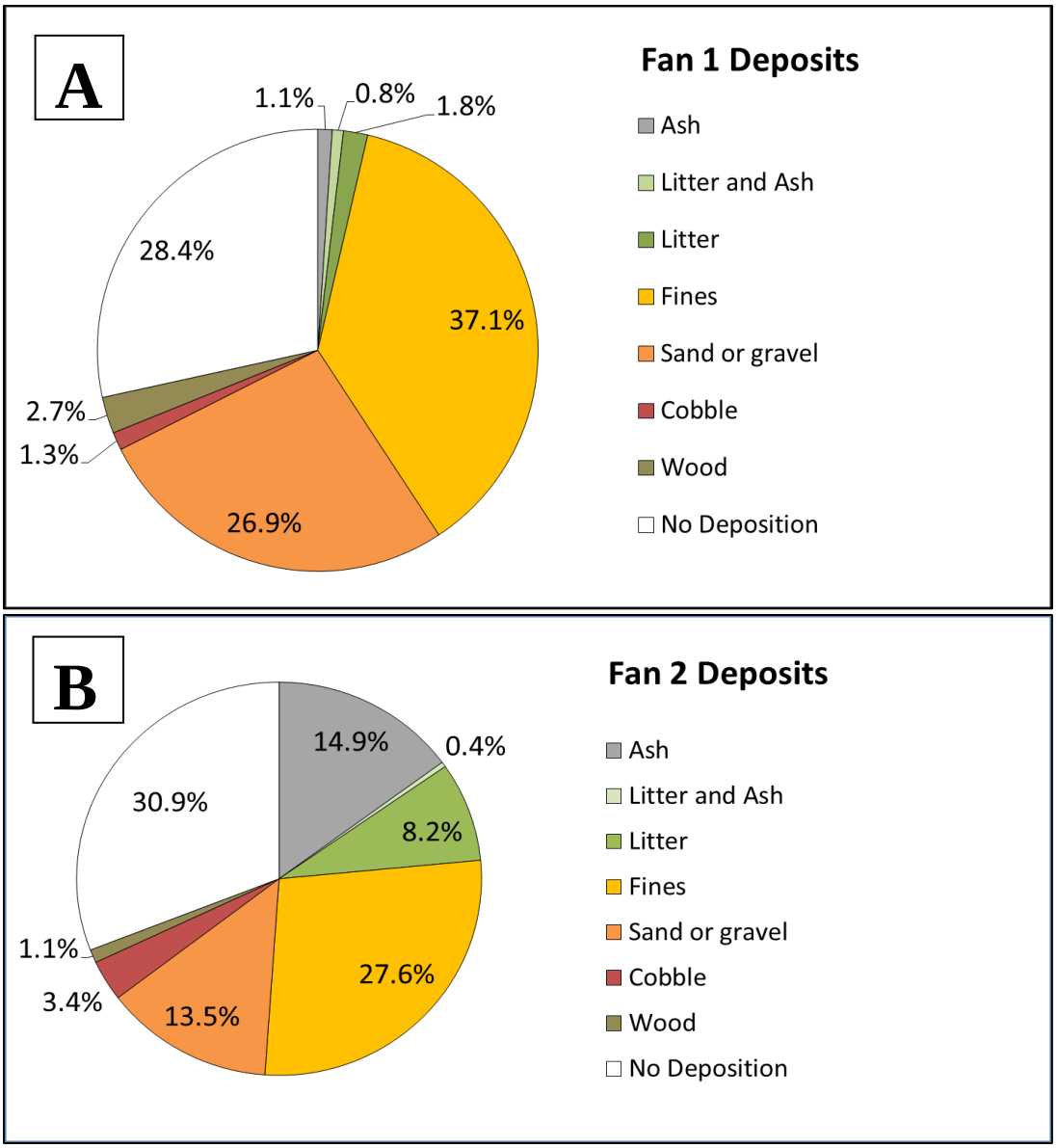

Figure A8. Areal percent coverage of deposit types along transects at (a) Debris Fan 1 and (b) Debris Fan 2.

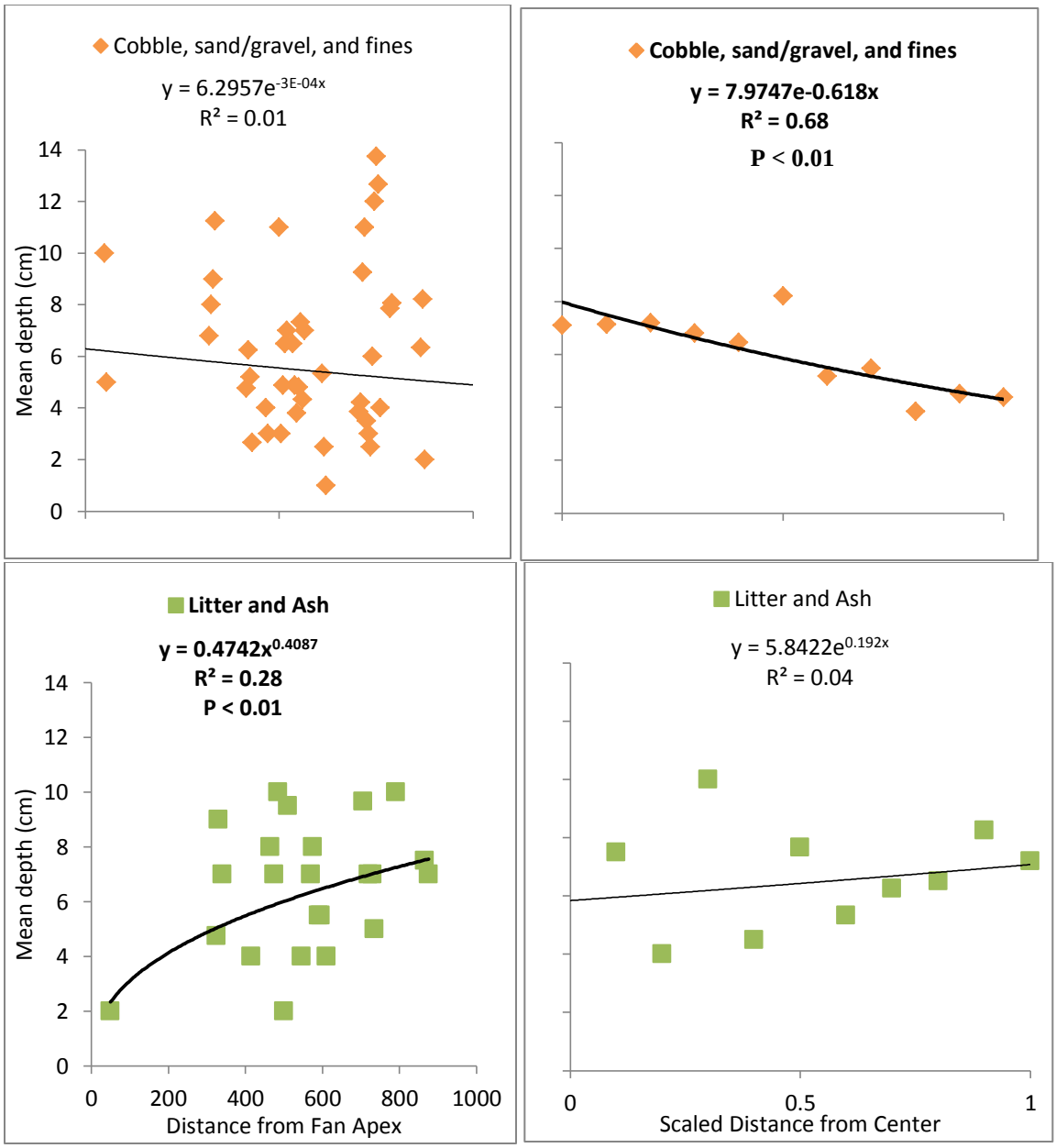

Figure A9. Spatial changes in deposit depth from fan apex to bottom (left panels), and from center of splay to edge (right panels), at Debris Fan 1 and Debris Fan 2, using binned means of the data. Bolded text and trendlines highlight the strongest empirical relationships.

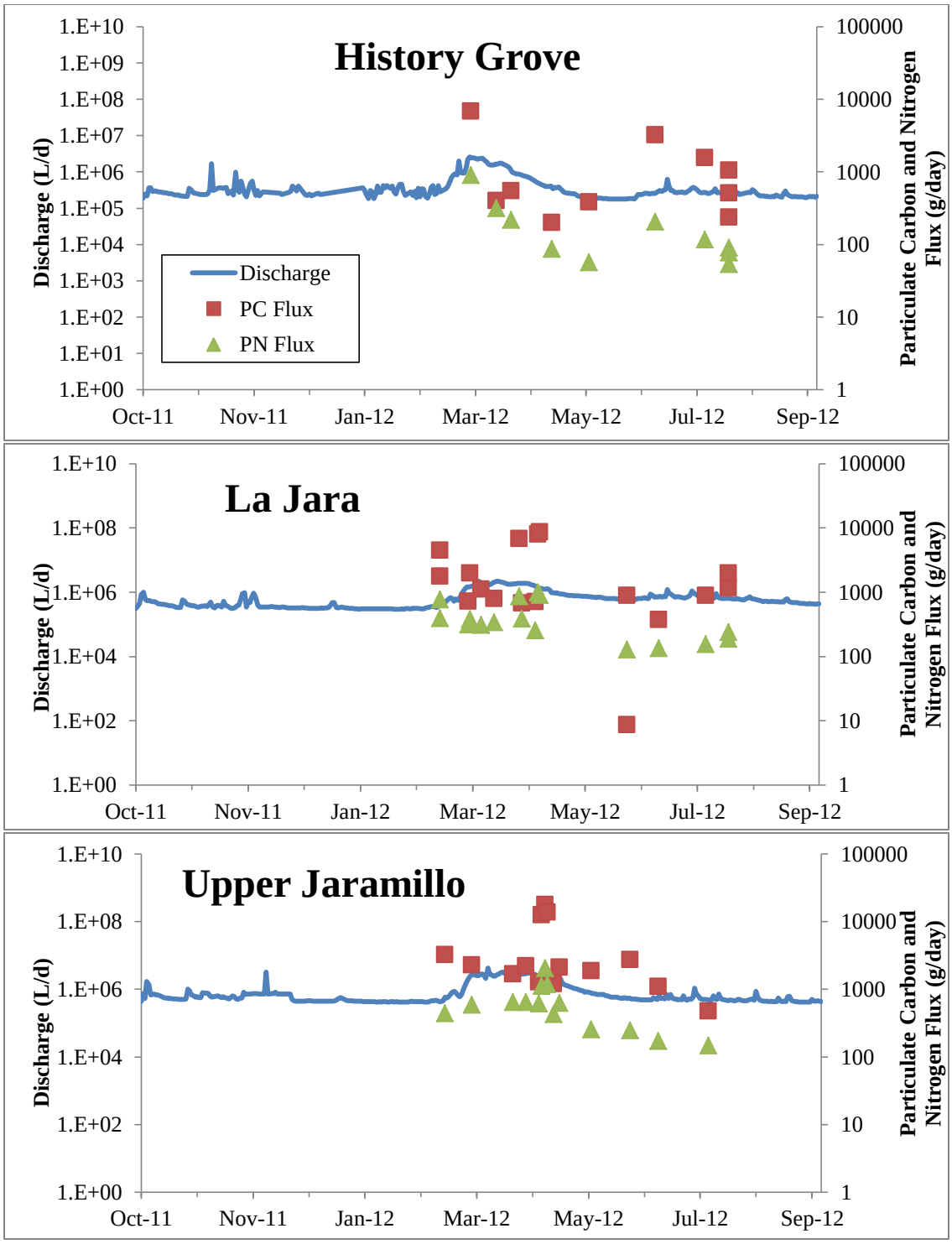

Figure A10. Discharge (L/day) and observed particulate carbon and nitrogen fluxes (g/day) at unburned Redondo Peak catchments, shown on a logarithmic scale to illustrate variability at low flows.

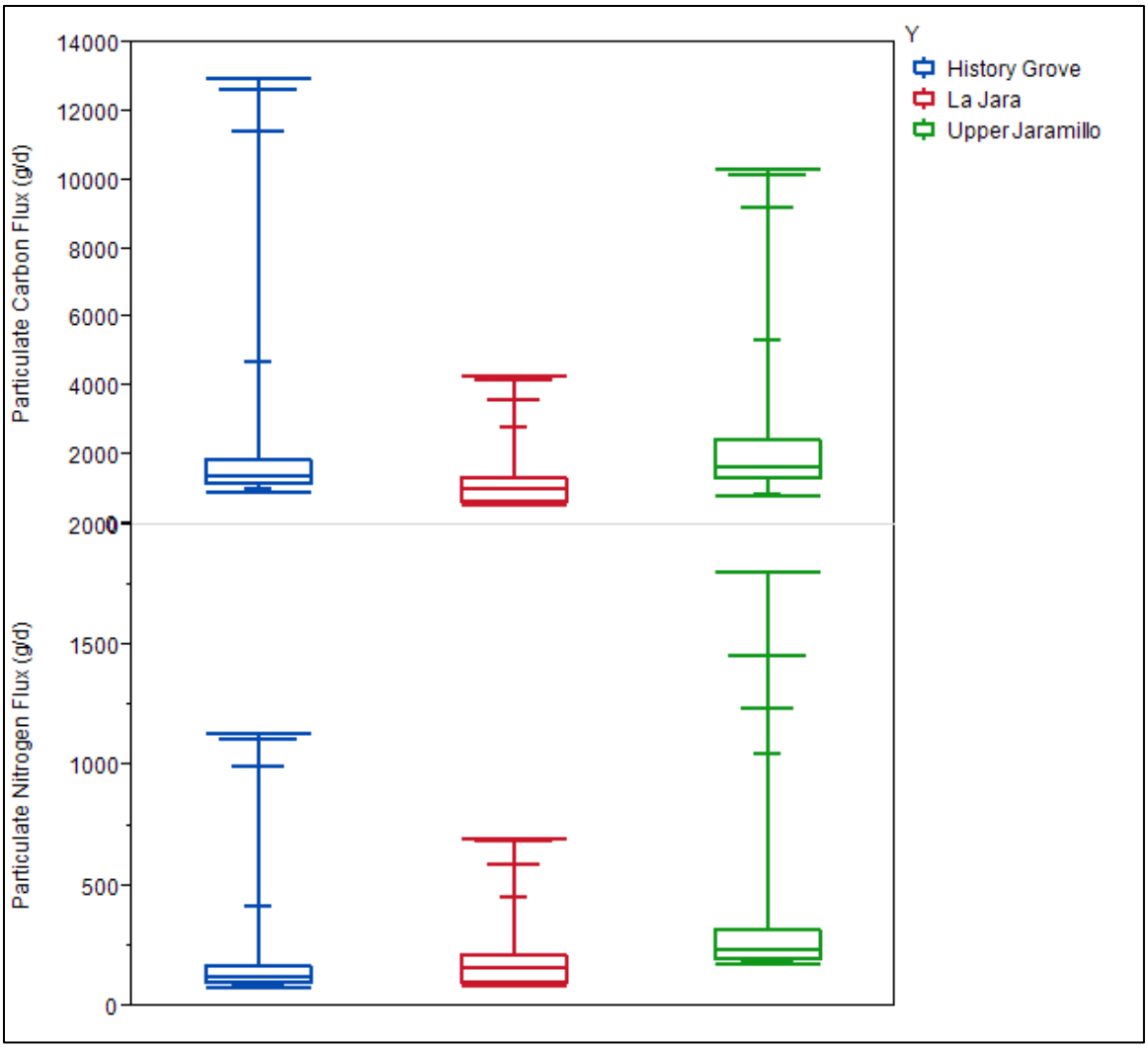

Figure A11. Quantile plots of predicted daily fluxes, in grams per day, of particulate carbon and nitrogen from Redondo Peak catchments over water year 2012, as calculated from flow rates and observed mean concentrations. N for each equals 366 days. Because the predicted fluxes are driven by discharge, high flux values can be interpreted as days of high discharge, predominately during snowmelt.

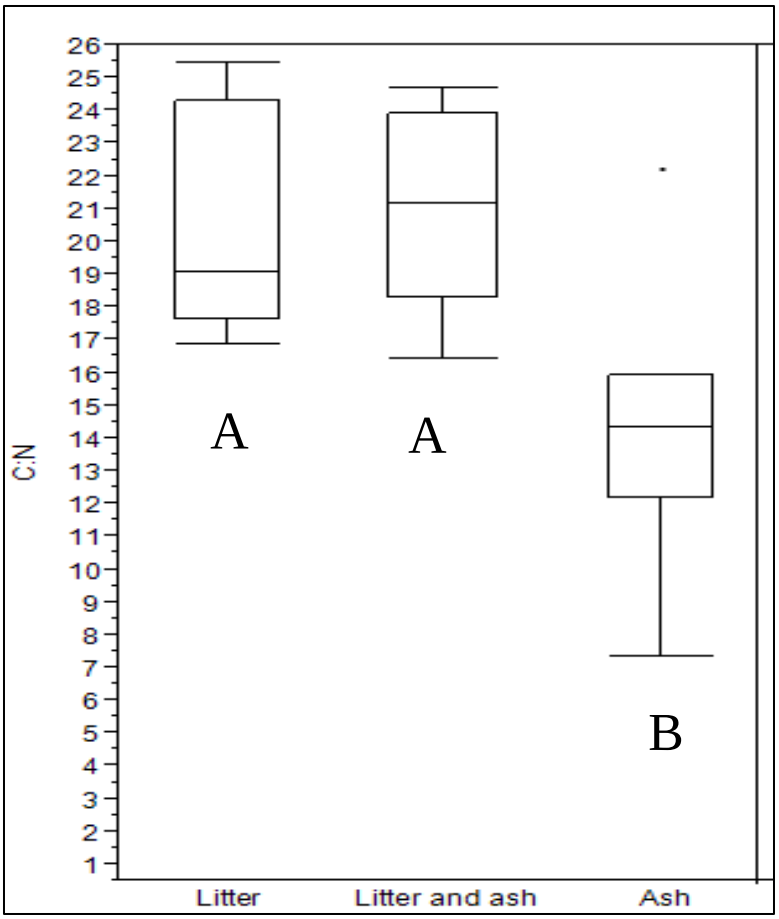

Figure A12. C:N ratios in alluvial deposits (litter, litter and ash, and ash categories) at Debris Fans 1 and 2. Different letters indicate significantly different means (Tukey-Kramer HSD, $P<0.05$).

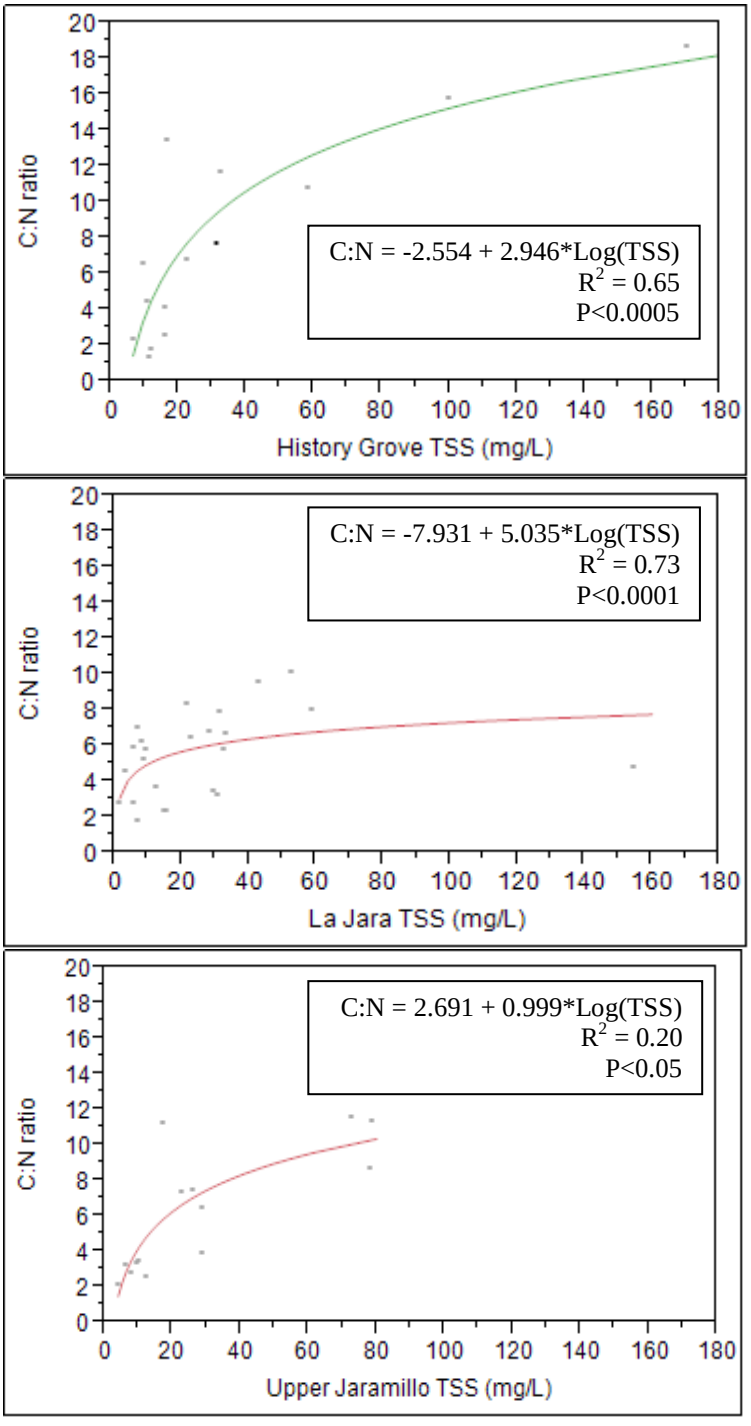

Figure A13. Logarithmic relationships between C:N and total suspended sediment concentrations (TSS, mg/L) at the Redondo Peak catchments.

Figure B1. Transect at Instrumented ZOB culvert, survey in June 2012.

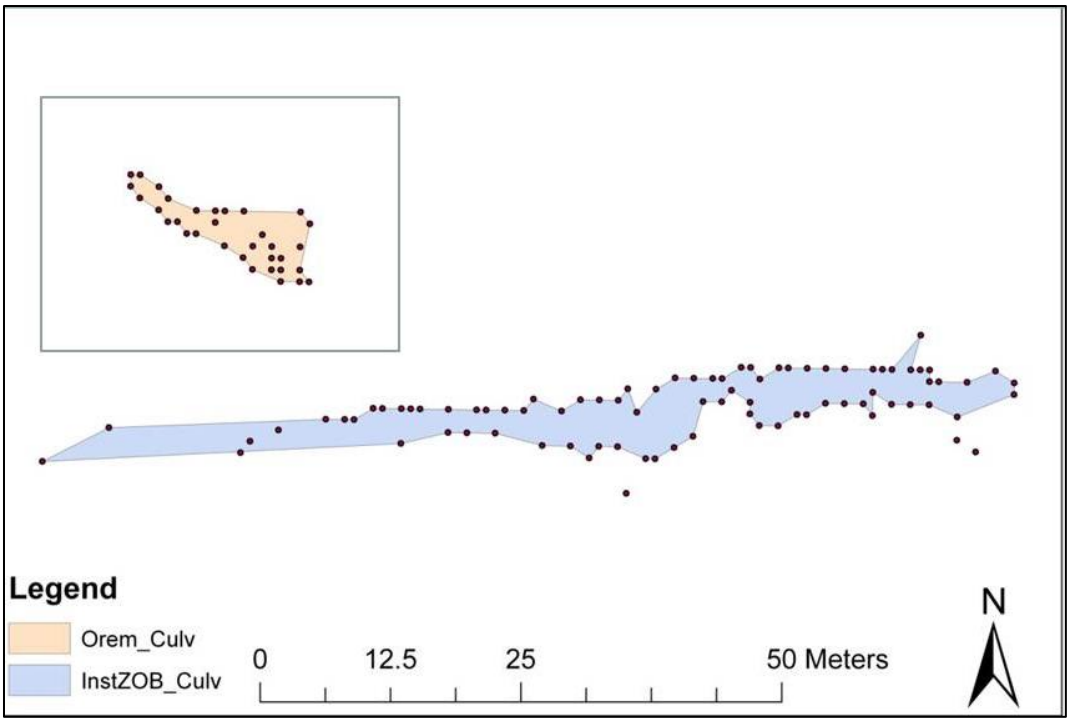

Figure B2. June 2012 survey points and outline of litter deposits at the Orem ZOB culvert (inset) and the Instrumented ZOB culvert.

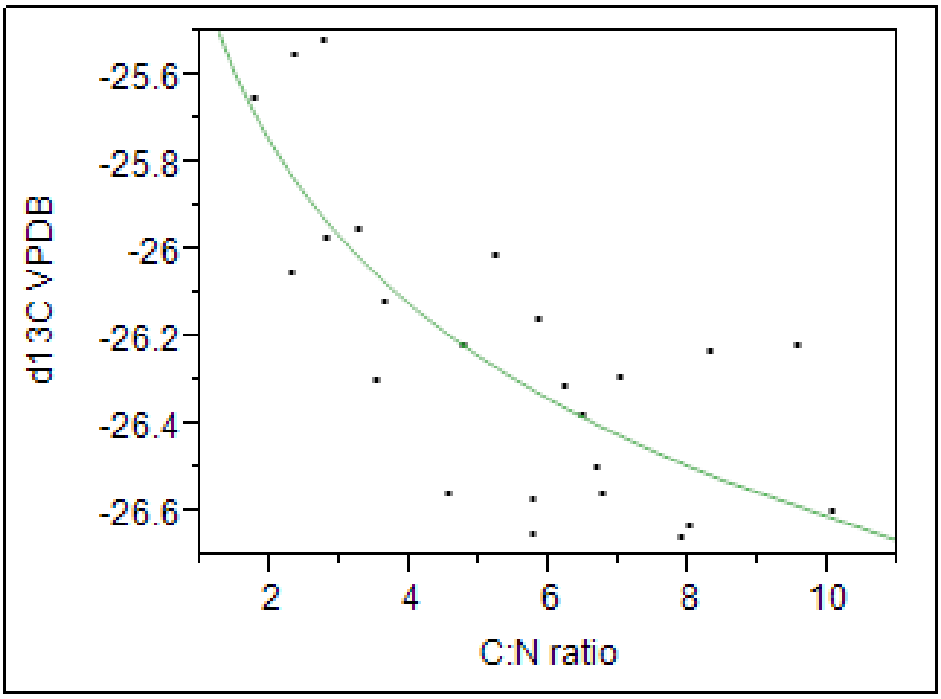

Figure C1. Logarithmic relationship between $\delta^{13}C$ (‰ VPDB) of particulate carbon and C:N ratio of total suspended sediments, at History Grove, with $R^2 = 0.59$ and $P<0.001$.

References

USDA Forest Service (2011) Burned Area Emergency Response (BAER) Imagery Support Data Download. In. United States Forest Service.